An analysis of anomalously wet summers in the South Western Cape of South Africa

by

Wade Matthew De Kock

Thesis presented for the degree of Doctor of Philosophy in the Department of Oceanography, University of Cape Town, Rondebosch, 7700

September 2022

I would like to dedicate this thesis to my Mother (Hildegard) and Stepfather (Sharlon) who has been the only father I know. To my brothers Gary and Leigh. Thank you to all for all the love and support. This work is memory of my late Grandmother, Anne Carolissen. Thank you for always believing in me.

Supervisors

Prof. Chris Reason
Department of Oceanography, University of Cape Town, South Africa

Dr. Ross Blamey
Department of Oceanography, University of Cape Town, South Africa

Funding

I am thankful for the funding from the National Research Foundation through the South African National Antarctic Programme. I am also thankful to the University of Cape Town for the Doctoral Research Scholarship and the Vice Chancellor's Scholarship.

Plagiarism declaration

I, Wade De Kock, understand the meaning of plagiarism and declare that all the work in the thesis, save for that which is properly acknowledged, is my own. This thesis contains less than 80,000 words including appendices, bibliography, footnotes, tables and equations, and has less than 150 Figures.

I confirm that I have been granted permission by the University of Cape Town's Doctoral Degrees Board to include the following publication(s) in my PhD thesis, and where co-authorships are involved, my co-authors have agreed that I may include the publication(s):

1. De Kock, W.M., Blamey, R.C. and Reason, C.J.C., 2021. Large summer rainfall events and their importance in mitigating droughts over the South Western Cape, South Africa. Journal of Hydrometeorology, 22(3): 587-599. https://doi.org/10.1175/JHM-D-20-0123.1

2. De Kock, W.M., Blamey, R.C. and Reason, C.J.C., 2022. Large-scale mechanisms linked to anomalously wet summers over the southwestern Cape, South Africa. Climate Dynamics, 1-15. https://doi.org/10.1007/s00382-022-06280-7

Signature: Signed by candidate

Date: 26 August 2022

Student Name: Wade Matthew De Kock

Student Number: DKCWAD001

Abstract

Unlike the rest of South Africa, the southwestern Cape (SWC) experiences most its rainfall in the austral winter (May-September). Due to interannual, intraseasonal and interdecadal variability, drought is a familiar occurrence. The SWC recently suffered from an extended dry period, known as the 'Day Zero Drought' during 2015-2018, where greater Cape Town nearly ran out of piped water supply. Despite most rainfall in the SWC occurring from May-September, considerable rainfall events have been known to occur during the summer (October-March). Such events could play a substantial role in mitigating winter droughts and multiyear droughts the region suffers from. Large Rainfall Events (LREs) during the summer of 2018/19 caused average dam levels in all major dams of the SWC to increase by more than 1%. The dam level increase is significant during the driest period of the year where dam levels decrease by several % per month. This study investigates all LREs during the summer (October-March) from 1979-2019 and their effects on major dam levels.

Most summer LREs are found to be linked to atmospheric rivers (ARs) or cut-off lows (COLs), which together account for up to 88% of the top 75 LREs. Apart from one study characterising the considerable effect of ARs on winter rainfall, to date little research on ARs has been done for the region. Furthermore, COLs have been suggested to occur mostly during transition seasons. This thesis reveals that although ARs are shorter in duration than COLs and lead to a smaller area receiving rainfall in the SWC, they both yield intense rainfall amounts with ARs concentrated around Greater Cape Town. After LREs have occurred, average dam volumes were shown to increase by up to 5% making LREs essential in drought recovery.

Anomalously wet summers, which typically contain more LREs than average, are also mostly associated with cooler temperatures and less extreme hot days (90% decile). Rainfall totals are inversely correlated (r=-0.44) with extreme hot days. In addition, extreme hot days also show a significant increasing trend of 2.8 days/decade from 1979-2019. Along with increased cloud cover, weaker winds over dam catchment areas can be associated with 4 out the 5 wettest summer seasons. Of the 5 wettest summer seasons, only one (2013/14) occurred in the last two decades. Anomalously cool and wet summers, reduce the water consumption impact on dam volumes as well as help reduce the impacts of drier than normal winter seasons. Wet and cool summer seasons also reduce fire risk in the region which is important considering that the region is agriculturally

productive and has experienced several devastating fires in recent decades, both in agricultural areas as well as in greater Cape Town.

Although the extended summer contributes only about 30% of the year's annual rainfall, summer LREs occur during the most water demanding part of the year. Notably, increased summer LREs usually correspond with anomalously wet summers. This thesis finds that anomalously wet summers can be characterized by increased rainfall days which are linked to increased cyclonic anomalies over the region and westerly moisture fluxes shifted anomalously equatorward in the South Atlantic. These changes in circulation patterns are found to be linked to a negative Southern Annular Mode pattern and in the late summer, also linked to ENSO and the zonal wave number 3 pattern. Overall, trends suggest decreases in rainfall days in the Greater Cape Town region and in the nearby mountain areas where most major dams are located for the mid to late summer (December-March). These decreases in rainfall days can be related to poleward expansions of the South Atlantic High Pressure (SAHP) which then lead to decreases in storms impacting the SWC.

With storm tracks occurring further poleward due to moisture corridor shifts and SAHP poleward expansions during recent years, there is a decrease in summer LREs in the SWC. Some of these poleward shifts are related to the tendency of the Southern Annular Mode to be in positive phase in recent decades. Since summer LREs are important in mitigating droughts in the region, future work needs to consider rainfall in all seasons rather than just the historical focus on winter rainfall which has been relatively well studied. This thesis shows the potential importance of anomalously wet summers as essential contributors to moisture in the region during the driest period of the year.

Acknowledgements

I would like to express the utmost gratitude to the following people for their contribution to this thesis in various ways:

My supervisors, Prof. Chris Reason, and Dr. Ross Blamey, for your expertise
and input throughout my journey is much appreciated. Thank you for the mentorship, time and guidance throughout my PhD journey. Thank you for creating a space for me to learn and grow in my field

Thanks to Mr Pierre-Louis Kloppers for cleaning up the rainfall station data provided by the South African Weather Service used in Chapters 4-6.

To my parents, Hildegard and Sharlon September, thank you for your motivational talks and support throughout my PhD journey. Thanks to my siblings (Gary and Leigh), who have kept me calm throughout my journey.

I would also like to thank my friends (Precious, Jesse, Salman, Tuscany, Cashifa) for providing the moral support and always listening.

Data Availability Statement

The rainfall data in this study are freely available on request using a disclosure form from the South African Weather Service (SAWS) (http://www.weathersa.so.za). In addition, Western Cape dam level data may be requested from the Department of Water and Sanitation (http://www.dwa.gov.za/). All reanalysis data from the ERA-Interim Project led by the ECMWF (European Centre for Medium-Range Weather Forecasts) as used by Dee et al. (2011) are freely available on request using the NCAR (National Center for Atmospheric Research, https://doi.org/10.5065/D6CR5RD9) Research Data Archive website (https://rda.ucar.edu/datasets/ds630.0/). In addition, all ERA5 reanalysis was sourced from the Copernicus Climate Data Store (https://cds.climate.coper nicus.eu/). The SAM and ENSO indices were obtained from the Climate Explorer portal (http://climexp.knmi.nl/). Extratropical cyclone data as seen in Gramcianinov et al. (2020) are available at (https://data. mendeley.com/datasets/kwcvfr52hp/3). OISSTv2 is available on the NOAA website (https://psl.noaa.gov/data/gridded/data.noaa.oisst. v2.highres.html) to calculate the SAOD and SIOD. Lastly, ETOPO2 which is a topography and bathymetry product of NOAA can be found freely on this website (https://sos.noaa.gov/catalog/datasets/etopo2-topography-and-bathymetry-natural-colors/).

List of Figures

List of Tables

List of Acronyms

ARs	Atmospheric Rivers
COLs	Cut-off lows
DJ	December-January
ENSO	El Niño Southern Oscillation
FM	February-March
JFM	January-March
LREs	Large Rainfall Events
MSLP	Mean Sea Level Pressure
ON	October-November
OND	October-December
ONDJFM	October-March
SAHP	South Atlantic High Pressure system
SAM	Southern Annular Mode
SAOD	South Atlantic Ocean Dipole mode
SIHP	South Indian High Pressure system
SIOD	South Indian Ocean Dipole mode
SST	Sea Surface Temperature
SWC	Southwestern Cape
WCT	West Coast Trough
ZW3	Zonal Wavenumber-3

Table of Contents

Chapter 1: Introduction

1.1 Background

In the Southern Hemisphere, Mediterranean-type climates, which experience most of their annual rainfall in austral winter, are to be found in the southwestern Cape (SWC) of South Africa (Reason and Rouault, 2005; Philippon et al., 2012; Mahlalela et al., 2019), southwest Western Australia, southeastern South Australia and most of Victoria, Australia (Cai and Cowan, 2006) and in central Chile (Garreaud, 2013). The rest of South Africa experiences mostly summer rainfall (Blamey et al., 2018; Mahlalela et al., 2020). High intraseasonal, interannual and interdecadal rainfall variability is experienced during the SWC wet season (May-September) (Reason et al., 2002; Reason and Rouault 2002). As with other Mediterranean type climate regions, multi-year droughts are not uncommon in the SWC (Reason and Rouault, 2005; Weldon and Reason, 2014; Muller, 2018; Burls et al., 2019); Sousa et al., 2019). Most recently, the prolonged drought of 2015-18 led to the possibility of water supply breakdown in greater Cape Town, the second largest city in South Africa with a population of ~ 3.7 million, and the event being termed the 'Day Zero Drought'. Dam levels became dangerously low throughout the region during this period and citizens were encouraged to limit water use to only 50l per day (Roffe et al., 2022), much lower than the typical daily water use per person in South Africa (~150-200l per day). The 'Day Zero Drought' emphasized the SWC's vulnerability to multi-year droughts, which are likely to increase in extent and frequency in the future (Otto et al., 2018; Mahlalela et al., 2019; Pascale et al., 2020).

The SWC contributes substantially to the agricultural sector of South Africa (Otto et al., 2018). Most of the large water supply dams are located in, or on the windward sides, of the substantial mountain ranges that characterize the region (**Fig. 1.1**). The pronounced topography, as well as distance from the neighbouring ocean areas, lead to strong rainfall gradients across the region (Mahlalela et al., 2019). Semi-desert areas (such as the Little Karoo) exist in rain shadows not far east and inland from the ocean. The majority of the SWC rainfall during the winter half of the year is brought from the ocean areas to the west and southwest.

Most of the SWC's rainfall is due to cold fronts often associated with extratropical cyclones tracking somewhat south of South Africa (Tyson and Preston-Whyte, 2000; Reason et al., 2002;

Burls et al., 2019). An additional source of rainfall may occur when the upper-level westerly wave becomes particularly amplified leading to cut-off lows (COLs) displaced from the main westerly flow further south. These cold-cored and deep (500hPa) convective systems are most common in spring and autumn (Taljaard, 1985; Singleton and Reason, 2007a; Favre et al., 2013; Omar and Abiodun, 2020) and have led to many of southern South Africa's flooding disasters (e.g., Taljaard, 1985; Singleton and Reason, 2006, 2007b; Favre et al., 2013; Molekwa et al., 2014).

Another moisture source associated with extratropical cyclones in the SWC are atmospheric rivers (ARs). ARs have been known to occur over the South Atlantic deriving from the South American tropics (Blamey et al., 2018; Payne et al., 2020). When they occur, ARs often cause very heavy rainfall in the region. Blamey et al. (2018) showed that 8 of the top 9 extreme winter rainfall events in the Western Cape resulted from ARs. ARs can be characterised as long (~2000km) and filamentous sources of low-level moisture transported from the tropics into midlatitude regions (Zhu and Newell 1998; Gimeno et al., 2014). Moreover, ARs have been known to cause widespread rain in other Mediterranean-like climate regions such as southern California (Ralph et al., 2013; Dettinger et al., 2011) or the Iberian Peninsula of southwest Europe (Ramos et al., 2015; Eiras-Barca et al., 2016; Gimeno et al., 2016).

To date, limited research has been done on wet summers and summers in general in the SWC. A better understanding of wet summer characteristics and associated mechanisms is needed as these are likely associated with wind changes along the west coast of the SWC (Jury, 2020). Previous work has shown that anomalously wet winters and transition seasons often involve westerly disturbances such as extratropical cyclones associated with ARs and COLs (Singleton and Reason, 2007a; Favre et al., 2013; Weldon and Reason, 2014; Blamey et al., 2018; Ramos et al., 2019) which transport moisture from the tropical and southwest Atlantic. However, there is little or no research to date on whether such strong weather systems may also lead to anomalously wet summers.

Much like the austral winter, one could expect wet summers to be associated with increased cyclonic activity, an increase in westerlies over the South Atlantic as well as an equatorward retreat of the semi-permanent South Atlantic High Pressure (SAHP) system (Taljaard, 1953) which allows for increased low pressure activity near the SWC. Generally, the SAHP moves further poleward and eastward during early summer along with a poleward shift in the subtropical jet. The poleward shift reduces frontal activity approaching the SWC and storms are redirected southward (Reason et al., 2006) resulting in relatively drier conditions. With south easterly winds dominating during

the austral summer, moisture is often steered away from the SWC in contrast to mainly westerlies during the winter and as a result, increasing impacts from cold fronts and other midlatitude disturbances.

Shifts in the SAHP and upstream moisture fluxes in the South Atlantic have been shown to be related to the SWC's interannual rainfall variability (Reason et al., 2002; Ramos et al., 2018; Sousa et al., 2018; Burls et al., 2019). Furthermore, changes in these circulation patterns have been shown to be related to sea-ice anomalies in the Southern Ocean (Blamey and Reason, 2007), sea surface temperature (SST) changes (Reason and Jagadheesha, 2005) as well as large scale modes of variability such as El Niño Southern Oscillation (ENSO) and the Southern Annular Mode (SAM) (Reason and Rouault, 2005; Phillipon et al., 2012; Mahlalela et al., 2019). Little to no research has been done on how anomalously wet summers are linked to these features and how they influence westerly moisture flux corridors over the SWC.

1.2 Aims

Given that the summer is typically warm, dry and windy with high evaporation potential, little or no work has previously been done on anomalous rainfall events during this season. However, if these rainfall events are large enough, they have the potential to reduce drought impacts from either the preceding or following winter (should those rainy seasons be drier than average) as well as reduce the risk of fires which often occur in the summer half of the year throughout the region. Most notoriously, the devastating fire on Devils Peak in late summer 2021 burnt several historic buildings on and near the upper campus of the University of Cape Town (Holmes et al., 2022). Thus, the aims of this thesis are to better understand rainfall variability and trends over the SWC during the summer half of the year (October-March), the occurrence of large rainfall events (LREs) in this season, and their potential to mitigate winter droughts or drier than average winter seasons. In particular, the mechanisms behind wet extended summers, the associated moisture sources, weather systems and large scale circulation patterns will be investigated. This thesis aims to investigate the role anomalously wet summers play in lessening drought effects but also in acting as important sources of moisture during the driest time of the year. In order to achieve these aims, the following questions are addressed:

Chapter 4

- Which rainfall bearing systems contribute to rainfall in the SWC during the extended summer?
- How is rainfall in the SWC distributed during the summer half of the year and which months are the driest on average?
- What is the interannual variability of rainfall during the summer half of the year?
- Do summer LREs make a significant contribution to summer totals and can they mitigate against the impacts of extended winter droughts?

Chapter 5

- How many wet summers are cooler than average?
- Is there a relationship between anomalies in rainfall and air temperature?
- Is there a relationship between anomalies in rainfall and wind?
- Are LREs associated with cooler seasons?

Chapter 6

- Are there any significant trends in rainy days during the summer?
- What are the circulation patterns associated with anomalously wet and dry summers?
- Are there any significant relationships between summer rainfall variability over the SW Cape and interannual climate modes?
- Do the characteristics of the semi-permanent high pressure system in the South Atlantic influence summer rainfall?

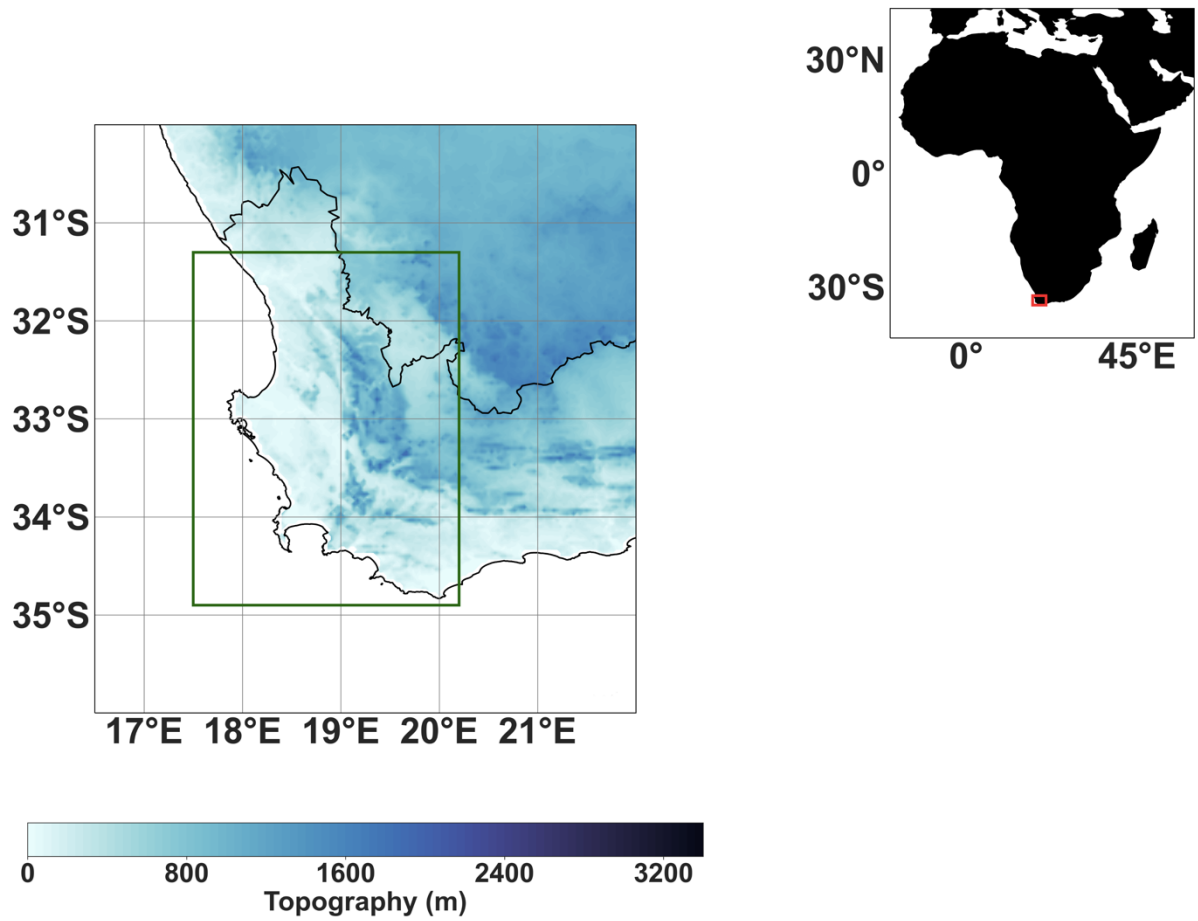

Figure 1.1:*The general topography (m) of the southwestern Cape (SWC) at the southwestern tip of southern Africa. Produced using ETOPO2 which is a topography and bathymetry product of NOAA. The green box represents the winter rainfall region.*

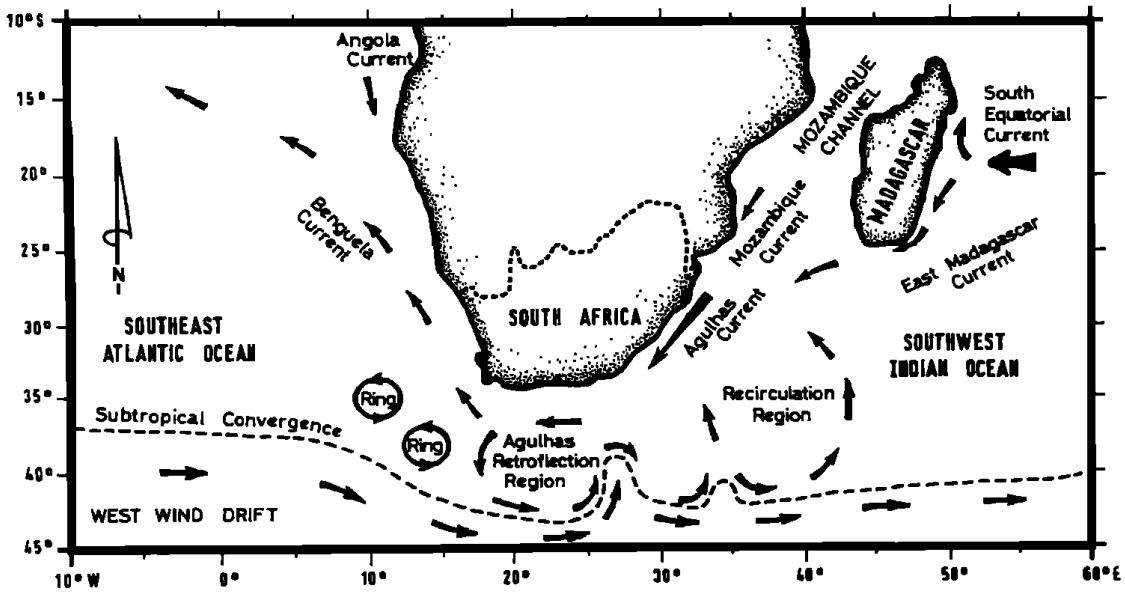

Figure 1.2: *Schematic showcasing the basic large scale features surrounding South Africa which includes the Benguela and Agulhas currents. Source: Walker (1990)*

Chapter 2: Literature Review

This chapter provides a comprehensive review of rainfall in the southwestern Cape. Previous studies have focused on austral winter rainfall as most of the region's rain occurs during May-September. As a result, little research has previously been done on summer rainfall since the extended summer (October-March) is considered the driest and warmest time of year for this region (Philippon et al., 2012; Mahlalela et al., 2019; Ndebele et al., 2020). The literature review furthermore discusses the mechanisms and circulation patterns that have been proposed to be linked to rainfall in the region.

2.1 Regional rainfall characteristics and systems

The southwestern Cape (SWC) of South Africa is unique in southern Africa in that it receives much of its rainfall during the austral winter (June-August; JJA) whereas most of southern Africa receives rainfall during the austral summer (Reason et al., 2002). Like other west coast subtropical regions, it experiences a Mediterranean-type climate but because of South Africa's narrow peninsula-like geography, the area occupied by this type of climate is relatively small compared to southern Australia, the west coast of the United States, and North Africa/ southern Europe.

With previous studies focusing on winter rainfall in the SWC, most of the region's known rainfall producing systems derive from westerly disturbances. The spatial distribution in rainfall across the region has been known to be moderated by the region's topography and the surrounding oceans (Blamey et al., 2018; Mahlalela et al., 2019). A relatively wet coastal region is separated by a drier interior largely due to the Cape Fold Mountain ranges and steep slopes. The SWC is at the south western tip of Africa where the South Atlantic and South Indian Oceans interact via rings and other eddy features shed off the Agulhas Current retroflection (Durgadoo et al., 2013; Loveday et al., 2014). This geography means that the strongest western boundary current in the ocean (Agulhas Current) terminates in close proximity to an eastern boundary current upwelling system (Benguela Upwelling System). Upwelling occurs along the west coast throughout the year between ~30-17°S and in the summer half of the year between ~34-30°S (Lutjeharms, 1981; Veitch et al., 2006). These cooler SSTs together with strong anticyclonic subsidence associated with the South Atlantic high-pressure system (SAHP) lead to the west coast climate quickly transitioning from semi-arid to hyper-arid in the Northern Cape and Namibia. Additionally, contrasting sea surface

temperatures (SSTs) from the Benguela and Agulhas currents (**Figure 1.2**) have been known to influence rainfall in the SWC (Reason et al., 2002; Reason and Jagadheesha, 2005; Mahlalela et al., 2019). Reason and Jagadheesha (2005) in particular, demonstrates how wet winters are characterized by anomalously warm SSTs in the southwest Atlantic which results in shifts of the jet stream position and the ability for fronts to enter the region. The air directly above warmer SSTs has been known to hold more water vapour which may enhance the vertical transport of moisture (Allen and Ingram, 2002; Held and Soden, 2006; Seager et al., 2010; Donat et al., 2016). Moreover, Donat et al (2016) notes that dry regions show areas of SST decreases in some parts of the ocean. Anomalies in SSTs in the open South Atlantic or in the cyclogenesis region in the midlatitude southwest Atlantic (Jones and Simmonds, 1993) have previously been related to changes in winter rainfall totals via latitudinal shifts in storm tracks, and westerly moisture fluxes approaching the SWC (Reason et al., 2002; Reason and Jagadheesha, 2005). Furthermore, Reason et al. (2002) suggests that warmer SSTs in the southwest Atlantic results in a more northward pattern in cyclonic activity and locally intensifies such rainfall systems, resulting in increased rainfall over SWC. In contrast, according to Mahlalela et al. (2019), drier winter seasons feature colder SSTs and an expansion of the SAHP.

Blamey and Reason (2007) suggested a relationship between extended winter (May-September) rainfall and Antarctic sea ice concentration (SIC) anomalies near the Antarctic peninsula and also in the sector due south of South Africa, with strongest correlations between SIC and rainfall for the core winter (May-July). This, and other studies, have shown anomalously wet SWC winters to be associated with cyclonic circulation anomalies over, and to, the south of South Africa. Wet winters also experience increases in westerly moisture fluxes and a stronger northward subtropical jet as seen in Weldon and Reason (2014) and Mahlalela et al. (2019). This results in intensified frontal behaviour impacting the SWC due to an increase in storms further north and more northward located anticyclones during winter months (Taljaard, 1953). Such wet winters with the fronts typically stronger and tracking further north than average, tend to also be cooler and windier than anomalously dry winters which are dominated more by anticyclonic conditions, often with berg winds (Mahlalela et al., 2019), leading to an increase in dry and warm (even hot) days where the maximum temperature near the coast can reach around 30^{o}C. Given the intensive use of irrigation in much of SWC agriculture, which exports considerable amounts of citrus and other fruit as well as wine internationally, anomalously dry and warm winters pose a substantial risk to one of the most important sectors of the local economy as well as increase fire risk (Van Wilgen, 1984; 2009; Holmes et al., 2022). More generally, Theron et al. (2021) and Grab and Craparo

(2011) have noted that temperature shows an increasing trend in the SWC. Such long-term trends are also likely to adversely impact the local economy, particularly water demand and agriculture.

A key factor in determining the climate of the SWC is the positioning and strength of the SAHP, a semi-permanent subtropical anticyclone over the South Atlantic. Early work (Vowinckel, 1955; Tyson and Preston-Whyte, 2000) indicated that on average the SAHP moves furthest east during October-December with a 13° westward shift during the winter (Preston-Whyte et al., 1977). Furthermore, Taljaard (1953) also notes that the SAHP moves about 4-5° north during the austral winter. In general terms, the retreat of the SAHP to the northwest and away from the SWC in the winter allows a relative trough of low pressure to exist over the SWC. This retreat of the SAHP brings rainfall (Jury, 1987) while the continental high is well developed over the interior, keeping the rest of South Africa relatively dry. Seasonal shifts in the SAHP also coincide with seasonal shifts in the circumpolar trough. An early study by Taljaard (1967) highlights an increase in storm activity poleward. The increasing poleward activity can be linked to southward shifts in the circumpolar trough during the summer and intermediate seasons. Furthermore, Taljaard (1967) highlighted increased cyclone density further equatorward with a band stretching from southern South America to the South Atlantic where it eventually merges with the circumpolar core south of South Africa. However, Jones and Simmonds (1993) notes that the South Atlantic band is not as defined as the South Pacific band which could account for variability in cyclone density in the South Atlantic. A more recent study by Gramcianinov et al. (2019) notes cyclogenesis in the South Atlantic occurring at three main locations off the southern Brazil and Argentinian coasts as well as the central South Atlantic around 45°S and 10°W.

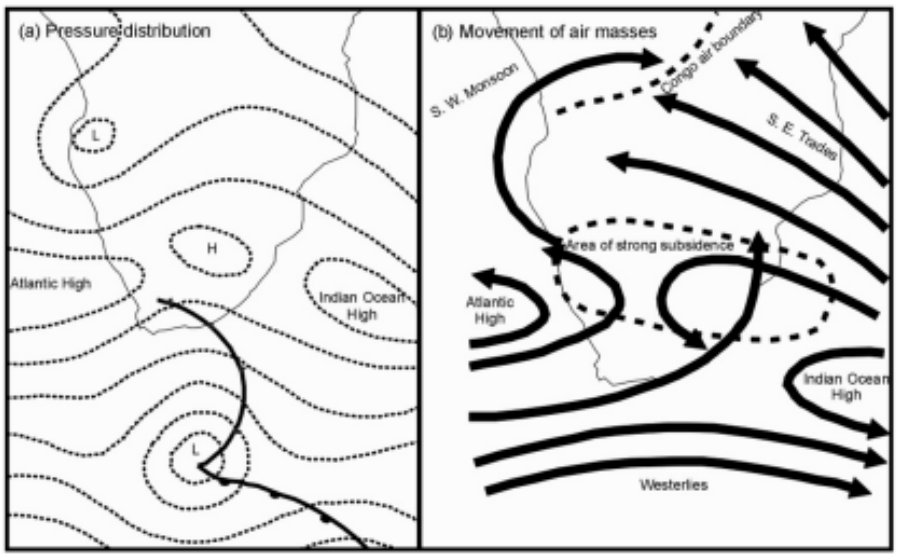

***Figure 2.1**: Schematic showing the typical pressure distribution and movement of air masses during the austral winter over southern Africa with the continental high over the interior and relative low pressure over the SWC. Source: Kruger et al. (2010)*

The intensity and position of the SAHP is well researched as its presence is also known to affect storm tracks and as a result, rainfall, in regions on the eastern and western basins of the South Atlantic (Vigaud et al., 2009; Telesca et al., 2012; Blamey et al., 2018; Gilliland and Keim, 2018; Sousa et al., 2018; Burls et al., 2019; Zilli et al., 2019; Al Fahad et al., 2020, Dyer et al., 2022). **Figure 2.1a** shows the general pressure distribution in the region while **Figure 2.1b** shows the general movement of air. Reboita et al. (2019) states that the SAHP expands in the winter and retracts eastward during the summer (Reboita et al., 2019). Reboita et al. (2019) also suggests that climate models predict a poleward shift in the SAHP as well as variability in its centre and position. Similar studies of SAHP expansion in recent years in the SWC (Burls et al., 2019; Al Fahad et al., 2020) indicate a drying trend, which may be due to the SAHP blocking rainfall systems such as cold fronts and extratropical cyclones from affecting the region. The positioning and intensification of the SAHP has also been linked to SST changes in the equatorial Atlantic (Zilli et al., 2019). Moreover, cold SST events in the South Atlantic have been associated with a strong SAHP during late summer (Lübbecke et al., 2014).

The SAHP position may influence the ability for extratropical cyclones to track (Reboita et al., 2018) towards the SWC. Extratropical cyclones have been known to play a key role in midlatitude and more specifically SWC rainfall (Reason et al., 2002; Blamey and Reason, 2007, Blamey et al., 2018). This is due to their role in the exchange of heat and moisture in the midlatitudes and how extratropical cyclones interact with other large scale atmospheric patterns (Simmonds and Keay, 1999; Bengtsson and Hodges, 2005). More specifically, Jones and Simmonds (1993) found that the southwestern Atlantic is an important region for cyclogenesis and storm tracking. Anomalously warmer SSTs in the South Atlantic promote cyclogenesis and the movement of storms equatorward. In general, Walker and Lindesay (1989) as well as Reason et al. (2002) suggest that such midlatitude storms affecting the SWC may be enhanced through warmer SSTs in the South Atlantic and that the spatial variability in SSTs additionally contributes to where these storms track. For example, warmer SSTs near the coast of the SWC, may locally enhance storm activity and aid in intensifying rainfall there (Reason et al., 2002). Furthermore, warmer SSTs off the Argentinian coast (Reboita et al., 2021), an important region for cyclogenesis (Jones and Simmonds, 1993), are also noted by Reason and Jagadheesha (2005) and Mahlalela et al. (2019) as potentially influencing SWC rainfall. Warmer SSTs here during the wet seasons may be

associated with increased cyclogenesis in the South West Atlantic and increased storm tracking towards the SWC.

Simmonds and Keay (1999) found decreases in storm activity in the Southern Hemisphere between 30-50°S and 50-70°S from 1972-1997. This decreasing storm activity can largely be accounted for by a decrease in low level baroclinicity (Geng and Sugi, 2003). Furthermore, Lim and Simmonds (2002) also link strong cyclones in the Southern Hemisphere to strong baroclinicity and suggest that this contributes toward the equatorward movement of cyclones. Studies consistently reveal a poleward shift in storm tracks (Taljaard, 1967; Bengtsson et al., 2006; Burls et al., 2019). However, the effects of a warming climate and SST changes are not yet fully understood (Schneider et al., 2010) so it is difficult to determine whether decreasing trends in storm activity persist or not as a result of climate change.

Rainfall bearing systems such as extratropical cyclones and ARs have been known to contribute towards rainfall in the region (Reason, 2002; Reason et al., 2002; Singleton and Reason, 2007b; Blamey et al., 2018; Ramos et al., 2019). Extratropical cyclones are often presented over the SWC as cold fronts or cutoff lows (COLs) depending on how far north these storms track (Tyson and Preston-Whyte 2000; Reason et al., 2002; Singleton and Reason, 2007b; Favre et al., 2013; Burls et al., 2019). COLs are cut off from a mid-latitude source region resulting in a closed, cyclonic vortex (Singleton and Reason, 2006), located equatorwards of the main westerly flow, and are frequently associated with strong winds and heavy rainfall. Such rainfall events have been known to bring considerable rain volumes particularly during the winter and transition months (Singleton and Reason, 2007a; Kruger et al., 2010; Weldon and Reason, 2014; Mahlalela et al., 2019; Barnes et al., 2021; Omar and Abiodun, 2021). Singleton and Reason (2007a) identified COLs to contribute to rainfall over the southwestern region of South Africa. Favre et al. (2013) suggests a 25% increase in COLs occurring from 1979-2006 but these are primarily for COLs along the south and east coast of South Africa. More interestingly for the SWC, Favre et al. (2013) found that COLs contribute 15% of annual rainfall in the Western Cape which is significant given that these rain bearing systems are not the largest contributors during the wet season (June-August).

Atmospheric rivers (ARs) are another weather system potentially associated with heavy rainfall over the SWC region. While they have been extensively studied in many other parts of the world (e.g., (Ralph et al., 2004; Gimeno et al., 2014), there has been little work on these systems in the South African region other than that of Blamey et al. (2018). These systems are characterised by narrow bands of intense, vertically integrated water vapour transported from the tropics to the

midlatitudes in the lower atmosphere (850hPa) (Zhu and Newell, 1994; Lavers et al., 2011; Gimeno et al., 2014; Cordeira et al., 2017; Payne et al., 2020). Blamey et al. (2018) showed that ARs are linked to around 70% of the top 50 largest rainfall events during the winter months (May-September). ARs are important sources of moisture for the region during the wet months even though they do not make landfall as frequently as their Northern Hemisphere counterparts (Blamey et al., 2018; Ramos et al., 2019). Furthermore, Ramos et al. (2018) suggests that years containing numerous ARs, have been known to bring about floods in the southern Africa. **Figure 2.2 a and b** below show AR prevalence in the SWC during the winter months.

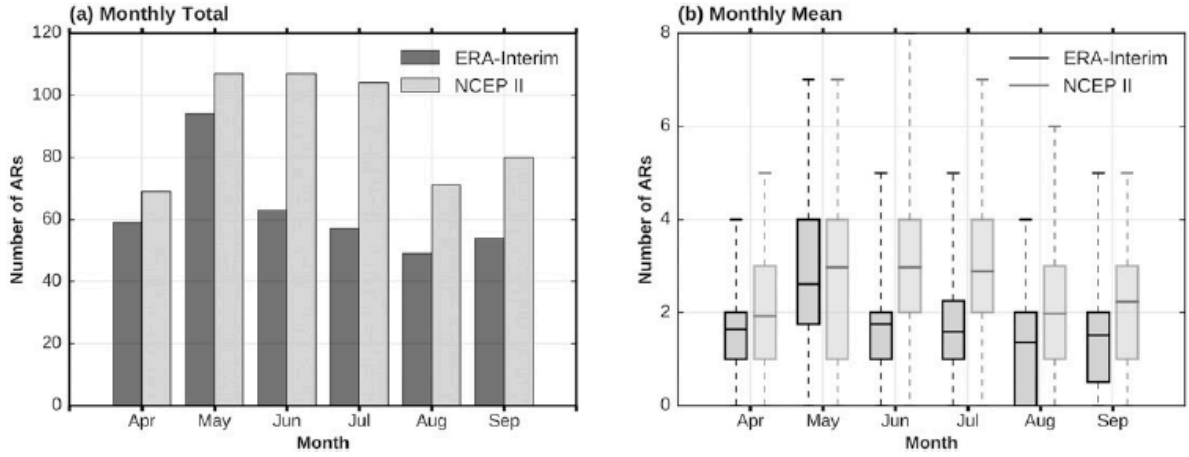

***Figure 2.2** : An indication on the number of atmospheric rivers (ARs) occurring off the west coast of South Africa during the wettest months of the year for the SWC (April-September). On average, ARs occur about three times a month during three of the wettest months. Source: Blamey et al. (2018)*

2.2 The recent 'Day Zero' drought

With the SWC experiencing considerable interannual and interdecadal variability in rainfall (Reason et al., 2002; Reason and Rouault, 2002), droughts are not an uncommon occurrence (Reason and Rouault, 2005; Weldon and Reason, 2014; Muller, 2018; Sousa et al., 2019; Burls et al., 2019). Most recently, the 2015-2018 drought (the 'Day Zero' drought) which was one of the worst SWC droughts since 1904 (Botai et al., 2017; Wolski, 2018) brought increased attention to the SWC's water supply and dam levels (Sousa et al., 2018; Burls et al., 2019; Mahlalela et al., 2019; Pascale et al., 2020).

The 2015-2018 'Day Zero' drought led to increased analysis on SWC drying in the past five years (Botai et al., 2017; Sousa et al., 2018; Wolski, 2018; Burls et al., 2019; Mahlalela et al., 2019; Roffe et al., 2021). Burls et al. (2019) showed that both a decrease in winter rainfall days as well

as in the intensity of the rainfall events contributed to the drought. The study also suggests that the decrease in rainfall days is related to Hadley cell expansion, which corresponds to an expanded SAHP. Sousa et al. (2018) considered the observed expansion in the SAHP and poleward migration of moisture corridors across the South Atlantic during the drought. Both studies show that this led to a poleward movement of extratropical cyclones and storm tracks which are important sources of rainfall for the SWC.

Recent changes in circulation such as SAHP expansion, shifts in the jet (Sousa et al., 2018; Mahlalela et al., 2019; Pascale et al., 2020) and moisture corridors, imply further drought risks in the future (Burls et al., 2019). With a large focus on winter already showing drying during the wet season of June-August (Mahlalela et al., 2019), there is a need to better understand patterns and trends throughout the year as the SWC population relies heavily on the rainwater collected in dam reservoirs (Sousa et al., 2018; Wolski, 2018; Burls et al., 2019). Although the recent 'Day Zero' drought can be classified as severe and rare (Wolski, 2018), drought risk through changes in circulation patterns and in conjunction with changing SSTs remains a problem. To compound the problem, not only does the winter rainfall season appear to be shortening (Mahlalela et al., 2019; Roffe et al., 2021) but rainfall duration shows decreases as well (Burls et al., 2019). The decrease in intensity is not surprising given the shift in moisture corridors which act as important pathways for rainfall systems such as ARs which have been shown to be important sources of moisture for the SWC.

Moreover, the poleward expansion of the SAHP implies fewer extratropical cyclones tracking in locations where they can significantly affect the the SWC, or a weakening of such cyclones, or both. As a result, cold fronts or COLs, which have been known to contribute considerable rainfall amounts to the SWC (Singleton and Reason, 2007a; Favre et al., 2013), may be weakened or steered away from the region. However, most COLs tend to occur in transition seasons (Singleton and Reason, 2007a), so further analysis is needed on their frequency and intensity to supplement the well-studied austral winter rainfall. Omar and Abiodun (2020) do showcase the importance of COLs during the 2015-2017 drought that brought much needed relief during the years 2015 and 2016. COL occurrences remained below average during 2017 and this may have aided extending the drought. Overall, COLs, together with ARs are seen as very important sources of moisture for the region and so any disruption or blocking along their path toward the SWC may result in drier than average conditions.

Mahlalela et al. (2019) characterizes wet winter seasons associated with a stronger subtropical jet and a weaker polar jet. The study also highlighted the Southern Annular Mode (SAM) as being important following earlier work which associated wet (dry) winters over a larger western South African region as being associated with a negative (positive) phase of the SAM (Reason and Rouault, 2005). This mode, as well as other large scale climate modes, is discussed further in the next section.

2.3 Large-scale modes of variability

The Southern Annular Mode (SAM) influences rainfall in the midlatitudes of the Southern Hemisphere (e.g., Hall and Visbeck, 2001; Silvestri and Vera, 2003; Reason and Rouault, 2005; Gillett et al., 2006; Abram et al., 2014). The SAM is barotropic and characterised by opposing pressure anomaly differences between the Antarctic and the midlatitudes. A positive SAM is associated with negative pressure around the Antarctic and positive pressure over the midlatitudes which translates to more poleward storm tracks as suggested by Gillett et al. (2006). During a negative (positive) SAM phase, western South Africa typically experiences wetter (drier) conditions (Reason and Rouault, 2005; Gillet et al., 2006; Nieto et al., 2014 and Mahlalela et al., 2019). The mechanism by which a negative SAM phase would favour increasing rainfall involves midlatitude storms be located further equatorward than average and the westerly wind belt shifting further north (Silvestri and Vera, 2003; Reason and Rouault, 2005; Pohl et al., 2010; Nieto et al., 2014; Reboita et al., 2015). A negative SAM phase also corresponds with an equatorward movement of the eddy driven jet (Codron, 2005) which is also highlighted by both Reason and Rouault (2005) and Mahlalela et al. (2019).

Regions with similar climates to the southwestern Cape, such as southern and southwestern Australia show a similar relationship with SAM (Pezza et al., 2008; Cai et al., 2011). This contrasts with central South Africa which shows that a positive SAM is linked to above average rainfall resulting from deep convection and southward shifts in westerly winds (Pohl et al., 2010). It is also necessary to note however that central South Africa has more a summer dominant rainfall whereas the SWC experiences a winter dominant rainfall. Pohl et al. (2010) also suggests that El Niño years are linked to higher probability of negative SAM phases. Over the Eastern Cape, where winter contributes less than 20% to the annual total on average, Mahlalela et al. (2020) found that the SAM (**Figure 2.3**) was significantly correlated with summer rainfall but not with spring. Silvestri and Vera (2003) in particular found SAM to be strongest during the winter and spring season when analysing links between rainfall anomalies in southeast South America and SAM. In contrast, dry

conditions have been associated with positive SAM phases in some areas of the Southern Hemisphere particularly those that correspond with La Niña years by restricting the passage for cold fronts in midlatitudes (Sun et al., 2017).

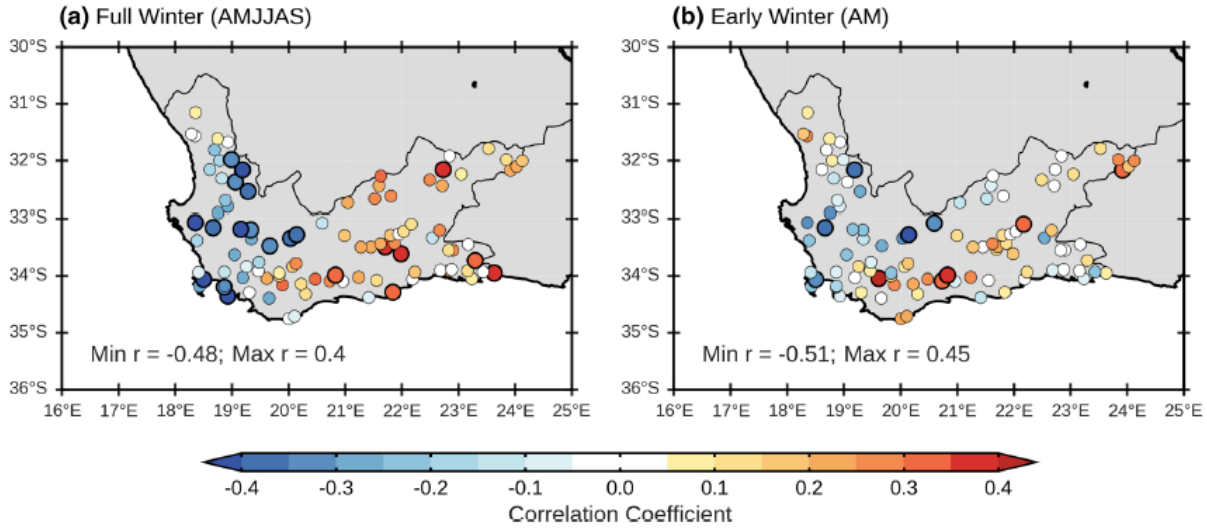

***Figure 2.3**: Schematic indicating the negative relationship the Southern Annular Mode (SAM) has with rainfall in the SWC compared to the rest of the region during the wet season (April-September). The relationship between rainfall and SAM is also shown to be slightly stronger during the early winter (April-May) with the rest of the Western Cape displaying a mostly positive relationship with SAM. Source: Mahlalela et al. (2019)*

The ENSO relationship with rainfall is not as obvious in comparison to the rest of South Africa (Philippon et al., 2012; Mahlalela et al., 2019). As shown by many authors (e.g. Lindesay, 1986, 1988; Nicholson and Kim, 1997; Reason et al., 2000), significant correlations are seen between summer rainfall over large areas of southern Africa and ENSO but this is not the case for the SWC. On the other hand, Philippon et al. (2012) suggests that longer wet spells during May-July rainfall may occur more during El Niño events. These authors also add that El Niño events may favour deeper rainfall bearing systems. Furthermore, studies have shown that ENSO strongly impacts on SSTs in the South Atlantic (Colberg et al., 2004; Lübbecke et al., 2014).

Another important mode of interannual SST variability in the region is the South Indian Ocean subtropical dipole (SIOD) which also influences summer rainfall over parts of southern Africa (Behera and Yamagata, 2001; Reason, 2001, 2002). When in its positive phase with above (below) average SST in the South West (South East) Indian Ocean, increased (decreased) summer rainfall sometimes occurs over parts of southern Africa. Hoell and Cheng (2018) found significant correlations between the December-March SIOD and rainfall in central South Africa, Botswana,

and Zimbabwe. However, many SIOD summers are also ENSO summers and it has been suggested that the rainfall impacts are strengthened (weakened) when ENSO and the SIOD are out of (in) phase (Hoell and Cheng, 2018). Located further north in the tropical Indian Ocean, the Indian Ocean Dipole has been shown to strongly influence September-December rainfall in equatorial East Africa (Saji et al., 1999) and, to lesser extent, the summer rainfall region of sub-Saharan Africa (Marchant et al., 2007).

While the SIOD is essentially driven by large scale changes in surface heat fluxes and Ekman heat transport associated with shifts in the strength and position of the SIHP (Hermes and Reason, 2005), the IOD like ENSO is a coupled ocean-atmosphere mode rooted in the tropics. Thus, planetary waves generated by the SST-anomaly induced shifts in tropical atmospheric convection, can lead to near-global scale rainfall impacts of both these modes. In the Southern Hemisphere, one well known teleconnection pattern is the Pacific South American pattern which is associated with SST anomalies and changes in the SAHP during ENSO over the South Atlantic (Colberg et al., 2004). Anomalies in the SAHP can then lead to changes in moisture transport towards southern Africa (Vigaud et al., 2009; Blamey et al., 2018; Sousa et al., 2018).

A dipole mode has also been proposed for the South Atlantic (SAOD) (e.g. Nnamchi et al., 2011). which has been suggested to influence West African precipitation (Nnamchi et al., 2013). The SAOD as defined by Nnamchi et al. (2011) can be characterised by warm SSTs near west and central equatorial Africa and cooler SSTs off the coast of Argentina, Uruguay and Brazil. Moreover, the southern pole is also an area in which cyclogenesis occurs (Jones and Simmonds, 1993; Hoskins and Hodges, 2005; Bengtsson et al., 2006) which can then affect South African rainfall (Reason et al., 2002; Blamey et al., 2018). More generally, the South Atlantic is an important region for moisture transport into the SWC (Blamey et al., 2018; Ramos et al., 2019).

The midlatitude circulation over the South Atlantic, and more generally the Southern Hemisphere, often exhibits a zonal wave number 3 (ZW3) pattern (van Loon and Jenne, 1972; Raphael, 2004). This type of pattern, or sometimes wave number 4, has been implicated in the SIOD evolution (Hermes and Reason, 2005) as well as in Antarctic sea ice anomalies (Venegas, 2003; Raphael, 2004). High (low) ZW3 activity corresponds to strong meridional (zonal) flow and tends to show peak signals in winter (positive) and summer (negative). A strong zonal flow is seen in transition seasons (austral spring and autumn) when ZW3 tends to be weaker. Raphael (2004) also suggests that ZW3 changes from strong positive to strong negative during a run of ENSO events. Whether or not these wave number 3 or 4 patterns strongly influence SWC rainfall remains to be shown;

however Mahlalela et al (2019) showed evidence of a link between wavenumber 4 and early winter rainfall over the SWC while spring rainfall over the Eastern Cape may be related to the ZW3 pattern (Mahlalela et al., 2020).

In summary, while various modes of climate variability have been investigated for their potential relationships with summer rainfall over eastern and northern South Africa or with winter rainfall over the SWC, there has been little research on the influence of large-scale modes of variability on summer rainfall in the SWC. Following the recent 'Day Zero' drought (Botai et al., 2017; Wolski, 2018; Burls et al., 2019) and interest in rainfall (**Figure 2.4**) occurring in other seasons in the SWC (Mahlalela et al., 2019), it has become increasingly important to better understand variability over the SWC during the summer half of the year. Thus, part of this thesis will consider potential relationships between SAM, ENSO, SAOD, SIOD and ZW3 on summer rainfall over the SWC.

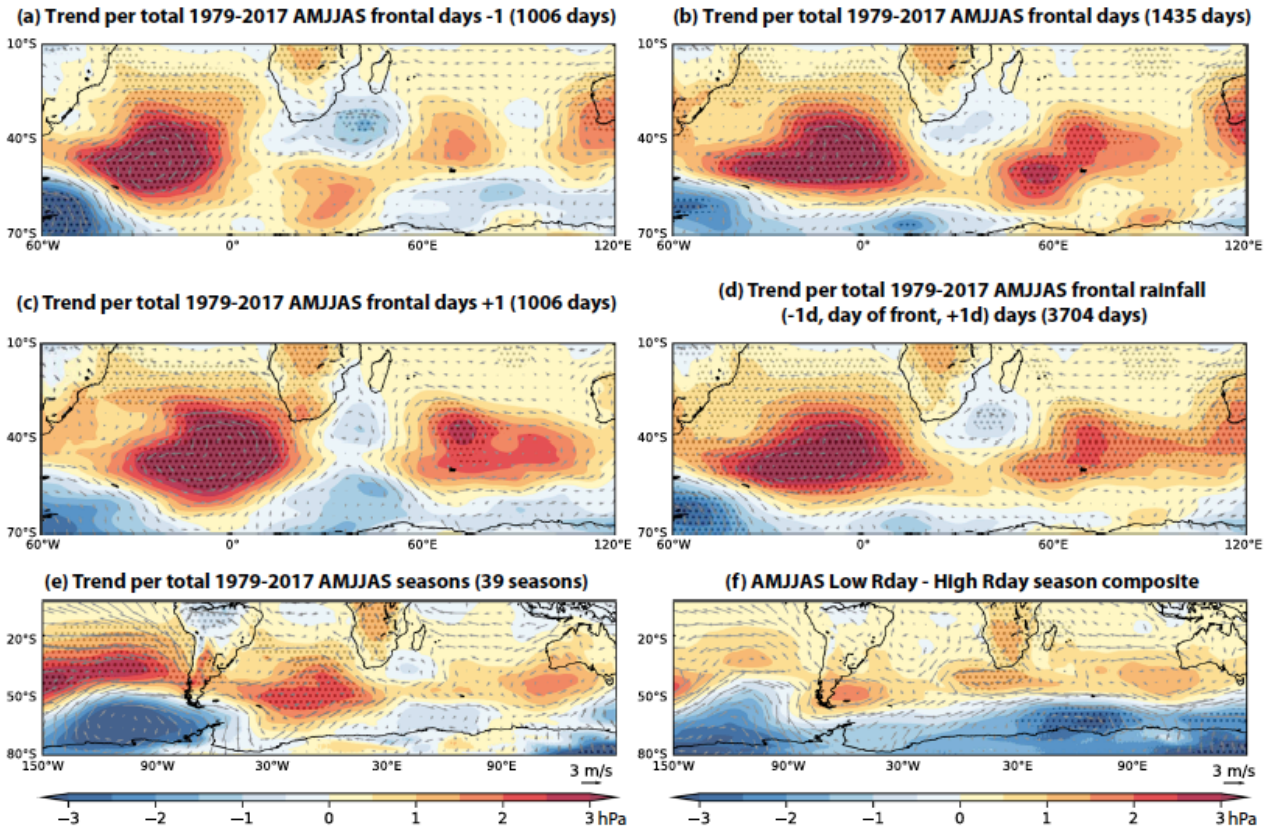

***Figure 2.4**: Schematic indicating suggested Hadley cell or South Atlantic High pressure (SAHP) poleward expansion trends during the wettest season of the year (April-September) for the southwestern Cape. The red accounts for positive pressure trends across frontal days from 1979-2019. Source: Burls et al. (2019).*

2.4 Summary

This Chapter reviewed the circulation patterns and weather systems that influence the weather and climate in the southwestern Cape (SWC) of South Africa as well as the South Atlantic region. Most of the region's rainfall occurs during the austral winter (April-May) and is brought about mostly through disturbances in the midlatitudes. Systems like extratropical cyclones and associated fronts, cut-off lows, and atmospheric rivers are the main contributors to winter rainfall as well as strongly affecting day to day changes in temperature and wind experienced over the region. Many studies have shown that the winter rainfall is highly variable and may be related to South Atlantic SST or sea ice variability or to large scale climate modes like the SAM.

The literature also suggests that the South Atlantic is an important moisture source for the SWC which makes the region, and its circulation features (particularly the SAHP and locations of the major westerly storm tracks), important for local rainfall. However, while the winter rainfall variability over the SWC and associated mechanisms have been relatively well researched, very little work has been done on rainfall characteristics during the summer, the driest part of the year. Anomalously wet extended summers (October-March) can supplement winter rainfall as well as have the potential to act as periods of relief following drier-than-normal winter conditions, or as insurance against the following winter rainy season being inadequate. Such wet summers also reduce fire risk in a fire-prone region and reduce irrigation demand by the economically important agricultural sector. Motivated in particular by the recent multiyear drought over greater Cape Town, as well as the possibility that rainfall seasons may shift in the future (IPCC 2021), this thesis investigates rainfall variability during the extended summer, the large rainfall events that sometimes occur then, and their associated mechanisms.

Chapter 3: Data

To avoid repetition in the data and methodology sections for *Chapters 4-6*, two of which have been published in the literature (De Kock et al., 2021, 2022), this chapter briefly summarises the data used in this thesis as well as the origin of the data. Full details on the methodology are given in *Chapters 4-6*.

3.1 SAWS Station Data

Station data was requested all along the SWC for years 1979-2019 for rainfall. Station data was used in contrast to satellite data given that SWC experiences a coastal resolution problem particularly with CHIRPS data. SWC stations with 95% of good or usable data (data that has not been flagged by the South African Weather Service) was considered in the thesis in order to obtain averaged rainfall volume and rainfall days. Averaging across different (to calculate LREs and for Zones A-D in *Chapter 5*) in the SWC based on location and rainfall patterns avoids considering one stations local rainfall amount which could differ due to change in elevation of stations or any local orographic differences within a zone.

3.2 ERA-Interim and ERA5 Reanalysis Data

ERA-Interim data with horizontal resolution of 0.75° (For Chapter 4) and ERA5 reanalysis data (Hersbach et al., 2020) with a 0.25°x0.25° horizontal grid (For Chapters 5 and 6) was considered. Both datasets are available on the ECMWF (European Centre for Medium-Range Weather Forecasts) website and is also freely available on request using the NCAR (National Center for Atmospheric Research, https://doi.org/10.5065/D6CR5RD9 for ERA-Interim) Research Data Archive website (https://rda.ucar.edu/datasets/ds630.0/) as well as the Copernicus database (https://cds.climate.copernicus.eu/cdsapp#!/home). Specific Humidity, wind data , geopotential height, was used to calculate moisture flux for LREs, proxy sounding data which were verified using sounding data at Cape Town International Airport from the University of Wyoming (http://weather.uwyo.edu/upperair/sounding.html). ERA-Interim data along with SAWS synoptic charts and NCEP reanalysis data was also used to determine LRE types from 1979-2019. Evapotranspiration data was also plotted using ERA-Interim.

ERA5 reanalysis data was used to calculate differences in physical variables between anomalously wet and dry composite seasons. Wind data was used to calculate the wind field around the SWC including the wind cross sections. Along with ERA5 wind data, specific humidity was also used to calculate moisture flux. Geopotential height and mean sea level pressure anomalies for dry and wet composite seasons were plotted. Moreover, ERA5 surface temperature, cloud cover and 10m wind speed data in Chapter 5 was considered in order to establish whether temperatures also respond to wet summer seasons. The storm track data taken from Gramcianinov et al. (2020) used in Chapter 6 was calculated using ERA5 as well. ERA5 SAM data was also considered and ZW3 was also calculate using ERA5 reanalysis data.

3.3 Sea surface temperature data

Optimum Interpolation version 2 sea surface temperature (OISSTv2) data from NOAA (National Oceanic and Atmospheric Administration) with a 1° x 1 ° resolution grid was used to calculate large scale ocean derived indices such as SIOD and SAOD for each bi-month in Chapter 5. For SIOD, the method used by Behera and Yamagata (2001) was considered and for SAOD the calculation method used by Nnamchi et al. (2011) was used. OISSTv2 is freely available on the NOAA Physical Sciences Laboratory website (https://psl.noaa.gov/data/gridded/data.noaa.oisst.v2.html).

3.4 El Niño index

For comparisons to rainfall, El Niño index 3.4 was considered and is freely available on the World Meteorological Organization's (WMO) Climate Explorer website (https://climexp.knmi.nl/). The ERA5 SAM data used was also downloaded from this website.

3.5 Dam level data

Reservoir dam level data in Chapter 4 for the SWC major dams (Theewaterskloof, Voëlvlei, Wemmershoek, Berg River Dam and Steenbras Upper and Lower) was requested from the City of Cape Town (https://www.capetown.gov.za/). This data was then cleaned up in order to compare dam levels during each LRE

Chapter 4: The importance of large summer rainfall events in drought mitigation over the South Western Cape, South Africa

This chapter address the questions listed below and represent the work as a published paper in the Journal of Hydrometeorology:

De Kock, W.M., Blamey, R.C. and Reason, C.J.C., 2021. Large summer rainfall events and their importance in mitigating droughts over the South Western Cape, South Africa. Journal of Hydrometeorology, 22(3): 587-599. https://doi.org/10.1175/JHM-D-20-0123.1

- Which rainfall bearing systems contribute to rainfall in the SWC during the extended summer?

- How is rainfall in the SWC distributed during the summer half of the year and which months are the driest on average?

- What is the interannual variability of rainfall during the summer half of the year?

- Do summer LREs make a significant contribution to summer totals and can they mitigate against the impacts of extended winter droughts?

Abstract

Although the South Western Cape receives most of its rainfall between May and September, there are substantial rainfall events in some summers. These events are of interest in themselves as well as for their possible role in mitigating the frequent winter droughts that the region suffers from. Most recently, greater Cape Town suffered a devastating drought during 2015-2018 known as the Day Zero drought due to the high risk of urban areas running out of piped water supply. Estimated data from the City show that major dam levels in the South Western Cape increased more than 1% in some cases after large rainfall events (LREs) in the summer of 2018/19. This increase is significant as dam levels often decrease by several % per month during the hot summer. In this study, LREs over the South Western Cape during the summer (October – March) are investigated together with dam level data.

Most summer LREs result from atmospheric rivers (ARs) or cut-off lows (COLs). ARs have not been previously studied in the South African region except for one study for winter which showed they are responsible for almost all the heavy rainfall events in the Western Cape. Although COLs are most common in the transition months, they can also occur in mid-winter and summer. COLs tend to last longer and cover larger areas than ARs which typically yield relatively short bursts of intense rainfall mostly concentrated around Greater Cape Town. After each summer LRE, average dam levels increase by up to 5% suggesting they are very important for drought recovery. In particular, summer LREs following the anomalously dry winters of 1980, 1984, 2003, 2004 and 2015-2018 played an important role in mitigating those droughts.

4.1 Introduction

The South Western Cape of South Africa, like other Mediterranean climate regions (southwestern Western Australia, southeastern South Australia, southern Europe, Morocco, central Chile and California) is mainly a winter rainfall region. Containing South Africa's second largest city of Cape Town, it occupies a small but highly economically and agriculturally productive part of the country, which apart from this region, is summer rainfall dominated. However, rainfall in the South Western Cape during the extended winter (May-September) is highly variable on intraseasonal, interannual and interdecadal scales (Reason et al., 2002; Reason and Rouault, 2002; Burls et al., 2019) and so the region frequently experiences drought. Such droughts here can become multi-year in nature if after a below average winter, the summer dry season is followed by yet another year of poor winter rains as occurred most recently during 2015-2018. The region is highly mountainous, with numerous rain shadow areas, and thus average rainfall is largely determined by topographic orientation to the South Atlantic coast, distance from this coast and altitude.

Most of the South Western Cape's rainfall is brought about by cold fronts associated with extra-tropical cyclones passing to the south of the country (Tyson and Preston-Whyte, 2000; Reason et al., 2002; Burls et al., 2019). Occasionally, such cyclones are further north than usual and more intense sometimes leading to cut-off lows (COLs), which occur most frequently over South Africa in October and April (Singleton and Reason, 2007a; Favre et al., 2013). COLs are characterised by a cold-cored, upper level (around 500 hPa) low pressure system which has been displaced from the main mid-latitude westerly flow (Nieto et al., 2008). In the cases affecting South Africa, a trough is cut off in the mid to upper troposphere from its source to form a closed low typically over the South Atlantic which then tracks towards South Africa. These systems have also been known to bring considerable amounts of rainfall to the Western and Eastern Cape of South Africa (Singleton and Reason 2006, 2007b; Favre et al., 2013; Molekwa, 2014) as well as to other regions with similar climates such as the Mediterranean and California (Nieto et al., 2005; 2008).

In winter, Atmospheric Rivers (ARs) also contribute to rainfall in the Western Cape (Blamey et al., 2018) and typically yield large amounts. These authors showed that ARs were linked to 8 of the top 9 heaviest winter rainfall events over the Western Cape since 1979. ARs are long (>2000 km) narrow plumes of moisture feeding into mid-latitude regions from the tropics (Newell et al., 1992; Zhu and Newell, 1998; Gimeno et al., 2014). These narrow plumes of moisture are mainly located in the lower atmosphere and are associated with strong winds and widespread rain,

particularly in regions with strong topography (e.g. Neiman et al., 2002; Ralph et al., 2004; Rutz et al., 2014). ARs are generally defined as areas that exceed a specific threshold in vertically integrated water vapour transport (see review by Gimeno et al., 2014). Other Mediterranean climate regions which experience ARs include the Iberian Peninsula (Ramos et al., 2015; Eiras-Barca et al., 2016; Gimeno et al., 2016) and southern California (Ralph et al., 2013; Dettinger et al., 2011). However, to date there has been no study of ARs anywhere over southern Africa for any season apart from the winter study for the Western Cape by Blamey et al. (2018).

COLs and ARs are less frequent contributors to winter rainfall over the South Western Cape than the relatively weak cold fronts which can pass over the region 1-3 times per week at this time of year but they often lead to more intense rainfall than fronts. Changes in the frequency or the intensity (sometimes via shifts in tracks) of rain bearing systems or in both of these factors can lead to severe drought in the region such as that which happened during the recent Day Zero drought in greater Cape Town between 2015-2018 (Sousa et al., 2019; Burls et al., 2019). A tendency towards early winter drying over the South Western Cape is another serious problem facing the region (Mahlalela et al., 2019). Given the strong rainfall seasonality and the tendency of the region to frequent winter drought, it is of interest to investigate whether occasional large rainfall events (LREs) during the generally dry summer half of the year are able to significantly mitigate severe winter droughts before the onset of the next winter rains and, if so, whether these LREs are mainly due to COLs or ARs.

4.2. Data and Methodology

Daily rainfall data were obtained from 27 South African Weather Service (SAWS) stations for 1979-2019 (see **Fig. 4.1a**). To reduce any risk with inhomogeneity in the data, all data is run through a cleaning process after Durre et al. (2010). Only stations which had at least 99% valid data throughout the 40-year period are used. To address the question of whether summer LREs can help mitigate a pre-existing winter drought, a sub-region for analysis was defined based on the major water supply dams for greater Cape Town and associated drainage basins (hereafter referred to as the South Western Cape; red box in **Fig. 4.1a**). In addition, a climatology of evapotranspiration during the extended summer (ONDJFM) was also plotted using ERA-Interim data to highlight the summer aridity. **Fig. 4.1b** shows the locations of these supply dams in relation to the city of Cape Town along with the region's topography. Both the number of rainy days (> 1 mm) and the mean total rainfall per dry season (ONDJFM) was analysed for each station. This definition of a rainy day is consistent with previous studies on rainfall variability in the region

(Burls et al., 2019) and with what constitutes a dry spell in southern Africa (Usman and Reason, 2004).

To define summer LREs, the identify and rank method for extreme rainfall events was used as initially proposed by Hart and Grumm (2001) and later adjusted by Ramos et al. (2015, 2018) for the Iberian Peninsula and South Western Europe. This method considers both the intensity of the event in terms of rainfall volume as well as the area covered by each event. The monthly average rainfall was calculated for each station and the 95th percentile determined. The mean anomaly (M[mm]) was then calculated for each of the events using the rainfall amount at each station. The fraction of stations that show a positive LRE for that area was then calculated as a percentage over the sub-region (N[%]). It was then possible to quantify the intensity and area covered for each LRE as:

$$R = M \times N$$

Each identified LRE has an R value with units mm-% which is an integrated measure of rainfall intensity over the region. M includes all rain days within the LRE for those stations exceeding the 95th percentile. More LREs were identified but these are either localised within the SWC and/or have very little impact on dam level increases.

Once the dates of the LREs are identified, their contribution to total seasonal rainfall is considered for each case. The percentage contributions of the largest LRE during the ONDJFM season were calculated for each year by obtaining the maximum rainfall amount across the sub-domain over the total rainfall for the season. A total of 75 events were calculated to have rainfall above the 95% threshold. Of these 75 LREs, a top 20 subset was created (**Table 1**) and the associated rain-bearing synoptic systems identified as well as their intraseasonal and interannual variability.

ERA-Interim reanalysis data (0.75°horizontal resolution) (Dee et al., 2011) were used to calculate the moisture flux (Q) of these rain-bearing systems at the 850hPa and 500hPa level for the AR and COL event respectively as the product of the horizontal wind and the specific humidity at that level. Due to limited radiosonde data available from Cape Town International Airport, pseudo-soundings were created from ERA-Interim reanalysis data from the nearest grid point (33.33°S, 18.28°E). ERA-Interim has been proven to be useful in creating proxy soundings which compare well with in situ measurements (Poli et al., 2010; Kishore et al., 2011; Jakobson et al., 2012).

Dam level data for the 6 major supply dams (Theewaterskloof, Voëlvlei, Wemmershoek, Berg River Dam and Steenbras Upper and Lower) for greater Cape Town were obtained from the South African Department of Water and Sanitation. To directly compare the effect of the top 20 LREs on dam levels and their potential for mitigating against drought, the dam levels were determined prior to and after occurrence of each LRE. The percentage increases were computed in proportion to dam volume so that the contribution of each dam to the total available water for greater Cape Town is weighted appropriately. Note that the Berg River Dam was only established in 2009, while Wemmershoek and Steenbras Lower dam level records start from 1989 and Steenbras Upper from 1993. The largest two dams of Voëlvlei and Theewaterskloof which make up 72% of total dam volume have records for the full 1979-2019 period.

4.3. Intraseasonal variability in LREs

Fig. 4.2 plots the average extended summer rainfall for the 27 weather stations across the South Western Cape as well as the number of days receiving at least 1mm of rainfall. Similar to the main winter rainy season, the seasonal totals are strongly influenced by topography, distance from the ocean and, to lesser extent, latitude. The latter factor is more evident along the full west coast of South Africa where conditions change from semi-desert north of about 33°S to hyper-arid in the Namib Desert which extends north of about 30°S along the coast up to southern Angola. Subtropical subsidence is stronger north of 30°S which, together with the upwelling favourable southerly winds driven by the South Atlantic Anticyclone, lead to very cold SSTs which further promote coastal aridity. Largest summer totals (200-300mm) occur near the mountains in the far south of the region (Overberg) while in the Greater Cape Town area (33.8°-34.2°S and 18.2°-18.6°E), two stations on the windward side of the Table Mountain chain (South African Astronomical Observatory and Kirstenbosch) also receive relatively high amounts (150-200 mm) on average. The number of rainy days is also highest in these regions (20-30 and 15-20 days respectively out of a maximum possible of 182 days). By contrast, on average the northern stations (32.9° - 33.6°S) are much drier (20-80 mm) with the number of rainy days ranging from 2-7 across this region.

Fig. 4.3 shows the number of LRE over the last four decades as well as the percentage contribution that the wettest of these for each summer made to the total summer rainfall for that year. It is clear that there were more LREs during 1979-1995 than for the more recent period since 2010. Several of the summers show no LREs in the top 75 whereas 1980/81, 1984/85 and 1995/96 experienced 6 or more out of the top 75. If the top 75 were equally distributed during 1979-2019, then close to

2 LREs per summer would be expected. Several summers with a large number of LREs (1980/81, 1984/85, 1998/99) follow anomalously dry winters. These winters (standard deviation of at least 0.5 below the mean) are marked with a red star in (**Fig. 4.3b**). On average, the strongest LRE can typically account for about 20% of the total summer rainfall (**Fig. 4.3b**) but this can increase to over 35% in some cases such as in 1998/99 and in 2004/05. In the case of the recent 'Day Zero' drought of 2015-2019, summer 2016/17 and 2018/19 each contained 1 LRE which respectively contributed about 29% and 22% to the summer total. Thus, this drought would have been even more severe without these 2 LREs. The percentage contribution of the wettest LRE to the extended summer total varies more evenly through the record with no apparent clustering towards any particular sub-period during 1979-2018. The summers of 1998/99 and 2004/05 in which the strongest LRE contributed more than 35% of the total summer rainfall are also seasons that follow dry winters (**Fig. 4.3b**). As expected, the wetter summers with the largest number of LREs (1980/81, 1984/85, 1994/95) show a lower percentage of seasonal rainfall contributions from their largest LRE.

Standardised rainfall anomalies in summer rainfall are plotted in **Fig. 4.4a** from which it is evident that some but by no means all of the wetter summers match up with those with more LREs in the top 75. For example, the slightly dry summer of 1979/80 has an average number of LREs (2). On the other hand, the wettest summer of 1980/81 has the second highest number of LREs (6) whereas the summer with the highest number of LREs (7 in 1984/85) is the second wettest. These differences result because of the relative strength of each LRE as well as the number of other days which received rainfall in a summer but not strong enough to be counted as a top 75 LRE. 1979/80 has neither of its events in the top 50 while 1980/81 has 4 of its 6 LREs in the top 50 (ranked 36th, 34th , 23rd and 1st respectively). Also, both 2016/17 and 2018/19 had below average rainfall but 1 LRE in the top 75 reinforcing the suggestion that the 'Day Zero' drought impacts would have been worse had these LREs not occurred. Overall, there is a decreasing trend in summer rainfall of 142 mm/decade, statistically significant at $p < 0.001$. With the exception of the very wet 2013/14 summer which had 4 LREs in the top 75, the entire decade from 2009/10 onwards shows below average summer rainfall. The decreasing tendency in summer rainfall is consistent with recent increases in mean sea level pressure over the mid-latitude South Atlantic (Zilli et al., 2019) and with the poleward migration of the subtropical highs under global warming (Scheff and Frierson, 2012; IPCC, 2013; Sousa et al., 2018) which has been found to be responsible for an early winter drying tendency over a larger region of western South Africa in recent decades (Mahlalela et al., 2019). A poleward shift in the subtropical highs in the summer and the upper-level jet stream means that extratropical cyclones which make their way across the mid-latitude South Atlantic

are displaced further south and the associated cold fronts are weakened reducing any rainfall over the SWC.

Fig. 4.4b shows the number of ARs and COLs experienced in each season. Weather system identification was done based on previous literature as well as looking at sources of moisture, synoptic charts, outgoing longwave radiation (OLR), satellite imagery and vertical profiles derived from ERA-Interim data. Although they account for 68 out of the top 75 LREs, there are occasional cases which are neither an AR nor a COL. For example, 1 of 3 LREs in 1998/99 resulted from a west coast trough (WCT) extending down the west coast with a cold front present to the south of Cape Town. For the top 20, 12 result from COLs and 8 from ARs (**Table 4.1**). The interannual variability of COLs in the top 75 is much greater than is the case for ARs. For the latter, ARs most typically contribute 1 event to a given summer when there is an LRE with only 1984/85 and 1989/90 showing 2 and 1995/96 experiencing 4 ARs. On the other hand, COL numbers per year with LREs range from 1-5 with only 9 out of 25 summers with LREs having only 1 COL. Singleton and Reason (2007a) suggested that annual COL numbers over the subtropical southern Africa region and neighbouring oceans (10°-40°E, 20°-40°S) were higher during La Niña events but this does not appear to be the case here with only the La Niña summers prior to 1998 tending to show increased COL frequency. On the other hand, there are reduced COL numbers during the mature phase El Niño summers of 1986/87, 1997/98, 2009/10, 2015/16 but not during 1982/83 or 2002/03.

Fig. 4.5a shows the occurrence of the top 75 and top 20 events calculated for 1979-2019 for each month from October to March. October and March are the months with the highest frequency of LREs in the top 75 events and February the least. For the top 20, October and November show the most LREs. Based on available satellite imagery, synoptic charts, OLR and circulation data, the weather systems associated with the top 75 were identified as COLs (46) ARs (22) or other (7). These 7 other events are clearly neither a COL nor an AR; in three cases they are WCTs but in the other four the synoptic situation is more complex and it is difficult to clearly determine a single dominant weather system. WCTs are systems that develop from a deepening of the easterlies over Namibia to extend down over the South Western Cape and can produce significant rainfall if the accompanying tropical air is sufficiently moist and unstable (Tyson and Preston-Whyte, 2000). Sometimes this deepening trough links up with a westerly disturbance passing south of South Africa to form a tropical - extratropical cloud band.

COLs are most frequent in October and March consistent with their tendency to be most common over South Africa in the transition seasons (Singleton and Reason, 2007a; Favre et al., 2013) but

with a mid-season peak in January when ARs are least frequent (**Fig. 4.5b**). ARs also show weak peaks in October and March whereas the small number of WCTs and other synoptic types are more or less equally distributed. Since ARs have only previously been documented over South Africa in winter (Blamey et al., 2018), it is of interest to note their occurrence during even high summer months of December – February. From **Figs. 4.4b**, **4.5b** and **Table 4.1**, it is clear that they are the second most important contributor to summer LREs over the region.

4.4. Moisture fluxes and vertical characteristics associated with LREs

Since the previous section has shown that 88% (100%) of the top 75 (20) LREs over the SW Cape are associated with either a COL or an AR, it is useful to consider the moisture fluxes and vertical characteristics associated with these two rather different types of weather system which tend to not only differ in their spatial rainfall distributions but also in their lifespan over the region (**Table 4.1**). As examples of each type, the largest cases of each rain bearing system are chosen for analysis. Rain bearing systems such as COLs and ARs differ intrinsically in their source, genesis and propagation. Two case studies have been selected based on showing the largest R value (**Table 4.1**) for a COL and AR respectively; namely, the COL of 22 January 1981 (**Fig. 4.6a-c**) which lasted 4 days over the region and the AR of 10 November 2008 (**Fig. 4.6d-f**) which lasted 2 days. The former led to devastating floods and more than 100 lives lost in the Laingsburg region on 25 January 1981 (Taljaard, 1985). The AR event caused 2 deaths and R1.139 billion in financial losses (de Waal et al., 2017).

Several important differences can be noted between the COL and the AR event in **Figs. 4.6-4.7**. Firstly, the AR involves a narrow plume of rain-bearing moisture impacting the region and associated cold front leading to a sharp drop in near-surface temperatures and increase in moisture between 9 and 10 November 2008 (**Fig. 4.6d-f**) as a warm dry continental air mass is abruptly replaced by a cool marine air mass. For the AR, a weak low-level inversion becomes apparent on 11 November 2008 the day after the wettest day and dew point temperatures quickly decrease from temperature above the inversion base at 900 hPa reinforcing the low-level nature of this synoptic system as the signature of the event weakened over the sounding location. As evident from the daily moisture flux plots (**Fig. 4.7d-f**), easterly winds from the western interior which adiabatically warm as they descend > 1000 m from the escarpment to the coast (Reason and Jury, 1990) were replaced by the cool moist northwesterlies of the AR. Most of the AR was located offshore of the South Western Cape as is typical (Blamey et al., 2018; Ramos et al., 2018).

On the other hand, the COL event shows similar near-surface temperatures throughout with only an obvious low-level moisture increase on 22 January 1981 consistent with the large extent of cloud cover and more gradual air mass changes associated with these weather systems. **Fig. 4.7a-c** shows a low of roughly 1500 km diameter and associated stratus cloud (not shown) advecting air over a large ocean fetch south of South Africa before impacting the South Western Cape thereby helping to keep low level temperature variations small. On this day of heaviest rainfall from the COL, high levels of convective available energy (CAPE) are apparent in the mid-troposphere. The COL persisted over the region for four days with rainfall recorded as late as 25 January 1981 over the study region and particularly in the Laingsburg region (about 100 km east of the eastern boundary of the red box in **Fig. 4.7**) where much devastation and loss of life occurred on the 24-25th (Taljaard, 1985).

Fig. 4.7 also shows different moisture sources between the COL and AR events. In the case of the COL, there is offshore flow of warm dry air over eastern South Africa which picks up moisture from the warm Agulhas Current which flows along the east and south continental shelf of South Africa. This moisture circulates over the Agulhas Current retroflection region south of the South Western Cape before broadly impacting the western landmass. This moisture flux pattern is very similar to the COL event that caused flooding over the eastern half of the red box in **Fig. 4.7** as well as an adjacent area further east in March 2003 and which was modelled by Singleton and Reason (2007b). On the other hand, the AR event (**Fig. 4.7d-f**) appears to get moisture from the far western tropical Atlantic on the first day (9 November 2008) as well as from the midlatitude South Atlantic due to a migratory anticyclone near 15°-45°W 30°-40°S. On the next day, there is an increase of moisture originating from South America and the tropical western Atlantic, consistent with the conceptual view of Ramos et al. (2018) but still with a little coming from the central midlatitude South Atlantic. The AR is no longer evident by 11 November, although the South American / tropical western Atlantic source remains. The key characteristic of the AR is the strong northwesterly wind which because of their tropical source leads to much higher magnitudes of moisture flux during a single 24 hour period than the COL but which do not impact the South Western Cape for long. Northwesterly winds may also occur at the beginning of a COL event affecting the region (**Fig. 4.7a-c**) but because their moisture source is more local and not tropical, the magnitude of the flux is less. However, the quasi-stationary COL lasts longer and hence can produce a large accumulated amount of rainfall over the South Western Cape. Thus, COL and AR events differ in duration (**Table 4.1**) and moisture source; the COL event originates from mid-latitudes whereas AR events obtain moisture from the tropics or sometimes subtropics. The COL then propagates towards southern Africa but may still receive some moisture from lower latitudes

as is weakly evident in **Fig. 4.7c**. It is important to note that the differences in COL and AR events relate to the vertical level. COLs are deep convective systems whose signature is most obvious above 500 hPa although they can sometimes have a near-surface meso-low present near the heavy rainfall (Singleton and Reason 2006, 2007b). On the other hand, ARs can be most clearly seen in the lower troposphere particularly when one is considering the region of heavy rainfall and immediately upstream thereof.

There are also subtle differences in the spatial distribution of rainfall across the South Western Cape box during COL and AR events (**Fig. 4.8**). For COLs, the heaviest rainfall tends to be more in the southeastern quadrant on the leeward side of the coastal mountains consistent with the larger scale of these systems and the more southerly nature of their moisture flux (**Fig. 4.7a-c**). Note that rainfall east of 19.5°E is not plotted; however, the distribution is consistent with previous studies of COL events over the broader Western Cape region (Singleton and Reason, 2007b; Favre et al., 2013). On the other hand, the AR events show larger rainfall contributions near Cape Town (associated with Table Mountain) and near the crests of the coastal mountains with relatively less in the far southeast compared to the COL events. ARs tend to provide more rain to the far south western parts of the region due to the lower atmosphere being saturated. This pattern is consistent with the northwesterly moisture flux incident on the topography (**Fig. 4.7d-f**) and noted by Blamey et al. (2018) for winter AR events. **Fig. 4.9** reinforces these results since it shows that stations in and near Cape Town have a probability > 60% of receiving rainfall during the AR events whereas this drops to about 30% during COL events. The extreme south western part of the region shows a larger probability of AR rainfall. Dams supporting the Greater Cape area therefore have a greater chance of recovery from AR events than from COLs (**Fig. 4.10**). The likelihood of rainfall caused by COL events increases in the southeast of the region so that catchment areas in the Overberg region receive more rain. This increase in rain further eastward can be seen in dam volume increases in Steenbras Upper and Lower dams (**Fig. 4.10**). Thus, the COL contribution to the Steenbras dams is almost double that of ARs. In the case of the 1981 COL event, **Fig. 4.7b-c** show relatively large amounts of moisture flux near the south coast and also east of the red box consistent with the general indication suggestion from **Figs. 4.8-4.9** of greater COL rainfall over the southeastern regions than further west.

4.5. LREs and Dam level analysis

Most of the rainfall events that occur during the extended summer months are brief in nature and only produce a few mm. Thus, they do not lead to much relief to any pre-existing drought nor do

they raise dam levels since their moisture is quickly taken up by the parched soils and high evapotranspiration (**Fig. 4.1a**) under intense solar radiation at this time of year. However, the LREs considered here (> 20 mm) which occur in some summers are particularly meaningful in catchment areas over river basins and water reservoirs and may provide some drought relief. Rainfall increases around water catchment areas that supply dams is very important as water consumption in the greater Cape Town urban area increases substantially during the extended summer months (Pienaar et al., 2017). Fire risk on the nearby mountain slopes is also much higher from about October and peaks in the late summer.

Theewaterskloof, Voëlvlei and Berg River dams are the three largest dams supplying water to the South Western Cape and in particular the >4 million inhabitants of the greater Cape Town area. **Fig. 4.10** shows that ARs contribute more than COLs to the water volume contained in these dams, as well as in the smaller Wemmershoek Dam, consistent with their location close to the coastal mountains (**Fig. 4.1b**). The two much smaller dams of Steenbras Upper and Lower are located furthest south and are contributed to more by COLs. From **Table 4.1** and **Fig. 4.11**, it is evident that the most intense LREs are able to increase dam levels by about 1-5% after each event. This is a significant amount since typically dam levels drop by 1.2-1.6 % per week during the dry summer months. Thus, a single LRE can mitigate against up to about 3 weeks of typical water draw down due to human consumption and evaporation off the dams. Furthermore, the rainfall associated with these events will also help the large agricultural areas in the South Western Cape (largely wheat, wine, citrus and stone fruit, sheep) and hence reduce irrigation demand by farmers. However, the timing is also important; if the LRE comes in the early summer it can mean the difference between the authorities having to impose less tough water restrictions than would be the case if there was no significant rainfall until much later in the summer. Thus, the October timing of the LREs in 1984 and 2004 was particularly helpful in mitigating the existing winter drought in those years because the dam levels in those Octobers (the first month after the end of the winter rains) was already below 60%. On the other hand, for the January 1981 COL event analysed above, a mid-summer example, the previous winter drought and ongoing dry summer had led to dam levels reaching as low as 32% by the time that COL event was able to increase them by over 4%. In the case of the most recent Day Zero 2015-2018 drought, only 3 LREs occurred during those summers and none was large enough to fall within the top 20 although the 2016/17 and 2018/19 LREs did make an above average percentage contribution to the below average rainfall recorded during those summers (**Fig. 4.3b**). Thus, had these 3 LREs not occurred, the severity of the Day Zero droughts impacts would have been worse.

4.6. Discussion and Conclusion

The South Western Cape has a Mediterranean-type climate with strong rainfall gradients associated with the complex topography of the region and with latitude. Semi-desert conditions are found in the coastal plain about 150-200 km north of Cape Town as well as about 100 km to the east or northeast in the rain shadows on the leeside of the coastal mountain ranges. The main winter rainy season shows great variability in rainfall totals on both interannual (Reason et al., 2002; Reason and Jagadheesha, 2005) and interdecadal time scales (Reason and Rouault, 2002) leading to frequent droughts. The large rise in population in the last three decades has placed ever increasing demands on the water supply dams and made the region more and more vulnerable to drought in a warming climate. Most recently, this problem manifested itself in the 2015-2018 Day Zero drought when the greater Cape Town area came close to running out of potable water in summer 2018 (Sousa et al., 2019; Burls et al., 2019).

To date, there has been little or no work on rainfall variability during the summer half of the year for the southwest region of South Africa. In this study, large rainfall events (LREs), occurring between 1-6 times in the summers are investigated. Such events offer the possibility of relief of the dry summer conditions and mitigating the impacts of pre-existing winter droughts before the onset of the next winter rainy season. This possibility assumes increasing importance with evidence that the early winters are showing a significant drying trend (Mahlalela et al., 2019). The LREs in years such as 1980/1981, 1984/1985, 2004/2005 and 2018/2019 follow particularly dry winters and would mitigate the drought to some extent. Some noticeable events such as the 1981 COL, the 1998 COL, the 2004 AR and the 1984 COL, all of which are in the top 10 largest events, contribute considerably to dam levels. The results presented in this study suggest that each of the 20 largest LREs can increase dam levels by about 1-5%. This amount is significant since under typical summer conditions, the levels drop by about 1.2-1.6% per week on average. Although the top 75 LREs contribute between 10-35% of the total summer rainfall, their importance is enhanced because the intense summer insulation and high solar evapotranspiration potential of the region will quickly eliminate the benefits of the lighter rainfall events.

Of the top 75 LREs, 46 arose from cut-off lows (COLs) and 22 from atmospheric rivers (ARs) with the remainder due to west coast troughs (WCTs) and other synoptic types. Due to the location of the supply dams, ARs appear to make a larger contribution to the region's water supply in summer than do COLs even though the spatial extent of the heavy rainfall tends to be greater for COLs. ARs are also typically shorter in duration (1-2 days) with more intense rainfall at particular

locations near the windward side of the coastal mountains than COLs which can sometimes stall over the region and last for 3-5 days. Although COLs have been previously studied over the region and, more broadly, subtropical southern Africa, with the exception of Blamey et al. (2018) for winter, ARs have not. Thus, this study is the first to show evidence of their occurrence in South Africa during the summer half of the year. An increasing concern is the tendency for ARs to be shifting southwards in winter over the South Atlantic which haver underlying SST and thermodynamic implications (Seager et al., 2010; Sousa et al., 2019). If this were to also occur in summer, which seems plausible given recent increases in sea level pressure over the midlatitude South Atlantic in summer (Zilli et al., 2019) and the projections of tropical expansion and poleward shifts in the subtropical anticyclones (Lu et al., 2009; Lucas et al., 2014; Sousa et al., 2018; 2019), then the likelihood of ARs occurring in summer in future should be reduced. Thus, their important contributions to summer rainfall in recent decades may very well decrease in future.

Tables and Figures

***Table 4.1**: Classification of the top 20 largest events based on their R values within the dam catchment area of the South Western Cape.*

Date	Month	Duration of event (days)	Mean Rainfall Anomaly (mm)	No. of Stations	R - Value	Type	Mean Dam level Before Event(%)	Mean Dam level After Event(%)
1981/01/22	Jan	4	51.39	27	4476	COL	32.2	36.5
2013/11/15	Nov	2	49.04	27	4271	COL	99.3	103.2
2008/11/10	Nov	3	52.1	24	4033	AR	98.7	103.8
2004/10/06	Oct	1	49.56	25	3997	AR	56.5	59.1
1998/12/14	Dec	1	46.66	25	3763	COL	84.7	86.5
2014/01/05	Jan	5	35.22	28	3181	COL	91.9	94
2004/10/20	Oct	3	30.73	29	2875	COL	58.9	60.4
1984/10/04	Oct	2	34.09	25	2749	COL	51.9	54.2
2007/11/20	Nov	6	38.54	21	2611	COL	90.5	93.8
2009/11/07	Nov	4	38.21	21	2588	AR	98.4	102.3
1995/10/24	Oct	1	28.58	22	2028	AR	99.1	101.1
1983/03/07	Mar	1	29.35	19	1799	COL	32.6	33.1
2003/03/22	Mar	3	37.91	14	1712	COL	60.5	61.9
1989/11/17	Nov	1	37.43	14	1690	COL	59.1	59.9
1995/10/11	Oct	1	23.42	21	1587	AR	97.1	99.3
1995/12/17	Dec	2	23.35	21	1582	COL	92.1	93.2
1990/02/19	Feb	2	31.13	15	1506	AR	40.2	41.4
1983/02/01	Feb	1	25.64	18	1489	COL	35.1	35.6
1985/03/14	Mar	2	22.82	20	1472	AR	43.5	44.8
1989/03/28	Mar	3	28	16	1445	AR	32.8	33.5

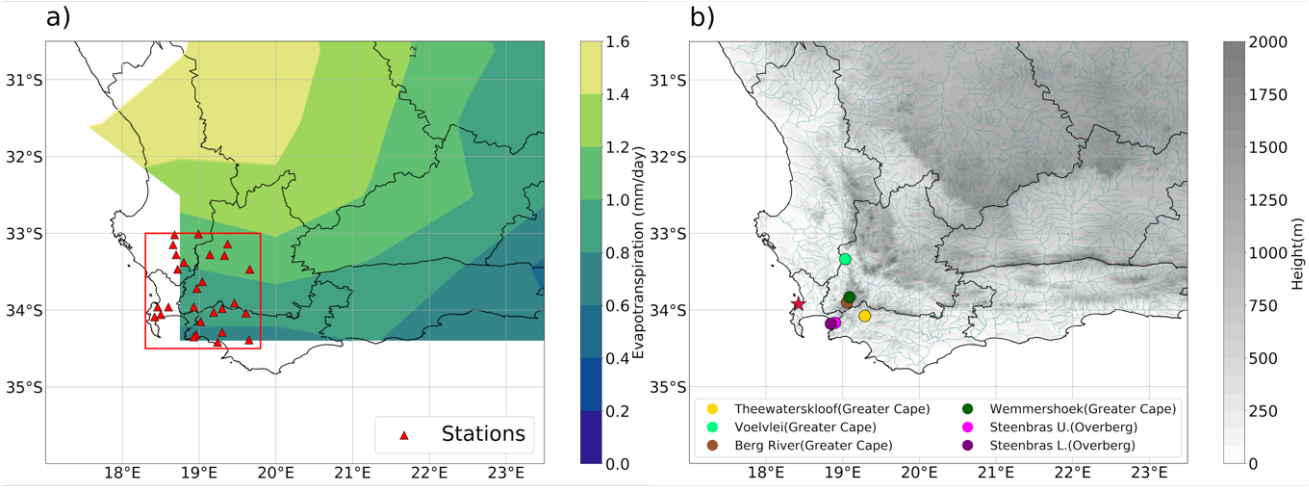

***Figure 4.1**: (a) Mean evapotranspiration of the South Western Cape of South Africa during ONDJFM from 1981-2019. A sub-region of stations (red box, red triangles) is shown closest to major dam locations and drainage basins that feed into them. (b) Indicates the location of the largest dams around the Western Cape in relation to Cape Town (red star) and the topography of the region.*

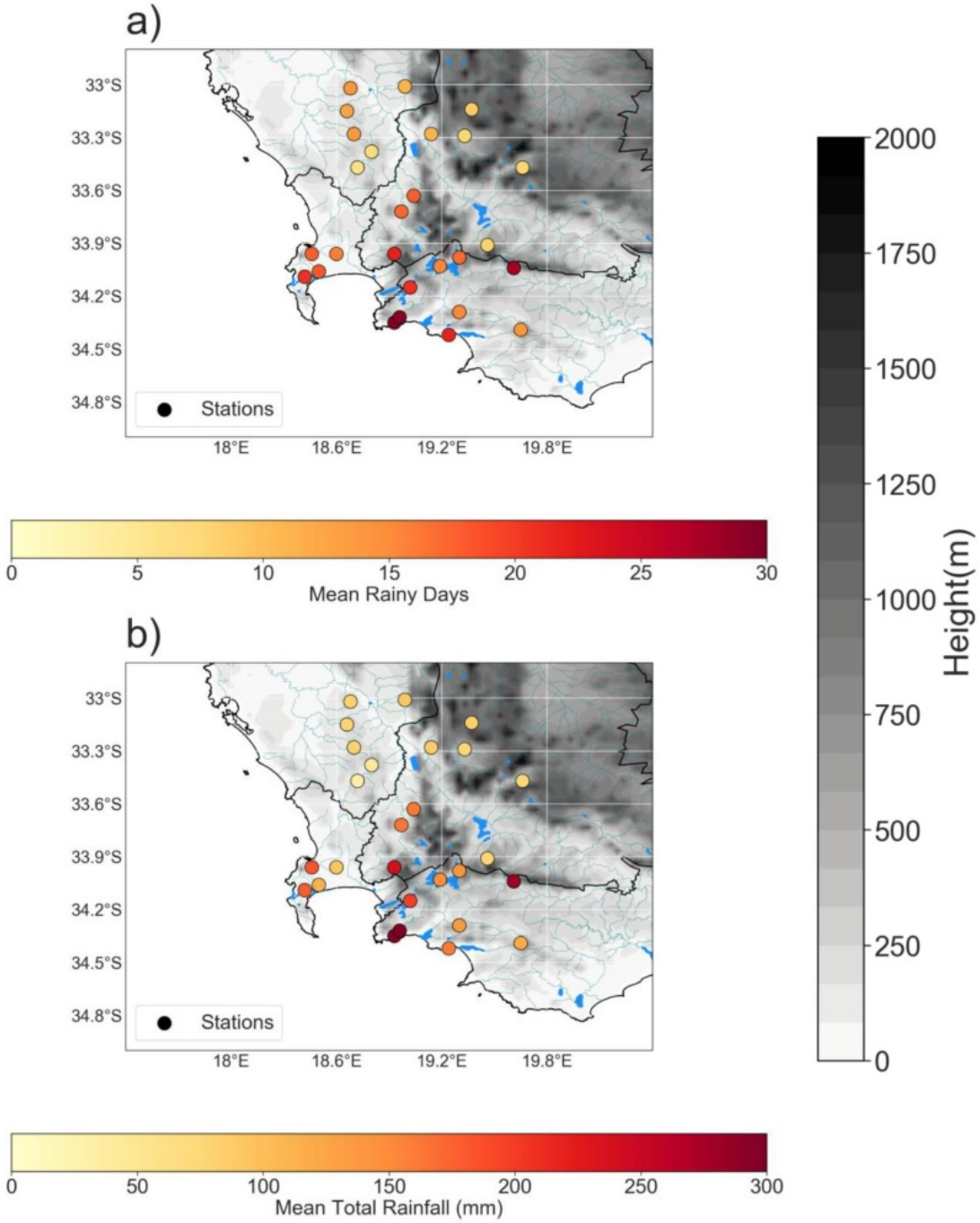

Figure 4.2: *(a) The mean number of rain days during the summer months at the 27 SAWS weather stations across the South Western Cape and, (b) the mean summer total rainfall (mm) at the stations. The topography (m) of the region is depicted by the greyscale background shading.*

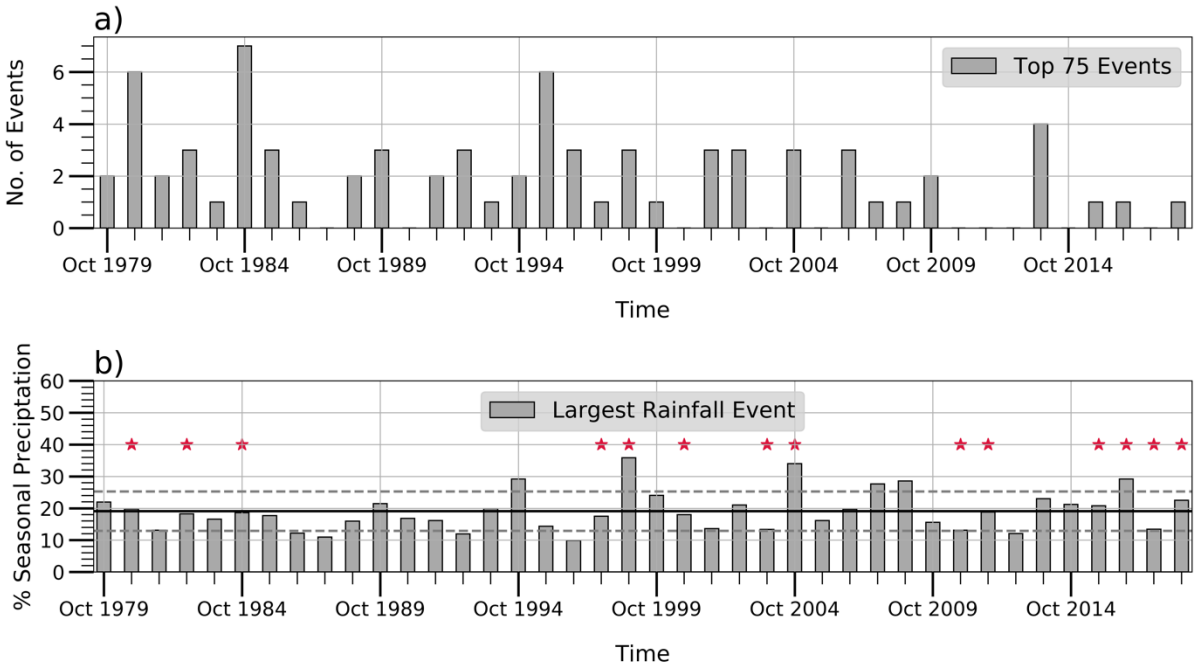

***Figure 4.3**: (a) The number of top 75 LREs per ONDJFM season and (b) percentage contribution of the largest rainfall event per season against total rainfall for ONDJFM across 27 SAWS stations. The red stars in panel b represent seasons following dry winters at least half a standard deviation below the mean.*

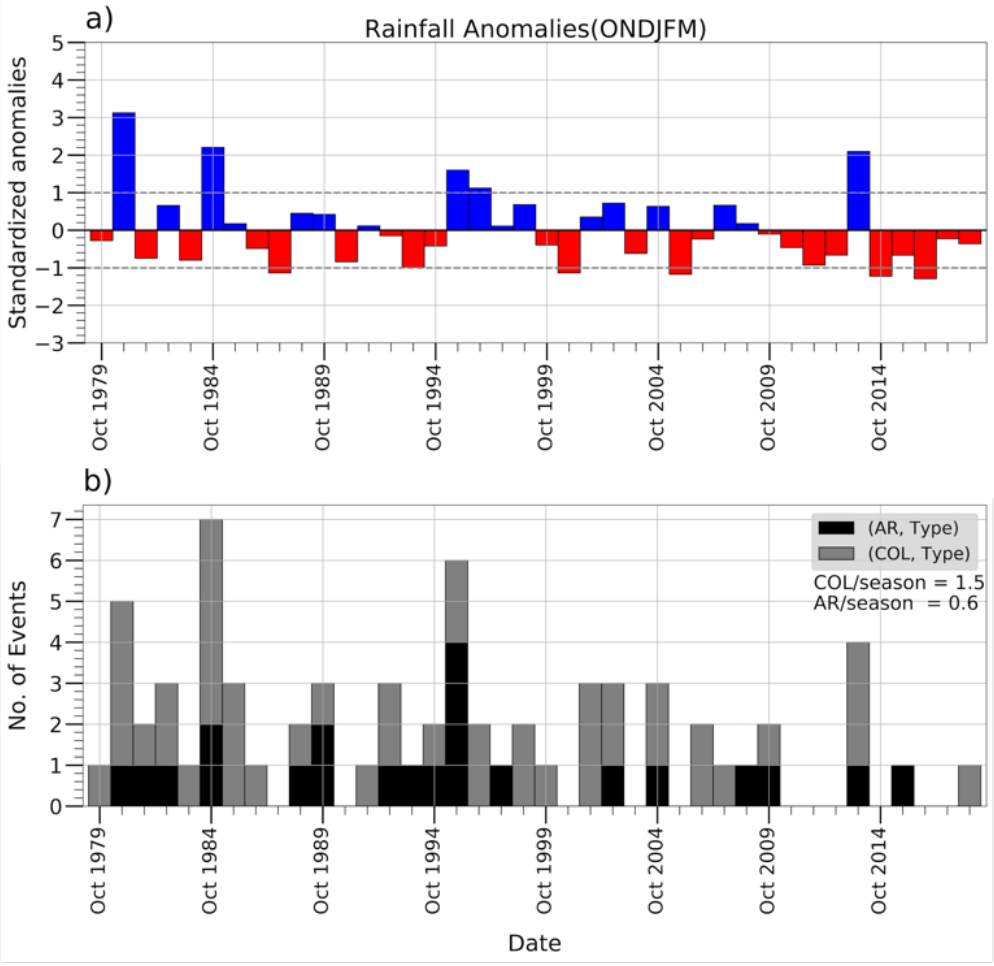

Figure 4.4: *(a) Standardized rainfall anomalies from 1979-2019 for the dam catchment area. (b) Represents the number of COLs and ARs events per season. These events range within the top 75 LREs.*

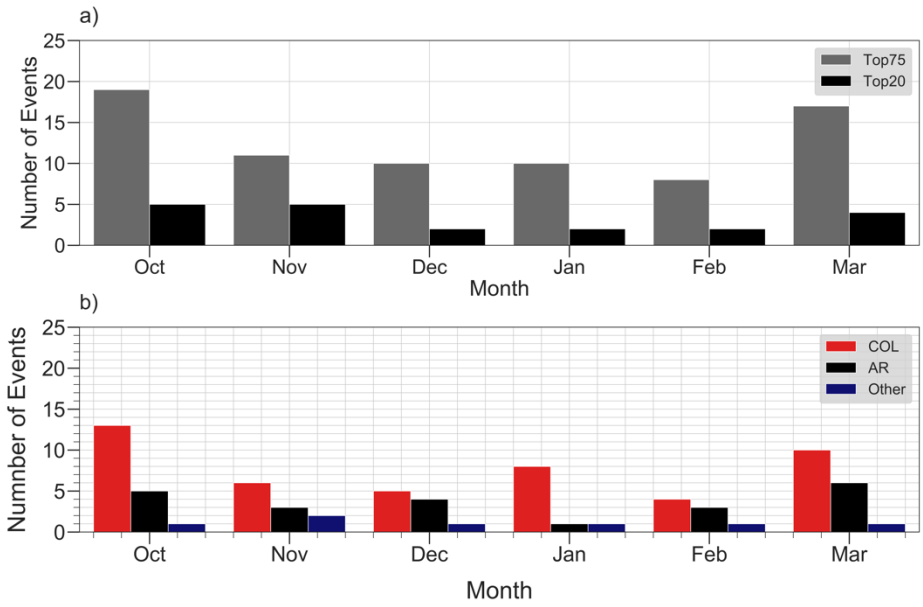

***Figure 4.5**: (a) Monthly totals of the top 20 and top 75 events and (b) monthly totals of the different rain bearing systems, which consists of COLs, ARs and other synoptic types (included in this category are 3 WCTs).*

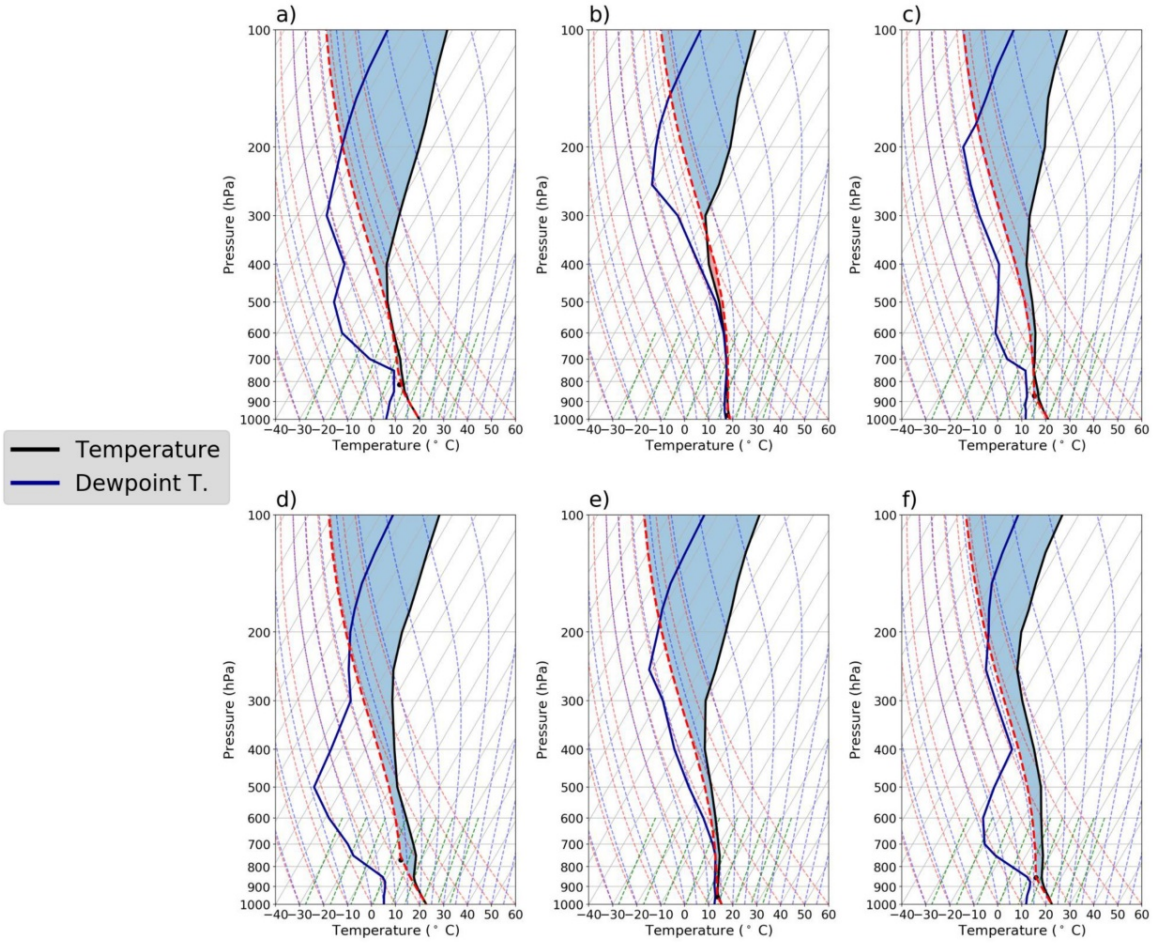

***Figure 4.6**: Proxy sounding data around near the Cape Town International Airport highlighting the differences between (a-c) a COL occurring from 21-23 January 1981 with most rainfall recorded on 22 of January 1981 (b) and (d-f) an AR on 9-11 of November 2008 with most rainfall recorded on 10 November 2008 (e). The red dashed line represents the parcel temperature while the blue shading represents the convective inhibition.*

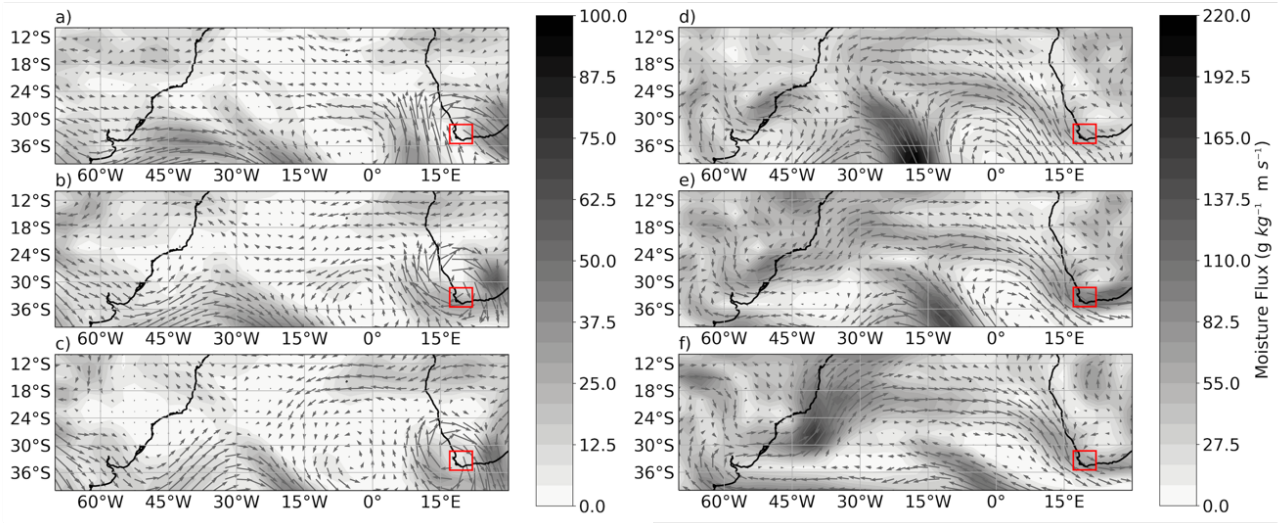

Figure 4.7*: Moisture flux examples around the South Western Cape (red square) during the largest COL and AR events. Panel (a-c) represents a COL occurring from 21-23 January 1981 with most rainfall recorded on the 22 of January 1981(panel b). The snapshots in panel (a-c) are taken at the 500 hPa level. In contrast, panel (d-f) represents an AR on 9-11 of November 2008 with most rainfall recorded on10 November 2008 (panel e). The snapshots of moisture flux in panel (d-f) are taken at the 850 hPa level.*

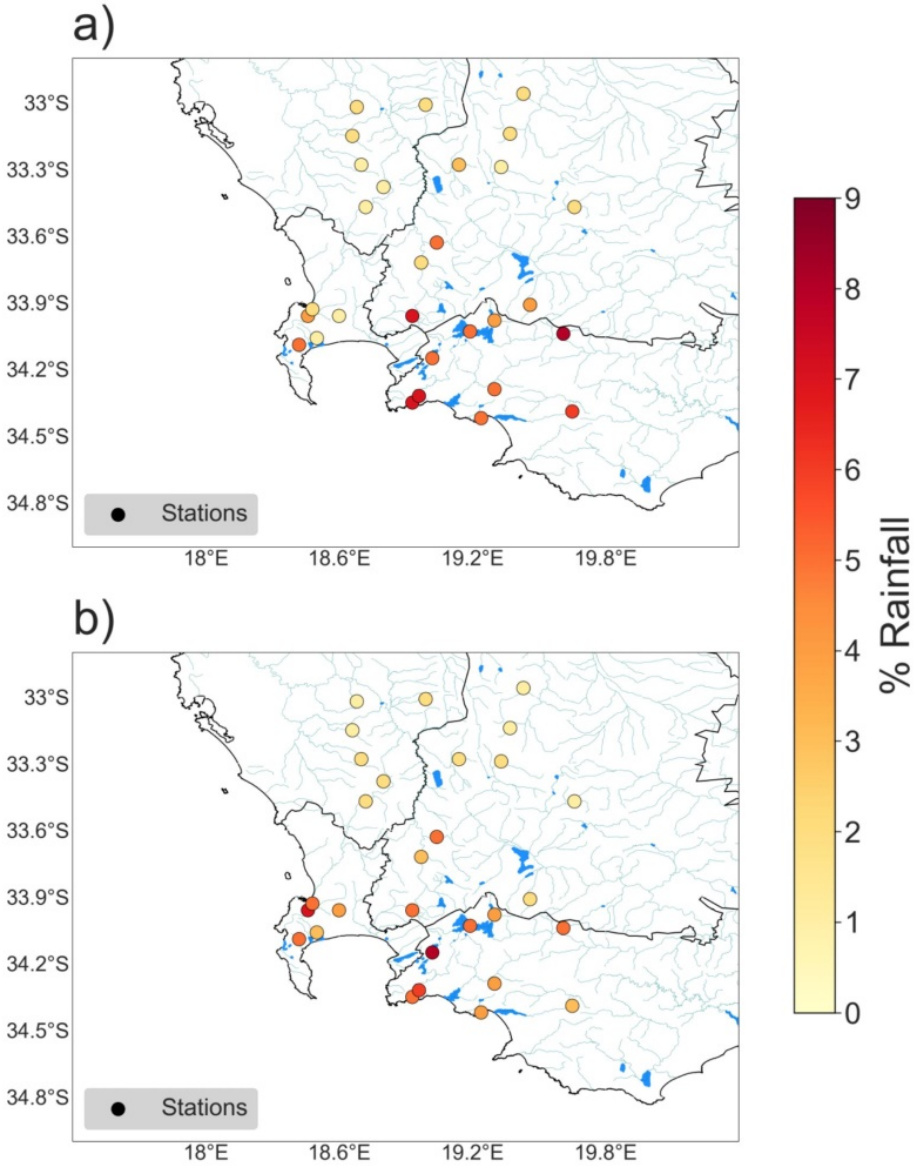

***Figure 4.8**: Average proportion of total rainfall for each rain bearing system across 27 stations in the dam catchment area for (a) during all COLs in the top 75 LREs and (b) all ARs in the top 75 LREs.*

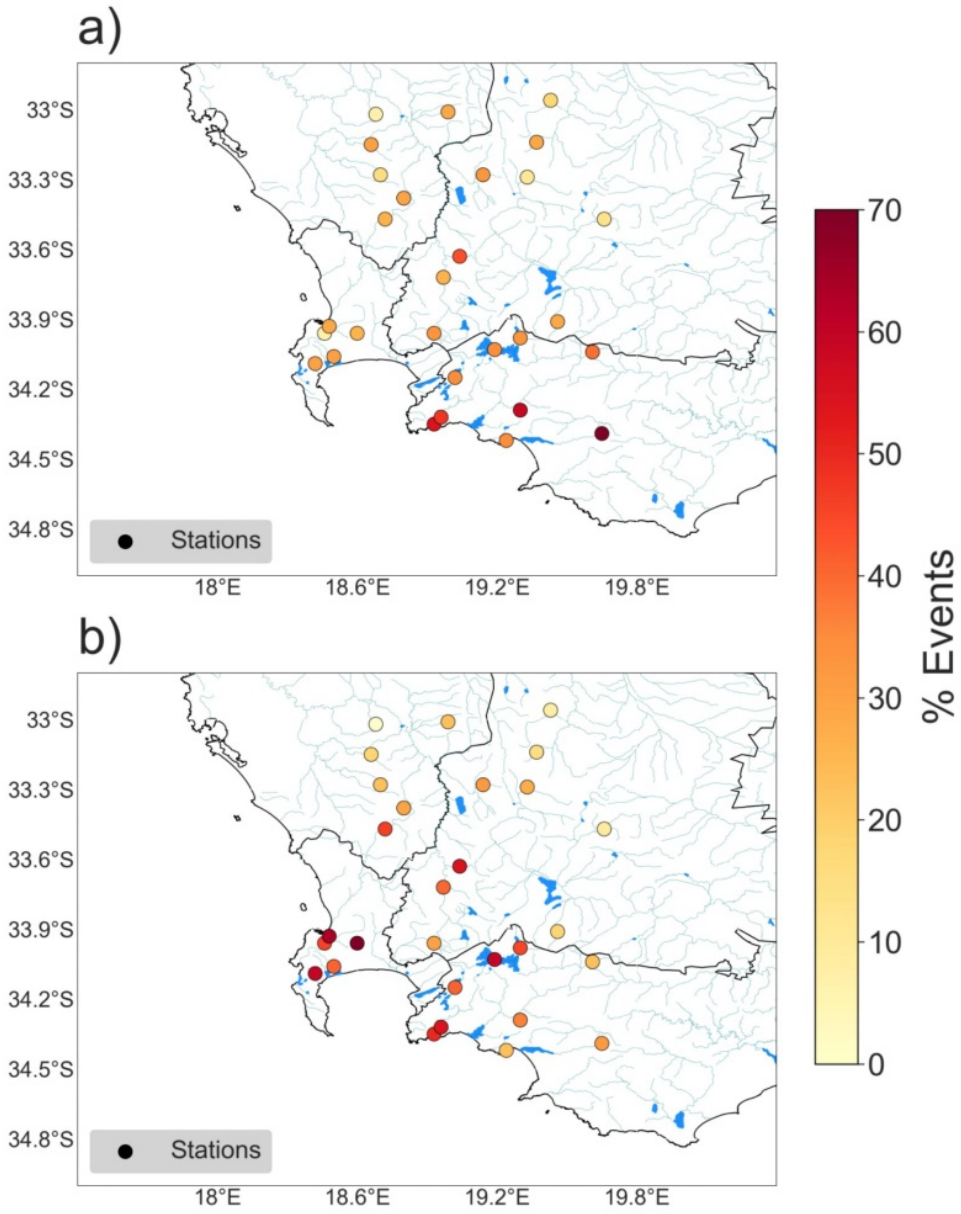

Figure 4.9: *The likelihood of a rainfall event occurring at a particular weather station once in effect for (a) COL system and (b) AR event during the ONDJFM months*

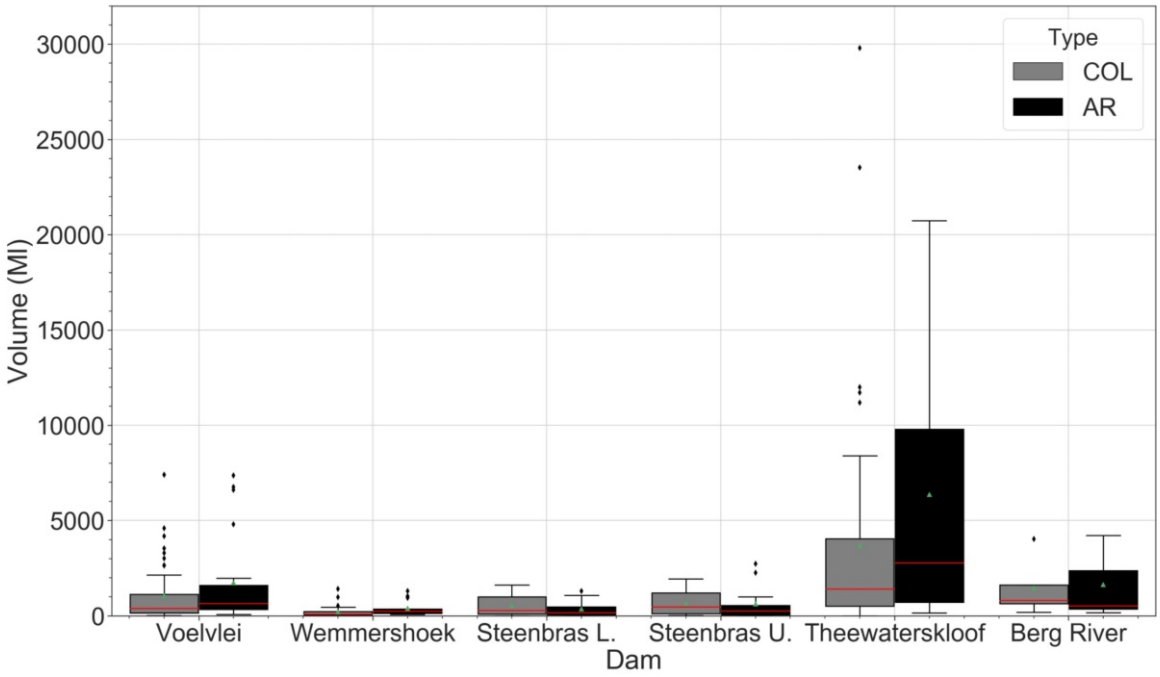

***Figure 4.10**: The contribution of ARs (black) and COLs (grey) to dam volumes of the 6 major dams in the region during the ONDJFM seasons from 1979-2019. The red line represents the median and the green dot represents the mean volume from 1979-2019.*

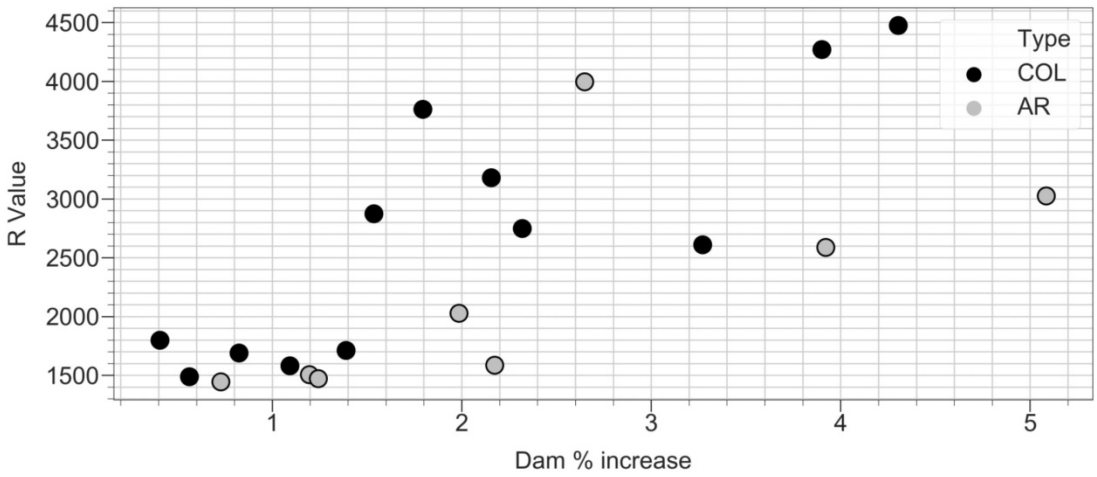

Figure 4.11: *The top 20 largest events during the ONDJFM season and links to how dam levels have increased after each individual event. The x-axis is the percentage increase in dam level and the y-axis is the R value (i.e. magnitude and spatial extent) of the event. The type of rain bearing system is also shown in the form of cut-off lows (black) and atmospheric rivers (grey).*

Chapter 5: Links between extreme hot days and rainfall during anomalously wet summers over the southwestern Cape, South Africa

This chapter addresses the following questions:

- How many wet summers are cooler than average?
- Is there a relationship between anomalies in rainfall and air temperature?
- Is there a relationship between anomalies in rainfall and wind?
- Are LREs associated with cooler seasons?

Chapter Abstract

The southwestern Cape (SWC) is an important agricultural region and experiences most of its rainfall during the austral winter (May-September). Most of the rainfall during the winter and transition seasons arises through cold fronts associated with extratropical cyclones, with atmospheric rivers (ARs) and cut-off lows (COLs) also making important contributions sometimes. Little to no research has been done relating anomalies in temperature to those in rainfall during the extended summer in the SWC. Since the population and economy in the SWC relies heavily on adequate winter rainfall, any failure of these seasonal rains causes significant hardship during the following summer, which climatologically is typically dry with warm to hot temperatures and high insolation. Unusually hot and dry summers lead to increased water consumption and fire risk as well as pose difficulties for agriculture. On the other hand, anomalously wet summers reduce these negative impacts. The previous chapter indicated how some anomalously wet summers can occasionally mitigate the effects of winter droughts in terms of rainfall and dam levels. Here, the potential relationships between these anomalously wet summers and air temperature and wind characteristics are considered.

It is found that summer rainfall totals (mm) are significantly inversely correlated (r=-0.44) with extreme hot days (90% decile). Furthermore, there is a significant increasing trend in the number of extreme hot days during summer (2.8 days/decade). Of the 5 wet seasons, 4 out the 5 wettest and coolest summers exhibit weaker winds over the catchment area and increased cloud cover. More interestingly, all 4 cooler and wetter seasons occur during 1979-2019 with only one season (2013/14) occurring in the last two decades. The latter season showed increased wind speeds and cloud cover. Anomalously wet and cool summers can help reduce the impacts of a below average previous winter rainy season as well as reduce water consumption by agriculture and other large users, thereby offsetting the risk of the following winter being drier than average.

5.1 Introduction

The southwestern Cape (SWC) of South Africa experiences a Mediterranean climate and receives most of its rainfall in the austral winter (May-September). The summer half of the year is typically dry, with warm to hot temperatures, high insolation and occasionally strong winds leading to high evaporation. Winter rainfall is typically associated with cold fronts associated with extratropical cyclones with the bulk of the wettest winters largely influenced by Atmospheric Rivers (ARs) which are low lying filamentous plumes of integrated water vapor (Blamey et al., 2018; Ramos et al., 2019). Cut-off lows (COLs) have also been known to contribute considerably to rainfall totals in the region, most commonly during transition seasons (Singleton and Reason 2007a; Omar and Abiodun, 2020; Barnes et al., 2021; Roffe et al., 2022). However, as shown in the previous chapter, both ARs and COLs can produce large rainfall events in some summers.

The spatial variability in rainfall over the SWC results from local factors such as distance from the surrounding ocean, topographic features, and the tracks of incoming rain-bearing systems relative to the local geography (Blamey et al., 2018; Mahlalela et al., 2019; Omar and Abiodun, 2020). The seasonal variability in rainfall results from the fact that the tracks of westerly disturbances (cold fronts, ARs) are typically much further poleward and weaker in summer with the South Atlantic Anticyclone shifted southeast towards the SWC along with strong subtropical subsidence compared to winter.

Higher summer temperatures coupled with low rainfall totals as well as frequent windy conditions suggest increased evaporation which can have serious negative impacts on dam reservoirs in the region (Botai et al., 2017). Water consumption by both the public as well as irrigated agriculture typically leads to large decreases in usable water in the region (Burls et al., 2019; Mahlalela et al., 2019) during summer. Furthermore, warm, windy, and dry conditions also promote the spreading of wildfires which is not uncommon in the region during summer (Van Wilgen, 1984; 2009; Holmes et al., 2022). Such fires can have devastating impacts on the economy, agriculture, and the population.

Major dam reservoirs are located to the east and northeast of the greater Cape Town urban area (see **Fig. 5.1**). These dams include, Steenbras upper and lower, Berg River, Vöelvlei, Wemmershoek and Theeawaterskloof and provide the vast majority of the SWC population with drinkable water. The catchment area of these dams relies heavily on winter rainfall to replenish them. Droughts are not uncommon in the southwestern Cape (Muller, 2018; Wolski, 2018; Sousa

et al., 2019; Burls et al., 2019) and long and dry summers followed by winters with below average rainfall can lead to multi-year droughts (Mahlalela et al., 2019). Theewaterskloof, the largest dam, decreased to as low as 17.5% during the 'Day Zero Drought' of 2015-2018 compared to the 31% and 53.9% in the preceding years (Muller, 2018).

While chapter 4 has shown how large rainfall events during some summers can help mitigate the effects of some previous winter droughts, the aim in this chapter is to examine whether there are any relationships between anomalously wet summers and surface maximum air temperatures, wind and cloud cover. These variables then impact on evaporation rates over the region and hence dam levels. Rainfall in the SWC is typically brought about by midlatitude systems with stratiform clouds. Hence, one expects wetter summers to have cooler, cloudier conditions. In contrast, hot days in the SWC are typically cloud free with dry, subsiding conditions. These features would not necessarily be the case in a tropical climate, or one dominated by convective rainfall since short term thunderstorms can be preceded by very hot and relatively clear conditions which is not as common in a Mediterranean climate. SWC rainfall events usually decrease temperatures in the region so wetter seasons tend to lower temperatures. In contrast, drier seasons with few rainfall events tend to have clear and hot days. Focus is placed on the on the catchment area defined as seen on **Fig. 5.1** which extends over 33.2-34.25° S and 18.78-19.38° E. Trends in temperature extremes are also considered.

5.2 Data and Methodology

To establish whether there is a relationship between anomalous rainfall and temperatures in and immediately surrounding the catchment area, 95% of good daily station data within the catchment area were used. To remove data inconsistencies and to ensure homogeneity, data were cleaned and processed according to Durre et al. (2010). Daily ERA5 reanalysis (Hersbach et al., 2020) temperature data were then obtained from the CDS Copernicus website (https://cds.climate.copernicus.eu/cdsapp#!/search) along with total cloud cover and wind data.

After defining dam locations and the catchment area (**Fig. 5.1**), the 90th percentile temperature values were obtained for each extended summer (ONDJFM) season within the catchment area. The maximum temperature as well as average wind speed data were plotted from 1979-2019 along with a trend line using a simple linear regression (**Fig. 5.2a and b** respectively). Results were also tabulated (**Table 5.1**) along with rainfall characteristics of each extended summer season and

average maximum temperatures and average temperatures. In addition, a Pearson correlation was done between rainfall and maximum temperatures in the catchment area (**Fig. 5.3a**). Given the effects warm and windy conditions may have on evaporation, a Pearson correlation was also done between average extreme temperature days per season and wind speeds. The significance of the relationship between rainfall and temperature maximums was also tested at the 95% level while the relationship between extreme temperature days and winds was tested at both a 95% and 90% level.

Since January and February are typically the driest and warmest months of the year, the October-December (OND) season was considered separately to January-March (JFM). In addition, OND is often much windier than JFM. Considering the five wettest seasons on record (taken from **Fig. 4.4** in *Chapter 4*), spatial plots of each variable characteristic were created for each OND or JFM season (**Figs 5.4-5.9**). For completeness, similar plots were done for the entire extended summer (ONDJFM) and are shown in **Appendix B-D**.

5.3 Results

Fig. 5.1 shows the catchment area of the major water supply dams for greater Cape Town together with the locations of the rainfall and temperature stations and the topography of the SWC. Over this catchment area, **Fig. 5.2a** shows that on average there are 17.4 days out of 182 in ONDJFM which can be characterized as extremely hot but there is considerable interannual variability (the standard deviation is 6.4 days). For example, the 1996/97 summer had only four such days whereas 2012/13 and 2015/16 each experienced 28 such days. Many of the summers with above average numbers of extremely hot days occurred in the last two decades of the record and indeed there is a significantly increasing trend of 2.8 days/decade. Only 2 seasons (2006/07 and 2014/15) in the last two decades (2000-2019) show below average numbers of extreme hot days compared to 12 seasons in the first 2 decades.

The increasing trend in extreme hot days appears to be related to rainfall totals. A significant inverse relationship ($r = -0.44$, $p < 0.05$) can be seen between rainfall totals and extreme hot days (**Fig. 5.3a**). Most seasons that experience more than 20 extreme hot days received below average rainfall. However, some dry summers also have a below average number of extreme hot days. While the three wettest seasons have well below average numbers of extreme hot days, there are also two seasons receiving more than 200mm (the average rainfall is 137 mm) which experienced near-average or above average numbers of extreme hot days. Much like extreme hot days, 10m

winds too show significant increases in recent decades at 0.04 m/s/decade (**Fig. 5.2b**) with four ONDJFM seasons in the last two decades showing below the average of 3.92m/s wind speeds. Four out of the five wettest seasons show below average wind speed. Furthermore, average wind speeds per season correlate with extreme hot days at 0.30 (**Fig. 5.3b**) but this only significant at a 90% level.

Table 5.1 lists temperature and rainfall details for the five wettest summers determined in Chapter 4 along with those for the five driest for comparison. As expected for the climatological dry season, the range in both rainfall totals and rain days is very large (respectively 31mm to 334 mm and 15-45 days out of a maximum possible of 182). Also, as already detailed in the previous chapter, anomalously wet summers also typically have LREs. However, not all the anomalously wet summers necessarily experience few extreme hot days. In particular, the fourth wettest summer (2013/14) in fact experienced an average number of extreme hot days (17) or two more days than three of the five driest summers. However, this summer occurred relatively late in the record compared to the other four summers. Its average extreme hot temperature (32.4°C) is the same as that for the most extreme dry summers and its average max temperature is similar to many of the five driest summers. Thus, in some sense this very wet 2013/14 summer appears somewhat of an outlier since its average maximum temperature is well over 1oC warmer than any of the other five wettest summers. Thus, this summer aside, all the anomalously wet summers experienced cooler maximum temperatures and fewer extreme hot days than average. However, it should also be noted that although very wet 1995/96 had below average numbers of hot days, the average maximum of these hot days was equal hottest (32.4°C). More interestingly, four of the five driest seasons and only one of the five wettest occur in the last two decades.

While **Fig. 5.2** and **Table 5.1** present information averaged over the dam catchment area, **Figs. 5.4-5.9** plot surface maximum air temperature, wind, and cloud cover, over the whole region. These plots were done separately for early summer (October-December) and late summer (January-March) due to January and February being the driest and warmest months of the year and the tendency for wildfire occurrence in late summer, early autumn (Van Wilgen, 2009). **Figs. 5.4a, 5.5a** show the climatological maximum air temperature for OND and JFM respectively with much cooler temperatures near the coast due to the effects of sea breezes (Burls and Reason, 2008) and cold SSTs (the region borders the southern part of the Benguela Current upwelling system). Areas of relatively cool inland temperatures can be related to high lying topography (**Fig. 5.1**). All the five wettest summers, except 2013/14, generally show cooler maximum temperatures across the whole region in OND (**Figs 5.4b-f**), particularly OND 1996 which was 2-3°C cooler than average.

On the other hand, OND 2013 was about 1°C warmer than average over the catchment area and closer to 2°C above average over most of the west coast region. For JFM, the 2013/14 summer again stands out compared to the other four cases (**Fig. 5.5b-f**) but its relative warmth is less obvious than was the case for OND (**Fig. 5.4d**). Most of the catchment area in JFM 2014 was close to average in terms of maximum air temperature with the eastern part of the region warmer than average and the western part mainly average or slightly cooler than that (**Fig. 5.5d**). While JFM 1996 also experienced close to average maximum air temperatures over the catchment area, the other three very wet summers are all generally cooler than average over the catchment area and indeed the whole SWC. In general, the magnitude of the anomalies for each season varies for the five wettest summers such that a particularly cool OND does not necessarily imply a particularly cool following JFM. When assessed over the entire ONDJFM extended summer, **Appendix B-D** shows that 1996/97 and 1980/81 were the coolest of the five wettest seasons. Furthermore, **Appendix E** also shows higher storm counts in the 30-50° S at the 10° E line which corresponds with less 0mm days of rain as well as shorter dry spells.

Another important variable for influencing dam levels and wildfire risk is wind. Wind during warm days may increase evaporation rates (Onoda and Anten, 2011; Burgess et al., 2016). Furthermore, strong winds can quickly spread fires (Hoffman et al., 2011). Surface winds for each of the anomalously wet seasons, along with climatology are plotted in **Figs. 5.6-5.7**. As expected, the ocean areas have stronger wind speeds than the land surface due to lower levels of surface friction and there are also relatively high wind speeds over low-lying coastal land or where winds are channeled by topography (Burls and Reason, 2008). Flatter areas in the interior (north and north-east of the domain) also tend to have stronger winds than the mountainous areas, again due to lower surface friction) (**Figs. 5.6a, 5.7a**). Out of the 5 seasons, 3 show weaker winds over the catchment area as well as large adjoining regions while OND 1984 shows very close to average speeds and OND 1980 stronger winds over the catchment area (**Figs. 5.6b-f**). Over the flatter areas near the coast which have higher climatological wind speeds and where fires often occur in summer, OND 1980, and to lesser extent OND 2013, experienced stronger winds while only OND 1995 and OND 1996 clearly show weaker winds, which together with increased rainfall, helps lower fire risk. For JFM, 1981 shows stronger winds than average over the catchment area but less pronounced than its preceding windy OND 1980. The other 4 JFM seasons show close to average or weaker winds over the catchment area as well as generally more obviously weaker winds over much of the coastal regions.

Cloud cover which can be brought on by LREs over the region, also has an influence on surface temperature. More cloud cover can be seen around the coastal region of the SWC where sea breezes advect humid marine air landwards (Figs. 5.8a, 5.9a). On average, the south coast and neighbouring coastal plain tends to be cloudier than the west coast because the prevailing southerly to southeasterly synoptic winds in the summer half of the year tend to advect low level moist marine air towards the south coast but away from the west coast. In OND, 1995 and 1996 seasons show above average cloud cover over both the catchment area and the whole domain (**Figs. 5.8d,e**). For the other three seasons, cloud cover is close to average over the catchment area but mainly slightly above (below) average elsewhere over the domain in 2013 (1980, 1984) (**Figs. 5.8b,c, f**). The cloud cover data set does not provide information about the type or height of cloud. Thus, although abnormally warm OND 2013 shows slightly above average cloud cover over most of the domain, this would be consistent with increased troughing down the west coast from Namibia which generally causes higher temperatures as well as high level cloud. On the other hand, cool, cloudier and slightly less windy 1995 and 1996 could result from low level cloud having been advected from the ocean areas to the south not being as readily dispersed by strong winds.

For the following DJF seasons, now 1996 and 1997 are generally less cloudy over most of the domain (**Fig. 5.9de**)., although for the latter the anomalies are close to zero over the catchment area. JFM 2014 also shows near average cloud cover over the catchment area (**Fig. 5.9f**) as well as average winds there (**Fig. 5.7f**). On the other hand, JFM 1981 (**Fig. 5.9b**) shows mainly decreased cloud everywhere whereas the reverse is true for JFM 1985 (**Fig. 5.8c**). Over the catchment area, the JFM 1981 winds are stronger than average (**Fig. 5.7b**) whereas they are weaker than average in 1985 (**Fig. 5.7c**) consistent with the cloud anomalies. Elsewhere in the domain, there is generally not an obvious relationship between stronger winds and reduced cloud. As already mentioned, the cloud data does not distinguish the height of the cloud and mid- or high level clouds may not be related to surface wind speeds. Furthermore, the complex topography of the region may also make it difficult to determine cloud – wind relationships. However, in some cases there do seem to be linkages between changes in wind and those in cloud over the catchment area of interest here.

5.4 Discussion and Conclusion

The catchment area shows a significant inverse correlation (r = -0.44) between rainfall totals and the number of very hot days. However, a few very wet seasons show above average numbers of these days. The extended summer of 2013/14 is particularly warm but does however, show the

fourth largest mean rainfall total at 222 mm. In addition, this summer experienced 5 LREs (well above average), highlighting the importance of these events for the rainfall. While it might seem counter-intuitive that such a warm season was also so wet, the large numbers of hot days were likely contributed to strongly by conditions occurring before the arrival of the LRE. Two of these 5 LREs in fact were in the top 20 LRE events during the record (*Chapter 4*). The very wet and relatively warm 1995/96 summer had a particularly large number of LREs (10), of which 3 fall within the top 20 recorded (**Table 5.1**). Of the wettest five extended summers, four showed generally cooler conditions than average but OND 2013, and to lesser extent, the following JFM 2014 were warmer than average. Thus, it appears that very wet summers often tend to be relatively cool but important exceptions exist. More LREs and light rainfall events bring cooler temperatures to the region and this results in a decrease in the average temperatures in the extended summer but this does not necessarily mean that extreme cannot coincide within the same season. That being said, seasons with more LREs tend to show cooler temperatures.

Although not as strong a relationship, weaker winds may be connected to cool conditions with four of the five wet seasons showing below average winds. The exception however is the wettest season, 1980/1981 which shows the strongest winds. Although wind can be associated with increased evaporation, wind gusts have been known to be associated strong storm activity. Barnes et al. (2021) demonstrates how COLs can be associated with formidable wind strengths with the largest COL from 1979-2019 occurring during 1980/81(from *Chapter 4*). Taken together, these anomalies in maximum temperature and wind strengths suggest that anomalously wet summers are likely to have reduced fire risk and water consumption through a combination of cooler, less windy conditions, and above average rainfall totals, but this is not necessarily always the case.

Apart from wind speed and temperature differences, other factors can cause changes in evaporation over the catchment area. Clulow et al. (2012) suggests that increased cloud cover may partially cause decreasing evaporation rates and therefore reduces fire risk. Apart from 1996/97 which only experienced 2 LREs, all anomalously wet seasons experienced at least 5 LREs; these events cause considerably increased cloud on the days they occur. This 1996/97 season was the 5th wettest season for the catchment area, and the coolest (**Figs. 5.4-5.5**) in terms of average maximum temperature as well as exhibiting the least amount of extreme hot days (**Table 5.1**). Other relatively cool and very wet seasons such as 1980/81 and 1984/85 had close to average winds over the catchment area and hence it is likely that evaporation losses there were average or below average while water consumption in the region would be expected to not be excessive. .

It is difficult to find consistent relationships between cloud cover and wind on the seasonal scale although in some seasons, changes over the catchment area do seem to show that stronger (weaker) winds are associated with less (more) cloud cover. The complex topography of the region and the different processes involved in cloud occurrence at different heights in the atmosphere are important factors that have not been explicitly considered here. In simple terms, stronger southeasterly winds (the prevailing wind direction in summer) should lead to less (more) cloud cover near the west (south) coast due to the orientation of these moisture-bearing winds in relation to that of the coastal mountain ranges. Other important factors are the depth and instability of this flow in relation to the mountain height (as measured by the Froude number) with a shallower and weaker layer of incident winds less able to flow over the topography and form cloud near the mountain crests than a stronger and deeper layer.

However, from the perspective of water availability for the region, a detailed field study over the catchment area to monitor and understand variations in evapotranspiration, runoff and infiltration into the soils would be needed. Such a hydrological study is beyond the scope of this thesis which has purely looked at the rainfall variability, or inputs into the water balance.

Of the anomalously wet seasons, 2013/14 clearly stands out as being the only such season during the 1998-2021 period, and for being particularly warm, in fact comparably warm to many anomalously dry summers. This season is an exception to the simple expectation of wetter summers being cooler than average - it received an average number of extremely hot days (2 more such days than three of the five driest summers). More interstingly, 2013/14 shows the least number of fires and smallest area burnt in recent years. Data from SAWS also reveals low fire counts for the other 4 anomalously wet seasons with all most fires occurring to the west of the catchment area before the Cape Fold Mountain ranges. The reduction in fire risk could be result of the anomalously wet summer bringing much needed moisture to the area during the driest time of the year. Whether or not future anomalously wet summers may also occasionally be considerably warmer than average is not known but it might happen in cases where there is increased troughing bringing more moist, tropical air southwards from Namibia than average. Projected trends in drying for the SWC have been shown by Mahlalela et al. (2019) and Naik and Abiodun (2020). However, only considering rainfall impacts in climate model projections (Abiodun et al., 2018) is likely to underestimate future drought; robust climate projections need to also consider the details of circulation changes as well as local factors affecting surface temperatures and evapotranspiration. **Fig 5.2** showed a significant increasing trend over the region in both the numbers of extreme hot days and in surface wind speeds. Theron et al. (2021) noted

increasing maximum temperatures in both the southeast and south of the SWC which have significant impacts on the agricultural industry where the recent 'Day Zero Drought' impacts were particularly severe.

Apart from temperature increases which in turn, increases evaporation (Naik and Abiodun, 2020), decreases in rainfall during transition seasons further increase drought risk (Pascale et al., 2020). Early summer (OND) and late summer (JFM) show variability in terms of temperature and cloud cover as well as winds which promote westerly disturbances and rainfall (**Figs 5.4-5.9**). Many of these cooler extended summer conditions follow LRE occurrences. LREs have considerable impacts on temperatures in the region which have several implications for agriculture and dam reservoir levels. Cool and wet JFM seasons stand out as particularly important during the dry season and contribute considerably toward decreasing drought effects.

Sizeable rainfall events during the extended summer, and particularly LREs, are important in not only adding surface water to dam reservoirs, either directly or via streamflow, but also (along with wind) help reduce evaporation rates during the driest time of the year. Furthermore, anomalously wet summer seasons also reduce fire risk and can mostly be characterized by cooler temperatures and, in some cases, decreased wind speeds and increased cloud cover (which contributes to decreasing evaporation) over the dam catchment area. However, further work is needed in order to quantitatively relate water availability over the region with changes in rainfall, evaporation and circulation. Since the winter rainy season is expected to be less reliable in future climate projections along with increasing temperatures, better understanding of rainfall and circulation trends during other times of the year is important. This chapter, and the preceding one, has considered rainfall variability and trends during the extended summer with a focus on anomalously wet summers and LREs. The following chapter considers large scale mechanisms associated with these anomalous summers.

***For 2013/14 fire area burnt see https://www.capenature.co.za/fire-management#:~:text=The%20Western%20Cape%20continues%20to,a%20result%20of%20climate%20change*

Tables and figures

Table 5.1*: The five wettest and driest seasons from 1979-2019 and their extreme hot day counts, average extreme temperatures, mean maximum temperatures along with mean rainfall totals, rainfall days and the number of large rainfall events. The mean maximum temperature over the catchment area is 26.1°C with an average mean maximum temperature of 32.2°C. The order is done in terms of date.*

ONDJFM Season	Wet/Dry	Extreme Hot Days	Average Extreme Temperature (°C)	Mean Maximum Temperature(°C)	Mean Total Rainfall (mm)	Rainfall days	No. of LREs
1980/81	Wet	6	31.9	24.8	334.5	45	6
1984/85	Wet	9	31.9	24.6	310.1	38	9
1987/88	Dry	15	32.4	25.7	73.1	28	0
1995/96	Wet	12	32.4	25.1	275.8	25	10
1996/97	Wet	4	31.7	23.5	180.0	28	2
2000/01	Dry	21	32.3	26.8	62.1	15	0
2005/06	Dry	21	32.4	26.6	59.4	20	0
2013/14	Wet	17	32.4	26.3	222.0	31	5
2014/15	Dry	15	32.0	26.5	68.9	18	0
2016/17	Dry	15	32.3	27.1	30.7	16	0

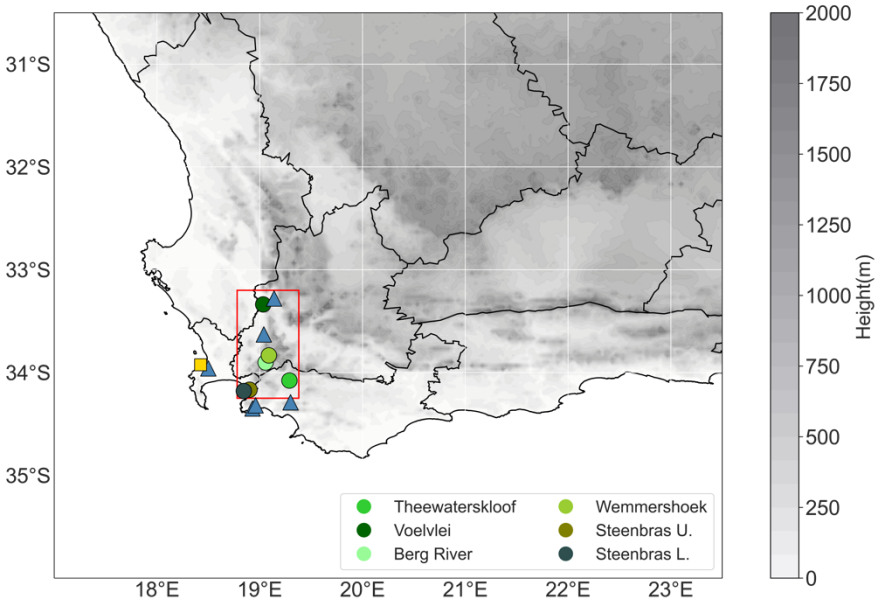

***Figure 5.1**: Map showing the SWC station locations(blue triangles) used as well as major dam reservoir locations (green circles). The red box represents the catchment area and yellow square the Cape Town urban area.*

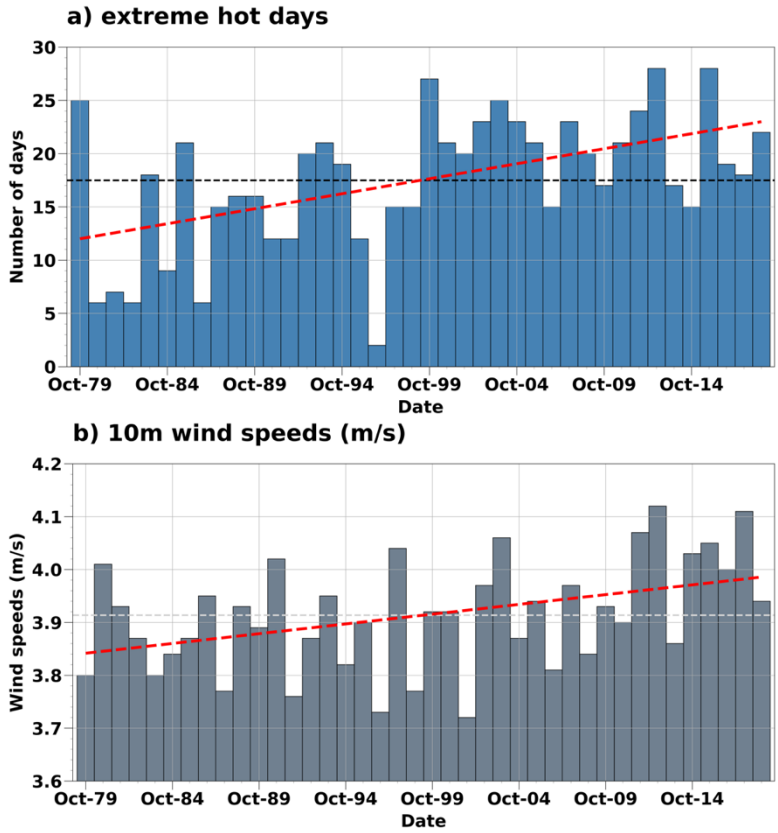

***Figure 5.2**: The number of extreme hot days per ONDJFM season within the catchment area(a). The teal line represents the average of 17.4 whereas the red line represents trends in extreme hot days significant at a 95% level ($p < 0.05$). (b) represents the average 10m wind speed per ONDJFM season. The grey line represents an average of 3.92 m/s and the red line represents the trend in wind speed and is significant at a 95% level ($p < 0.05$)*

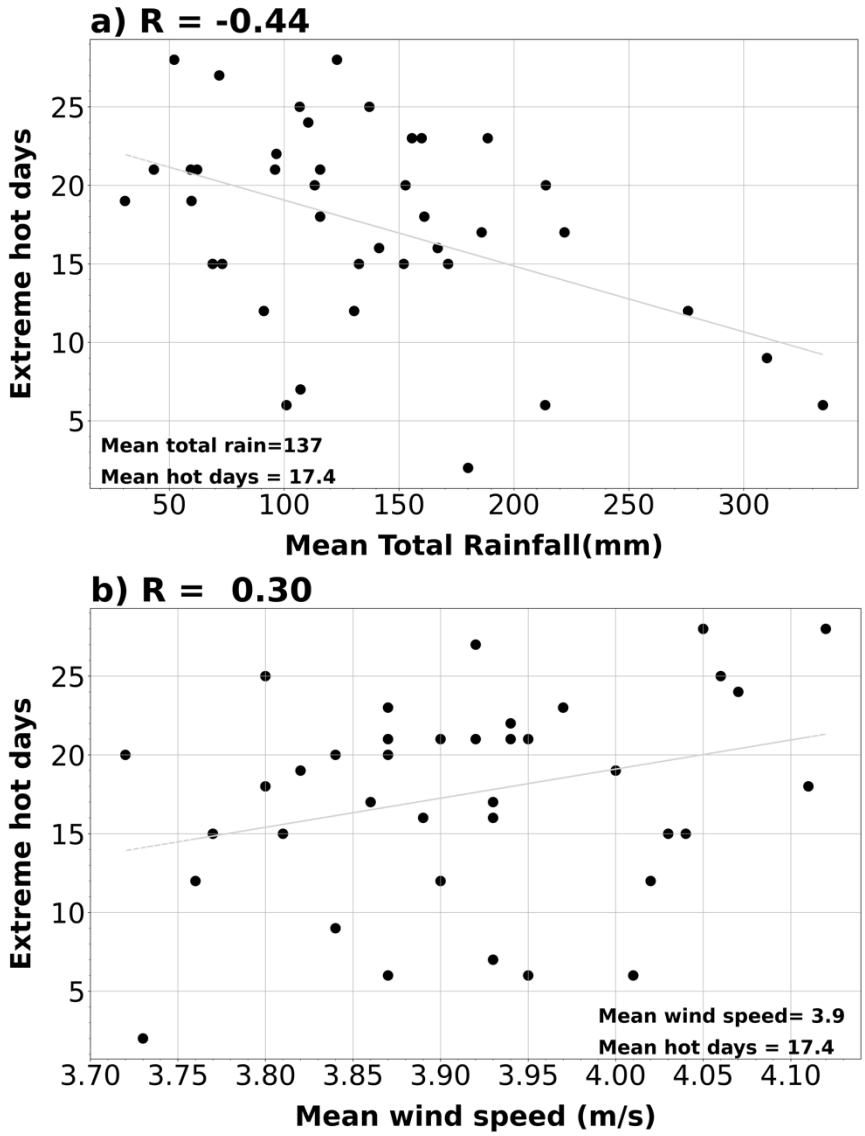

Figure 5.3*: The relationship between mean rainfall totals and extreme hot days in the catchment area over the ONDJFM season (a). The negative relationship of -0.44 is found to be significant at a 95% level. (b) represents the relationship between extreme hot days and wind speed which shows a positive relationship of 0.30 but only significant at a 90% significance level.*

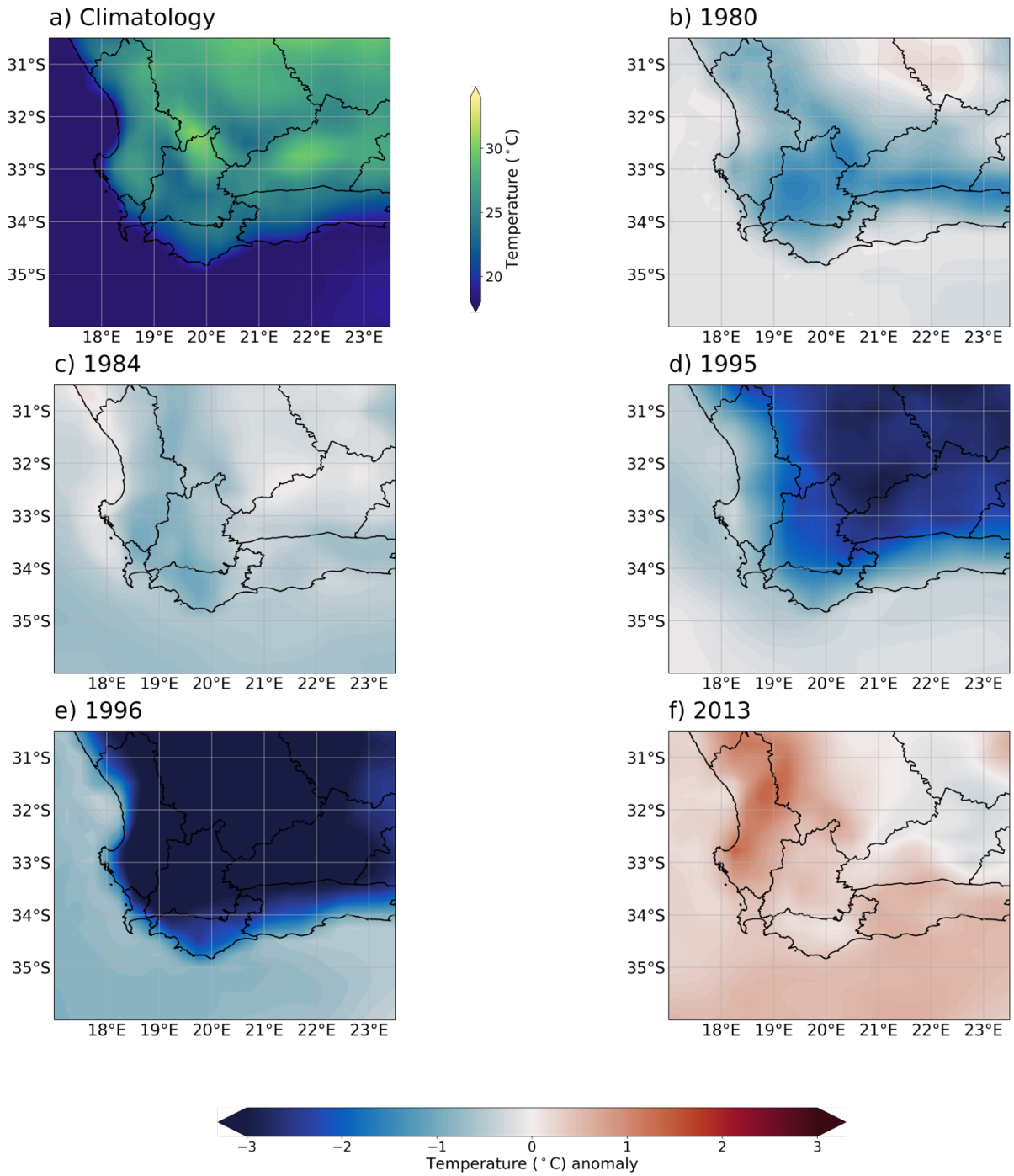

***Figure 5.4**: Climatology (a) of mean maximum day temperatures (°C) for October-December for the SWC followed by anomalies in mean maximum temperature (b-f) for the five wettest ONDJFM seasons.*

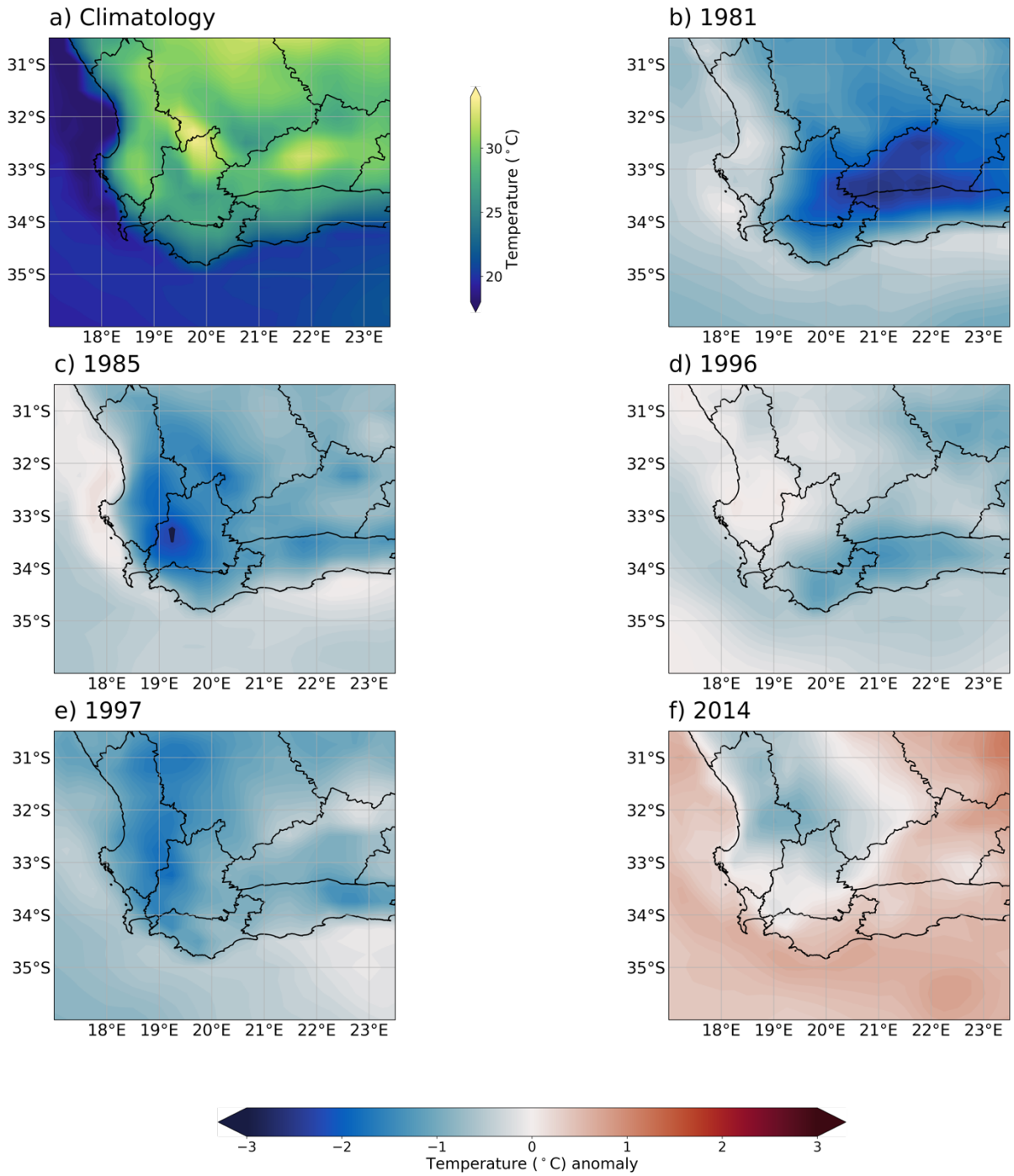

***Figure 5.5**: Climatology (a) of mean maximum day temperatures (°C) for January-March for the SWC followed by anomalies in mean maximum temperature (b-f) for the five wettest ONDJFM seasons.*

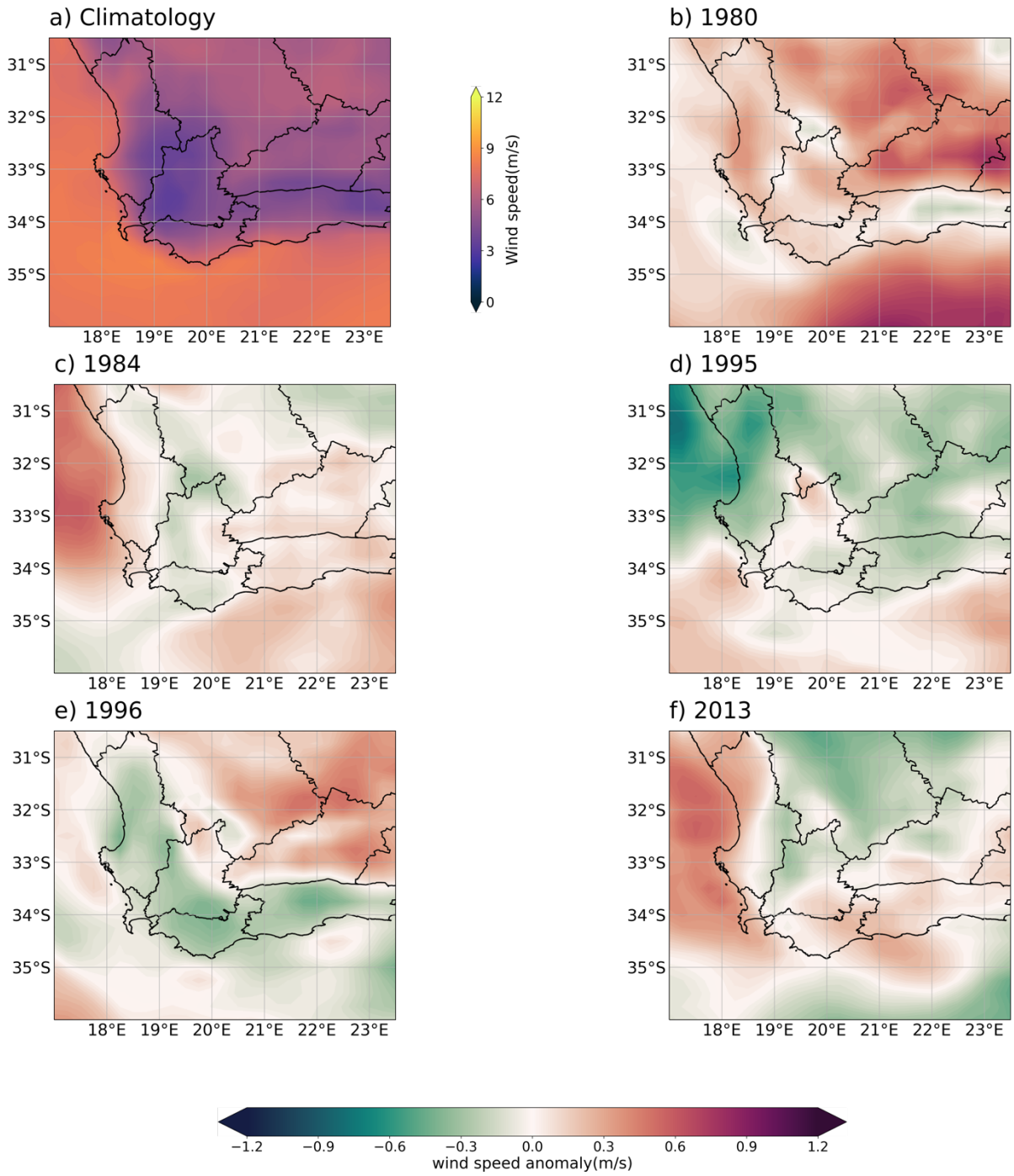

***Figure 5.6**: Climatology (a) of mean 10m wind speed (m/s) for October-December for the SWC followed by anomalies in mean 10m wind speed (b-f) for the five wettest ONDJFM seasons.*

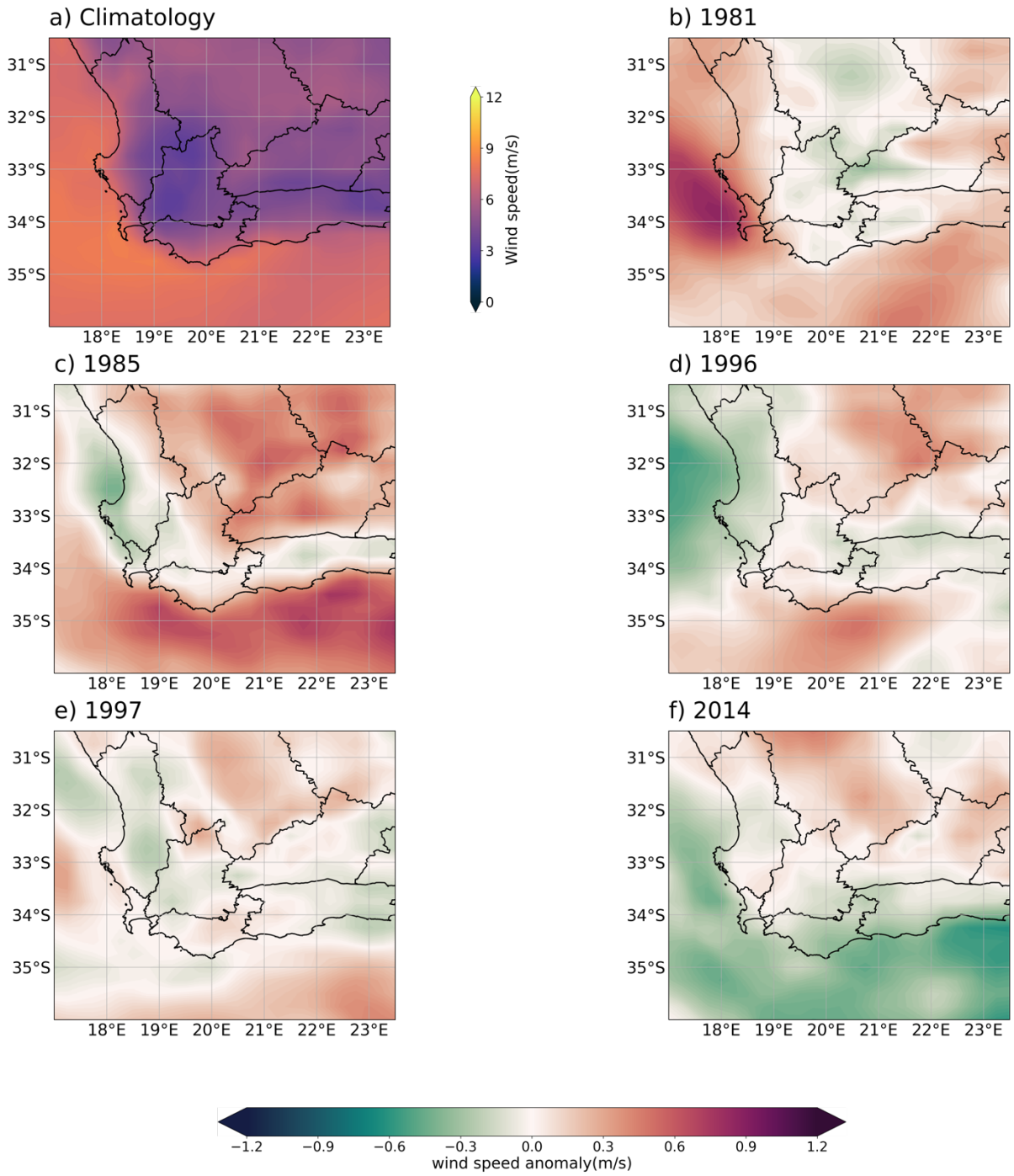

***Figure 5.7**: Climatology (a) of mean 10m wind speed (m/s) for January-March for the SWC followed by anomalies in mean 10m wind speed (b-f) for the five wettest ONDJFM seasons.*

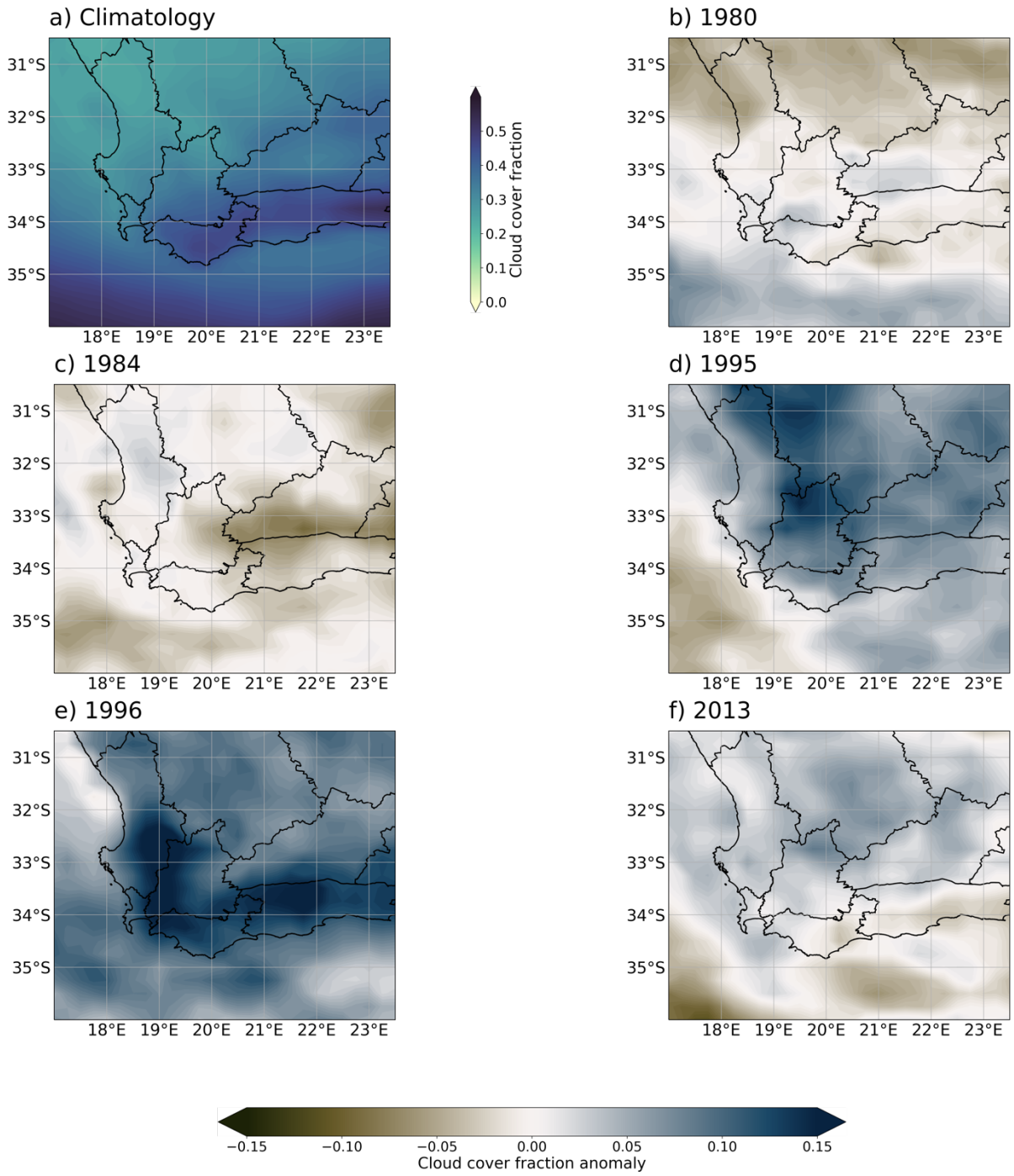

***Figure 5.8**: Climatology (a) of mean cloud cover for October-December for the SWC followed by anomalies in mean cloud cover (b-f) for the five wettest ONDJFM seasons.*

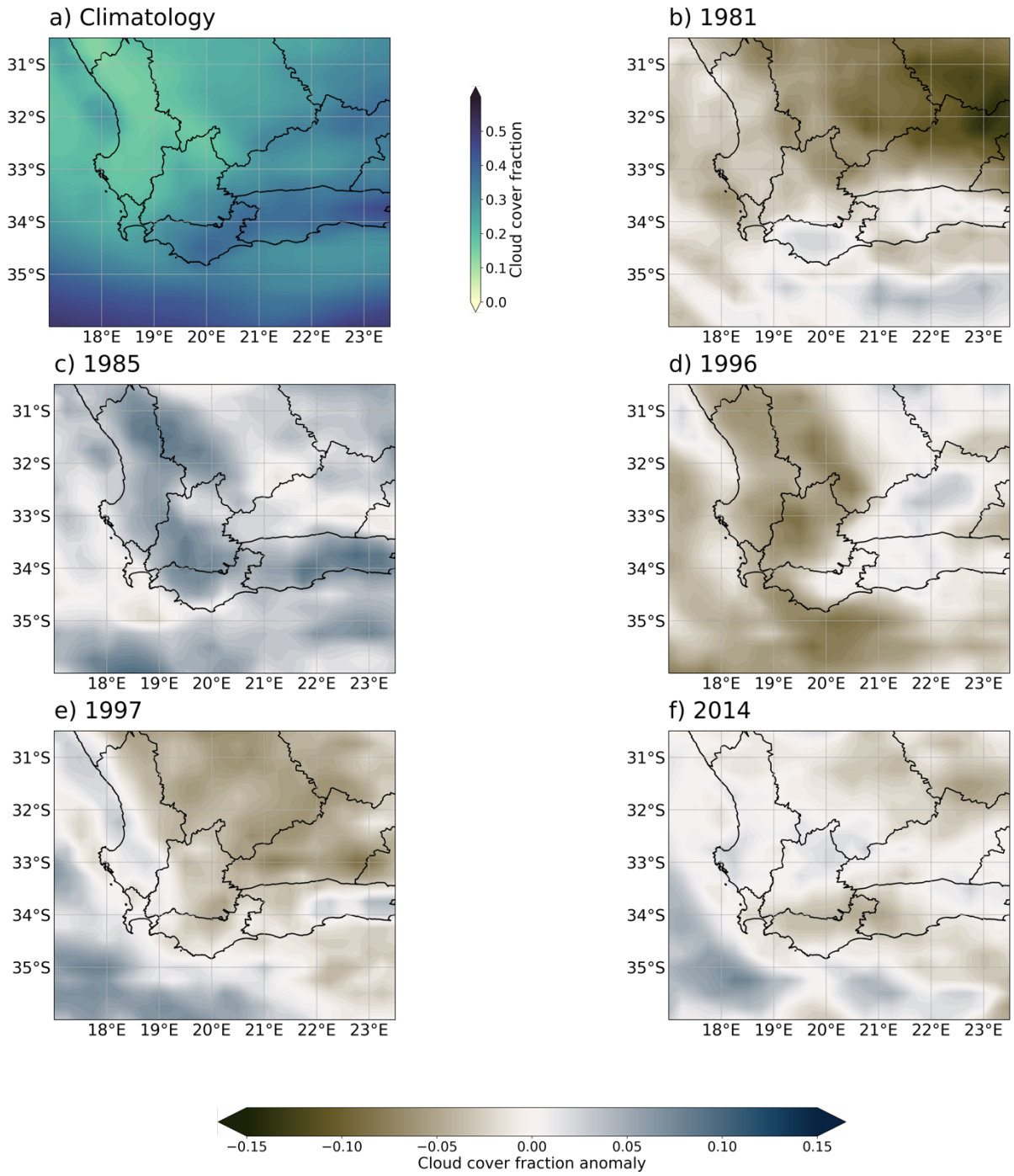

***Figure 5.9**: Climatology (a) of mean cloud cover for January-March for the SWC followed by anomalies in mean cloud cover (b-f) for the five wettest ONDJFM seasons.*

Chapter 6: Large-scale mechanisms linked to anomalously wet summers over the southwestern Cape, South Africa

This chapter address the questions listed below and represent the work as a published paper in Climate Dynamics:

De Kock, W.M., Blamey, R.C. and Reason, C.J.C., 2022. Large-scale mechanisms linked to anomalously wet summers over the southwestern Cape, South Africa. Climate Dynamics, 1-15. https://doi.org/10.1007/s00382-022-06280-7

This chapter addresses the following questions:

- What are trends in rainfall days in the SWC and which months show the strongest change in rainfall days?
- How do anomalously wet and dry extended summer seasons differ?
- Are there links between rainfall days and large-scale features and/or modes of variability?
- What are the major potential contributors to increases or decreases in SWC rainfall?

Abstract

Although on average, the southwestern Cape (SWC) of South Africa is a winter rainfall dominated region, almost 30% of the total rainfall occurs during the extended summer (October-March). A previous study showed that anomalously wet summers may help mitigate the effects of severe winter drought. Apart from that study, very little work has been done on summer rainfall variability over the SWC or the mechanisms associated with it. Here, station data and ERA5 reanalyses are used to investigated summer rainfall day variability and associated mechanisms.

Interannual variability in summer rainfall day frequencies appears related to that in the South Atlantic High Pressure (SAHP) and westerly moisture fluxes across the midlatitude South Atlantic. Increased rainfall days are associated with cyclonic anomalies over the region and enhanced westerly moisture fluxes. Some of these circulation changes are related to the Southern Annular Mode, and in late summer, also to ENSO and changes in the zonal wavenumber 3 pattern. Significant decreasing trends in rainfall days were found in the mid- and late summer for the southern part of the region where most of the population lives and the main water supply dams are located. These trends seem associated with significant trends found in the southern boundary of the SAHP and in decreasing (increasing) South Atlantic storm counts in the 35-45°S (50-60°S) latitude bands.

6.1. Introduction

The southwestern Cape (SWC) of South Africa receives most of its rainfall during the austral winter months (June-August), while the summer months (December – February) are mostly warm and dry (Reason et al., 2002; Burls et al., 2019; De Kock et al., 2021), and is therefore a Mediterranean-type climate region much like southwestern Australia and central Chile. The rest of South Africa mainly receives rainfall in summer, except for the south coast which is an all-year rainfall region (Weldon and Reason, 2014; Engelbrecht et al., 2015). The SWC is very important to the national economy with key agricultural, fisheries, transport and services industries as well as containing the second largest city (Cape Town). Recent prolonged droughts in the SWC have had significant negative effects on the local economy (Shepherd, 2019). However, droughts are a relatively common occurrence in the SWC, but what makes them particularly damaging is when they last for consecutive years like the 2003-2004 extreme drought (Muller, 2018) or the more recent "Day Zero" drought from 2015-2018 (Sousa et al., 2018; Wolski, 2018, 2021; Archer et al., 2019; Mahlalela et al., 2019). In the 2003-2004 case, the extended 2003-04 summer received below average rainfall while this was true for all the extended summers in 2014-2018 (De Kock et al., 2021).

However, in some cases, anomalous large rainfall events (LREs) during the extended summer (October-March) can play an important role in mitigating the effects of extended droughts in the SWC (De Kock et al., 2021). In addition to summer rainfall totals being important for drought mitigation, it helps reduce the demand for irrigation in the extensive cropping areas and also lowers the risk of severe bush fires. These are most common in the late summer and early autumn (Van Wilgen, 1984, 2009) before the winter rains start. In recent years, such fires have led to significant loss of life in informal settlements around Cape Town as well as destroyed large tracts of indigenous vegetation in the surrounding mountain areas. Summers with anomalously high rainfall in the SWC are also likely to be associated with changes in the upwelling favourable southerly winds along the west coast of South Africa (Jury, 2020) and hence have impacts on the rich fisheries of the southern Benguela Current upwelling system (**Fig. 6.1**). Thus, a better understanding of what causes some summers to be anomalously wet is of considerable interest but to date, there has been limited research into summer rainfall variability in the SWC and its associated mechanisms.

Winter rainfall in the SWC is primarily produced through cold fronts originating in the South West Atlantic (Reason et al., 2002; Blamey et al., 2018; Burls et al., 2019). Other westerly disturbances, such as cut-off lows (COLs), may on occasion produce considerable rainfall over the region although they tend to be more common in autumn and spring (Singleton and Reason 2007a; Favre et al., 2013; Weldon and Reason, 2014). Most of the extreme wet winters in the region result from atmosphere rivers (ARs), which transport large amounts of moisture from the tropical south west Atlantic or Brazil towards the SWC (Blamey et al., 2018, Ramos et al., 2018). Both ARs and COLs have been associated with large rainfall events during the summer half of the year over the SWC (De Kock et al., 2021).

One might expect that both anomalously wet winters and summers could result from an equatorward expansion of the midlatitude westerlies over the South Atlantic along with a retreat northwestward of the semi-permanent South Atlantic High Pressure (SAHP). Typically, as the subtropical jet shifts poleward, the SAHP moves southeast towards the SWC in late spring and early summer and helps weaken approaching fronts and steer them further south compared to winter (Reason et al., 2006). In summer, low level moisture tends to diverge away from the SWC in summer due to the southerly or southeasterly flow along the west coast whereas it tends to be advected towards the region by the westerlies in winter. Several studies have related interannual rainfall variability over the SWC to changes in the SAHP and westerly moisture fluxes upstream over the South Atlantic (Reason et al., 2002; Ramos et al., 2018; Sousa et al., 2018; Burls et al., 2019). In turn, these circulation changes may be related to South Atlantic SST or sea-ice anomalies (Reason and Jagadheesha, 2005; Blamey and Reason, 2007) or to El Niño-Southern Oscillation (ENSO) (Phillipon et al., 2012) or the Southern Annular Mode (SAM) (Reason and Rouault, 2005). To date however, these has been little or no research into whether similar changes in the SAHP, the subtropical jet or westerly moisture flux corridors may lead to some summers being anomalously wet over the SWC.

Given the occurrence of multiyear severe droughts over the SWC in recent times (e.g., 2003-2004 and 2015-2018) and the role of some anomalous summer large rainfall events in helping to mitigate such droughts (De Kock et al., 2021), the objective in this study is to better understand the variability in summer rainfall totals, rainfall days and associated circulation anomalies. The question of any long-term trend will also be considered since there is evidence of an early winter drying trend in the SWC (Mahlalela et al., 2019).

6.2. Data and Methodology

Data from weather stations across the Western Cape were obtained from the South African Weather Service (SAWS) and processed using the quality control methods after Durre et al. (2010). Only stations with more than 95% of valid data was considered from October 1979 to March 2019, which resulted in only 20 stations being available. Since rainfall days and average rainfall totals vary across regions in the Western Cape (**Fig. 6.2a, b**), stations were grouped into zones based on rainfall frequency and variability as well as geographical location. This resulted in four clusters namely; (A) West Coast, (B) Cape Metropole and Winelands, (C) Overberg and (D) Central Karoo district (**Fig. 6.2c**). The major dam reservoirs that supply the greater Cape Town region are primarily situated in zones B and C.

Given that the extended summer is the dry season, the focus was placed on rainfall days rather than rainfall totals. There is a strong linear relationship between rainfall days and rainfall totals across all four of the zones (**Fig. 6.3**). For this analysis, seasonal totals for days with rainfall >1mm and rainfall >10mm during the extended summer (ONDJFM) were calculated. The criteria for rainfall days and rainfall totals is consistent with previous studies on rainfall variability in southern Africa (De Coning, 2013; Kruger and Nxumalo, 2017; Burls et al., 2019). Rainfall days were then counted for each of the four sub-regions and split into three sets of bi-monthly values; early summer as October-November (ON), core summer as December-January (DJ) and late summer as February-March (FM). Here, ON and FM represent seasonal transition periods before and after the core summer, respectively.

ERA5 reanalysis data (Hersbach et al., 2020) were used to recreate the synoptic patterns associated with the five wettest and driest sub-seasons. These five wet and dry cases are based on combining the rainfall days across zones B and C and are provided in **Table 6.1**. These two zones were chosen as they are wetter than the other two zones and contain the large water supply dams as well as most of the SWC's population. Here, monthly mean sea level pressure (MSLP), zonal (u) and meridional (v) winds, specific humidity and geopotential height data were obtained for the period 1979-2019. All ERA5 reanalysis data are on a 0.25°x0.25° horizontal grid. The composite anomalies using the different variables are presented as differences between the wet and dry case (effectively the difference between the anomalously high numbers of rainfall days and the anomalously low numbers of rainfall day composite).

The MSLP data were used to determine the location and intensity of the South Atlantic High Pressure (SAHP). The latitude and longitude of the centre of the SAHP is defined here as the location with a maximum in the MSLP field (after applying a 9x9 grid-point spatial smoothing filter) within the climatological mean area (40°W-15°E; 0°-45°S and values over land were masked). Alternative methods have been implemented to find the centre of the various subtropical high pressure systems, such as second-order Taylor series (e.g. Murray and Simmonds, 1991, Mächel et al., 1998) or nearest neighbour approaches (e.g. Sinclair, 1997; Zarrin et al., 2010, Reboita et al., 2019). However, the approach adopted here does not appear to influence results, with the methodology used here being tested with output from an analysis of SAHP by Gilliland and Keim (2018). For the purpose of this study, the northern, southern, eastern and western extension of the SAHP is determined as the outer boundary of the 1018 hPa contour in the MSLP. This contour level is chosen as it is easily identified as closed contour level around the SAHP, which is not intersected with the neighbouring land masses in either the early (ON) or late (FM) summer periods. Trends were evaluated using the Theil-Sen slope estimator (Theil, 1950; Sen, 1968) and the non-parametric Mann-Kendall test (Mann, 1945; Kendall, 1975). These methods are relatively insensitive to outliers with the Mann-Kendell test making no assumption about the distribution of the underlying data. Statistical significance was assessed at the 95% level (90% for individual stations in **Fig. 6.10**).

An analysis of the relationship of DJ and FM rainfall and ENSO, SAM, the South Atlantic subtropical dipole (SAOD), the South Indian Ocean subtropical dipole (SIOD) as well as the midlatitude zonal wave number 3 (ZW3) pattern. Prior to running correlations, all data were detrended and a Student t-test was used to test for statistical significance. The Niño 3.4 index (SST anomalies over 5°S–5°N, 120°–170°W) is used to represent ENSO in the analysis, while the SAM index, calculated as the zonal MSLP differences between 40°S and 65°S after Marshall (2003), is determined from ERA5 data. The ERA5 data was also used to calculate the ZW3 index data using the 500hPa geopotential height. Raphael (2004) suggests using 500hPa zonal anomaly which is constructed by removing zonal means from each grid point. The ZW3 index is the average of the anomaly values at three selected grid points namely, 45°–60°E, 161°–171°E and 71°–81°W with a latitude range of 45°–50°S (Raphael 2004) and is calculated as follows:

$$ZW_i = \frac{X_m - \bar{X}_m}{\sigma_m}$$

for each of the three grid points where X_m is a three-monthly value, $\bar{X}_m$ is a three month climatological mean and σ_m is the three monthly mean standard deviation.

The SIOD and SAOD were calculated using SST data from Optimum Interpolation of SST version 2 (OISSTv2) reanalysis from the National Centers for environmental Prediction (NCEP). The SIOD index is defined in Behera and Yamagata (2001) as the SST anomaly difference between the 55-65°E, 37-27°S pole and the 90-100°E, 28-18°S pole. The SAOD was calculated using the Nnamchi et al. (2011) index defined as the SST anomaly difference between the 10ºE-20ºW, 0º-15ºS pole and the 10º-40ºW, 25º - 40ºS pole.

Lastly, the tracks of extratropical cyclones in the South Atlantic (Gramcianinov et al., 2020), were obtained from Mendeley Data. This daily storm track dataset, available from 1979-2019 and based on ERA5 reanalysis, is used to investigate potential changes in cold fronts impacting on the SWC. The core (DJ) and late summer (FM) periods are considered when analysing storms with SAHP behaviour because SAHP seasonal signals are stronger and less noisy compared to months where the transition of spring or autumn takes place. Further to that, recent studies also suggests that December-February shows the most evidence of change in the SAHP (e.g., Sun et al., 2017; Al Fahad et al., 2020).

6.3. Results

(a) Summer rainfall variability

The extended summer (ONDJFM) experiences between 28-37% of annual total precipitation across the stations in zones A-D in the SWC (**Appendix A**). Zone B (Cape Town Metropole and Winelands) experiences more rainfall days and rain totals (**Fig. 6.2**) than either zone A or D due to its higher latitude (weaker subtropical subsidence). Orographic effects and distance from the coast also make zone D drier than it would be otherwise. The differences between zones B and C are less obvious but, generally zone C inland stations (e.g., near 34°S, 19.5-20°E), are drier than either those near the south coast or on the windward side of the mountains in zone B.

Given that the extended summer is relatively dry, anomalies in the number of rainfall days rather than in rainfall totals is a more useful metric. It is also useful from an applications viewpoint because non-rainfall days in summer are commonly cloud free and relatively windy leading to high evaporation, drying out of soils and vegetation, and increased fire danger. On the other hand, even a light rainfall day substantially reduces these adverse effects. As shown in **Figure 6.3**, the number of rainfall days is also highly correlated with rainfall totals. When averaged over each zone, it is

clear that zone B is by far the wettest in terms of both rainfall days and totals but this average is significantly biased upwards by a few stations located very slightly west of 19°E near the windward crests of the mountains (**Figs. 6.1b, 6.2**). More interesting in **Figure 6.3** are the extremes which are as much as 46 rainfall days out of 183 and over 700 mm or as little as 13 rainfall days and less than 200 mm in zone B. The differences between the extremes in the other zone are somewhat less but all zones show considerable interannual variability in both rainfall day numbers and rainfall itself. There are also a number of summers with considerably more rainfall than the average in each zone (e.g. in zone B, 9 out of 40 summers received 450 mm or more as compared to the long term spatial average of 363 mm or 32 or more rainfall days compared to the mean of 27).

This interannual variability in the number of rainfall days averaged over each zone for the summer half of the year is further evident in **Figure 6.4** which also breaks down the total into bi-monthly contributions. Every bi-month also shows a decreasing trend during the record which is significant for February-March (FM) at each zone. The only exception is a very weak increasing tendency in October-November (ON) for zone C. For ON and December-January (DJ), the decreasing trends are significant for 2 out the 4 zones but these 2 significant zones are different for ON and DJ. respectively. On average, the most recent 20 years experienced about 4 rainfall days less per summer than 1979-1999 and was therefore somewhat drier. Particularly concerning are the large decreasing trends in rainfall days and totals in DJ and FM in zones B and C since most of the SWC large dam reservoirs supplying greater Cape Town are situated here.

As a result of these large trends in DJ and FM, and because these two bi-months show the largest seasonal differences from the winter circulation on average, the remainder of this study focuses on them rather than the ON sub-season.

(b) Circulation patterns during anomalous summers

To better understand the circulation patterns and potential mechanisms behind anomalously wet summers, the five wettest DJ and FM sub-seasons are contrasted with the five driest. Note that the DJ years are not necessarily followed by the FM of that year for either the wet or the dry case (**Table 6.1**). Both DJ and FM have four out of their five driest seasons occurring between 1999 and 2019 (**Table 6.1**); this tendency is consistent with the trends in **Figure 6.4** and is discussed further in a later section. Given that zones B and C are the largest contributors to rainfall in the SWC (**Figs. 6.2-6.4**) and these zones are where the largest dam reservoirs and most of the

population are located, the wet and dry composites are derived for rainfall days averaged over these two zones.

Figure 6.5 indicates that the wet summers are characterised by lower pressure relative to the dry summers over and south of the SWC in both sub-seasons. In DJ, the SAHP appears to be shifted further southwest in the wet summers with the circumpolar trough weakened in the Atlantic and southeast Pacific sectors (**Fig. 6.5a**) whereas in FM, there is evidence of a negative SAM pattern in the wet summers (**Fig. 6.5b**) and strong cyclonic anomalies off the southern coast of Argentina where cyclogenesis often occurs (Jones and Simmonds, 1993). Note that wet winters over the SWC have previously been associated with a negative SAM (Reason and Rouault, 2005; Mahlalela et al., 2019). At mid-levels, Figure 6.6 shows cyclonic anomalies over and just upstream of the SWC in both sub-seasons in the composite difference which would be favourable for strengthening rain-bearing systems as they approach the region, consistent with increased rainfall. Taken together, (**Figs. 6.5-6.6**) imply an enhanced midlatitude westerly influence in FM in the wet versus the dry summers. For DJ, the situation is more complex with the cyclonic anomalies along the west coast of southern Africa suggesting an increasing tendency for southward advection of tropical air and west coast trough formation over the SWC as fronts approach from the midlatitude southeast Atlantic.

Upper level wind differences (**Fig. 6.7**) reflect a negative SAM in FM and a more complex pattern in DJ. In both sub-seasons, the subtropical jet is strengthened over and upstream of the SWC in the wet summers relative to the dry case. A transect of zonal wind differences along 10°E, or just upstream of the SWC, indicates that in both sub-seasons, the subtropical jet is shifted north and stronger in the wet versus the dry summers (**Fig. 6.8**). Near the surface, the easterly component over the South Atlantic in the 32-35°S band weakens substantially in both sub-seasons in the wet composite (**Figs 6.8b, d**), consistent with increased rainfall. Furthermore, the gradient between the tropical easterlies and the midlatitude westerlies strengthens in DJ and, to lesser extent, FM, implying stronger westerly disturbances approaching the SWC in the wet versus the dry case.

Consistent with Figure 6.5, the moisture flux differences show a more southwesterly stream towards the SWC in DJ as the SAHP is located slightly further to the southwest (**Fig. 6.9a**), implying increased advection of cooler, moist marine air from the South Atlantic over the region in the wet versus the dry case with relative uplift as this flow impacts the coastal mountains (not shown). SST anomalies indicate warming upstream of the SWC in the wet case versus the dry (not shown) which would also favour increased rainfall days. There is also a large area of warming east

of Argentina where cyclogenesis often occurs (Jones and Simmonds, 1993), favourable for more storms being advected towards the SWC. For FM (**Fig. 6.9b**), the midlatitude westerlies are shifted north to directly impact the SWC in the wet summers, with again increased uplift relative to the dry case (not shown) as this flow reaches the mountains. The SST composite difference (not shown) also shows warming upstream of the SWC as well as in the cyclogenesis region east of Argentina. In addition, there is warming to the south of the SWC over the Agulhas Current retroflection region, favourable for the strengthening of cold fronts as they make landfall.

(c) Summer rainfall and large scale modes of variability

The strongest correlations with ENSO, ZW3 and SAM occur in FM for stations in zones B and C (**Fig. 6.10**) where only those significant at 90% significance level are shown. The strong negative correlations in FM for SAM and ZW3 are consistent with the negative SAM pattern in **Figure 6.6** which also shows a weakening wavenumber 3 pattern (cyclonic anomalies in the ridging areas downstream of the three continents). For ENSO, the SWC is on the edge of the regions of strong circulation anomalies typically occurring in summer over the South Atlantic and South Indian Oceans during these events (Reason et al., 2000; Colberg et al., 2004) so it is not surprising that sign of the correlation changes across the zones. For the SAOD, **Fig. 6.10gh** shows positive correlations which are stronger in FM than DJ. The same applies for the SIOD except that the correlations are negative (**Fig. 6.10ij**).

Taken together, **Figs. 6.5-6.10** suggest that interannual variability in rainfall days over zones B and C of the SWC is influenced by changes in atmospheric circulation over and upstream of these zones which reflect changes in the SAHP and, in FM, the SAM and ZW3 patterns. The latter sub-season also shows relationships with the SIOD and the SAOD since these SST dipole modes are themselves driven by changes in the SAHP and the South Indian Ocean high pressure and hence related to the wavenumber 3 pattern (Fauchereau et al., 2003; Hermes and Reason, 2005).

d) Trends

A pattern evident across the four clustered zones is the decreasing trend in rainfall days during the core (December- January) and late (February-March) summer (**Fig. 6.4**). Zones B and C, containing the southern stations, reveal a significant decreasing trend in both DJ and FM, whereas the decreasing trend is significant only in FM for the northern zones A and D. The significant

decrease in rainfall days across all four clusters during the late summer (FM) complements Mahlalela et al. (2019) who found evidence of the drying during early winter months in the SWC. If this trend continues, then it has significant implications for water management since water consumption is typically large during the seasonally hotter months of December-April when wild fires are also likely. Trends in SAHP and storm activity are now considered to see how they may be related to the decreases in rainfall day numbers.

Figure 6.11 shows variations in the spatial boundaries and centres of the SAHP during 1980-2019. Both the central latitude and the southern boundary of the SAHP have shifted south in DJ but only the latter trend is significant, implying that over the ~40-year period, the southern boundary of the SAHP has extended over 2° further south. Since the southernmost point of Africa (and the SWC) lies equatorward of 35°S, such a shift in the SAHP suggests that midlatitude disturbances such as cold fronts are less likely to impact as strongly on the region than previously. **Figure 6.12b** supports that suggestion since there is a clear reduction in midlatitude storms passing through 15°E, or just upstream of the SWC, in the most recent 15 years compared to the first 15 years of the record. The DJ storm tracks (**Fig. 6.12a**) helps explain why the SWC is much drier in summer than winter; although both midlatitude and subtropical storms are generated in the western Atlantic as far north as 20°S (near the South Atlantic Convergence Zone in Brazil), the SAHP tends to steer the vast majority of them south of the SWC in DJ. The few storms apparent along the west coast of South Africa and Namibia either reflect unusually far western located tropical-extratropical cloud bands (west coast troughs) whose tropical origin is around 15-20°S or the occasional cut-off low.

If one breaks the transect in **Figure 6.12b** down into latitude bands, then there is a statistically significant decrease in storms passing through 15°E in the 35-45°S band and an increase in those in the 50-60°S band (**Fig. 6.13**). Moreover, **Figure 6.12a** suggests that on average, storm tracks during 2004-2019 are located further south and also show a larger concentration in the 40-55°S band whereas 1979-1994 are more spread out with relatively a higher number in the lower latitudes so the average location of storms during 1979-1994 is further north. These trends are consistent with the poleward trend in the southward boundary of the SAHP seen in **Figure 6.11b** and help explain the decreasing trend in DJ rainfall days in zones B and C. Similar, in fact slightly stronger, trends in storm counts are found if **Figs. 6.11-6.13** are derived for DJF. However, the trend results are no longer consistent in the FM. This apparent inconsistency occurs because the change in the monthly average SAHP position between February and March is much greater than that between December and January or between January and February, leading to essentially a double-centred

SAHP when this system is analysed in terms of FM. As a result, a FM analysis of SAHP trends is not meaningful.

6.4. Discussion

The trends in the SAHP shown in the previous section are consistent with overall trends evident elsewhere in the subtropics (e.g., Gillett et al., 2003; Gillett and Stott, 2009; Nguyen et al., 2013; Grise et al., 2018; Staten et al., 2018). The poleward shift of the SAHP and the other subtropical anticyclones are largely attributed to the expansion of the tropical circulation belt and poleward shift of the Hadley Cell edge due to tropical upper tropospheric warming and high latitude lower stratospheric cooling (Gillett and Stott, 2009; Grise et al., 2018). A poleward expanding SAHP implies that the main mid-latitude storm track in the South Atlantic (**Fig. 6.12a**) would also shift poleward. Such a mechanism has been found to help multi-year winter droughts in the SWC (Sousa et al., 2018; Burls et al., 2019) and the results presented here suggest that it may also help account for declining summer rainfall days. Jury (2020) supports this finding and suggests an increasing drying trend in the core summer, with warmer temperatures as well as a further extension of the dry season in the Cape Town Area (Zone B). Fewer storms were shown in this study occurring upstream of the SWC (10°E) during DJ between ~35°-45°S during the most recent 15 years (2004-2019) compared to the earliest part of the record (1979-1994) while there was an increase in storms polewards of ~50°S. The poleward shift in the mid-latitude storm tracks shown here is consistent with the hypothesis that the subtropical belt (30-40°N/S) will get drier in response to a warming climate (Scheff and Frierson, 2012). A potentially important factor not explicitly considered here is the orientation of the post-frontal ridging with respect to that of the coastal mountains. For example, a more zonally oriented anticyclonic ridging following frontal passage (with a westsouthwesterly flow) is less likely to lead to further rainfall than one where the anticyclone is more meridionally oriented and directs a colder, moister southsouthwesterly airstream towards the coastal mountains.

In addition to the poleward expansion of the Hadley circulation, recent decades have shown a greater tendency for the SAM to be in positive phase (Pezza et al., 2007, 2008). The positive phase of SAM is characterised by a poleward shift in the eddy-driven jet (~50°S), resulting in a poleward shift in the storm track with higher surface pressure in the midlatitudes and lower surface pressure in the high latitudes (Hartmann and Lo, 1998; Pezza et al., 2008). Earlier work showed that the SAM is inversely related to winter rainfall over the SWC (Reason and Rouault, 2005). **Figure 6.10** showed that the SAM is also inversely correlated with summer rainfall day frequency at several of

the southern stations in the SWC in DJ and particularly FM. A significant correlation also exists between the SAM and the SAHP southern latitude ($r=-0.57$; p-value<0.05) as well as between the SAM and the proportion of storm frequency between 40-50°S vs 50-60°S ($r=-0.44$; p-value<0.05) during DJ (**Fig. 6.13b**). Similar correlation results occur for DJF but are weaker when March is included, likely due to the large shift in the position of the SAHP centre between February and March, previously mentioned. This suggests that when SAM is in its positive phase, the SAHP together with storm tracks in the South Atlantic are located further polewards leading to less summer rainfall days and rainfall in the SWC.

6.5. Conclusion

To date, very little work has been done on rainfall variability and trends in the summer half of the year in the SWC region of South Africa despite around 30% of rainfall and rainfall days occurring during this period on average, and evidence that anomalous large rainfall events then can sometimes play an important role in mitigating severe multi-year winter droughts (De Kock et al., 2021).

Using daily station data from October 1979 to March 2019, an analysis of local rainfall characteristics was presented. As is the case in the main winter rainy season, strong spatial gradients exist in summer rainfall totals and rainfall days in the region with a relatively wet coastal region in the southwest and southern parts and a relatively dry north and interior. These gradients result from distance from the ocean moisture source, orographic effects and increasing subtropical subsidence with latitude and are expected since the rain-bearing weather systems in both the summer and the winter are largely cold fronts and cut-off lows. Although west coast troughs (which involve a tropical inflow of moisture from Namibia) only occur in summer, they do not often lead to rainfall over the SWC and therefore do not influence the spatial gradients to any extent. Since a few anomalously large rainfall events might distort the rainfall characteristics during the summer, the results were determined using the number of rainfall days rather than rainfall totals as the variable of interest. However, summer rainfall days and rainfall totals are highly correlated ($r = 0.84$-0.96 across the region) implying that the results can be extended to totals with confidence.

Interannual variability in summer rainfall days in the SWC is related to changes in the SAHP and moisture fluxes upstream over the subtropical / mid-latitude South Atlantic Ocean together with circulation anomalies over the region itself. Summers with increased rainfall days appear to be

associated with cyclonic anomalies over the SWC region as well as a northward shift in the westerly moisture fluxes immediately upstream. Some of these circulation anomalies appear to be associated with SAM and, in FM but not DJ, changes in the zonal wavenumber 3 pattern and ENSO.

In addition to pronounced interannual variability, significant decreasing trends in rainfall days were found in both DJ and FM in the two southern zones of the SWC; namely, the greater Cape Town region and that immediately to its east on the other side of the coastal mountains (Overberg). The two northern (and drier) zones exhibited significant decreasing trends in FM as well as ON but the decreasing trend in DJ was not significant at 95%. The decreasing trends in the greater Cape Town and Overberg regions are particularly concerning since this is where the majority of the population lives, and the largest water supply dams are located. Both the summer trends found in this study and those associated with winter droughts (Sousa et al., 2018; Burls et al., 2019) are associated with a poleward expanding SAHP and southward shift of westerly moisture fluxes. Since these poleward shifts appear related to ongoing Hadley cell expansion in a warming climate (Al Fahad et al., 2020), there is the potential for droughts to become more severe in future in the main winter rainy season, and for anomalously wet summers, such as studied here, which can play a role in mitigating these severe winter droughts, to become more scarce or less effective in reducing water demand in this semi-arid region with a fast-growing population.

Table and Figures

***Table 6.1**: The top 5 wettest and driest seasons based on standardized anomalies of rainfall days and totals for October-November (ON), December-January (DJ), February-March (FM) from 1979-2019.*

Wet				Dry			
Months	**Date**	**Std dev.**	**Mean Total(mm)**	**Months**	**Date**	**Std dev.**	**Mean Total(mm)**
ON	1980	1.57	326.2	ON	2016	-1.69	26.5
ON	1996	1.22	273.2	ON	1987	-1.11	38.6
ON	2013	1.88	259.0	ON	1994	-1.13	54.9
ON	2010	1.86	252.2	ON	1990	-1.08	61.7
ON	2009	1.12	250.3	ON	1999	-1.19	64.5
DJ	1980/81	3.14	397.4	DJ	2009/2010	-1.23	11.0
DJ	2004/2005	1.61	260.6	DJ	2005/2006	-1.31	15.5
DJ	2001/2002	1.93	250.5	DJ	2012/2013	-1.18	32.7
DJ	1994/1995	1.42	229.9	DJ	2000/2001	-0.61	35.6
DJ	1984/85	1.1	206.6	DJ	1988/1989	-0.62	38.6
FM	1989	2.39	204.9	FM	1999	-0.84	24.3
FM	1983	1.69	202.9	FM	2001	-1.37	24.8
FM	1985	2.29	198.9	FM	2017	-1.11	32.5
FM	1981	1.49	191.4	FM	1980	-0.61	37.7
FM	1992	1.66	184.9	FM	2009	-1.17	38.0

***Table 6.2**: Pearson correlations between areas of the South Atlantic High Pressure (SAHP) and the respective large-scale mode of variability, namely; the El Niño Southern Oscillation Index (ENSO), The Southern Annular Mode (SAM), Zonal Wavenumber 3 (ZW3), the South Atlantic Indian Ocean Dipole (SAOD) and the South Indian Ocean Dipole (SIOD) during December-January (DJ) and February-March (FM). The bold values represent significant correlations at 95%.*

	SAHP Cen. Lon.		**SAHP Cen. Lat.**		**North**		**South**		**West**		**East**	
	DJ	FM	DJ	FM	DJ	FM	DJ	FM	DJ	FM	DJ	FM
ENSO	-0.10	-0.05	0.07	-0.18	**0.39**	-0.17	-0.17	0.08	**-0.36**	0.08	0.24	-0.26
SAM	0.02	0.11	-0.29	-0.22	0.18	-0.11	**-0.57**	**-0.51**	-0.28	-0.09	**0.36**	0.02
ZW3	**-0.37**	0.17	**-0.38**	-0.33	-0.02	-0.24	**-0.42**	-0.13	**-0.37**	-0.06	0.08	0.02
SAOD	0.23	**0.36**	-0.03	0.14	-0.31	-0.04	0.10	0.18	**0.37**	0.33	-0.13	0.10
SIOD	0.01	0.10	-0.06	-0.30	0.25	0.00	-0.24	-0.26	-0.27	-0.30	**0.33**	0.26

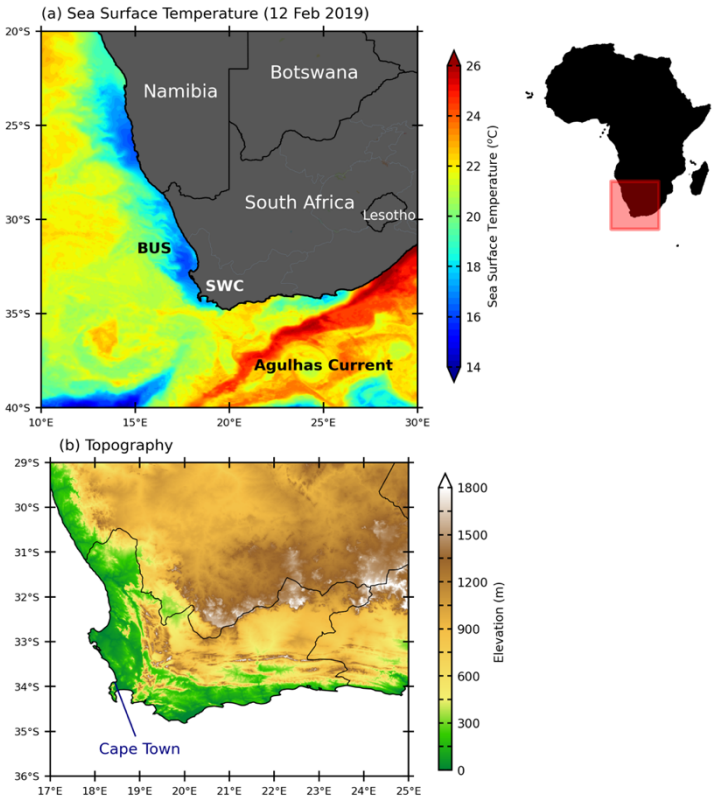

***Figure 6.1**: (a) SSTs (°C; based on MUR SST) surrounding southern Africa for a particular summer day (12 February 2019), with extremely warm SSTs along the east and south coast (Agulhas Current) and cold upwelled water along the west coast (Benguela Upwelling System). The location of the southwestern Cape is denoted by the acronym SWC on the map. (b) local topography of the SWC and the location of the city of Cape Town.*

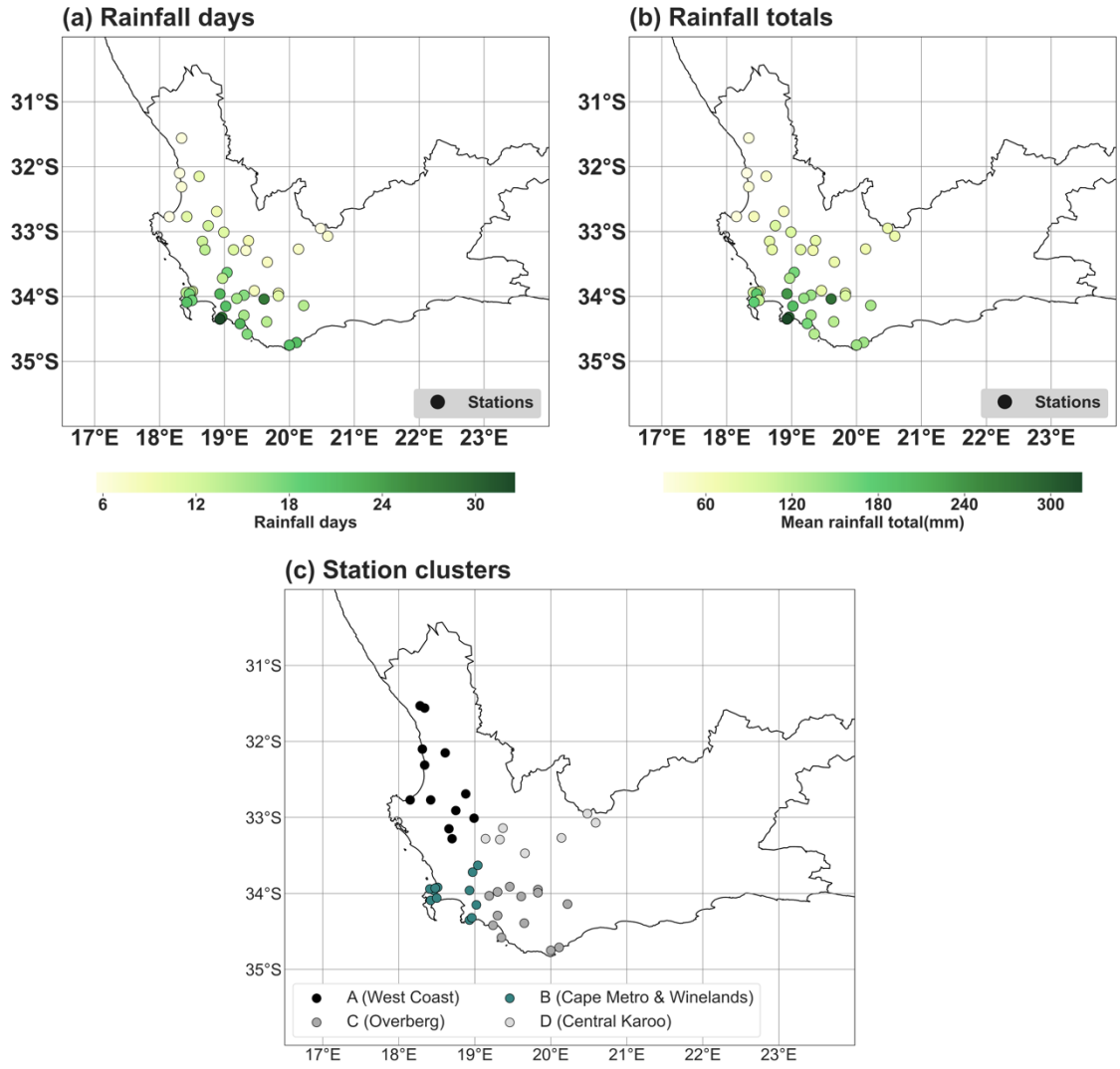

***Figure 6.2**: ONDJFM average rainfall days (a) and rainfall totals (b) at individual stations. (c) represents a Map of the Western Cape with the location of SAWS weather stations divided into four distinct rainfall day zones showing Zone A (West Coast; black), Zone B (Cape Metropole and Winelands; teal), Zone C (Overberg; dark grey) and Zone D (Central Karoo; light grey).*

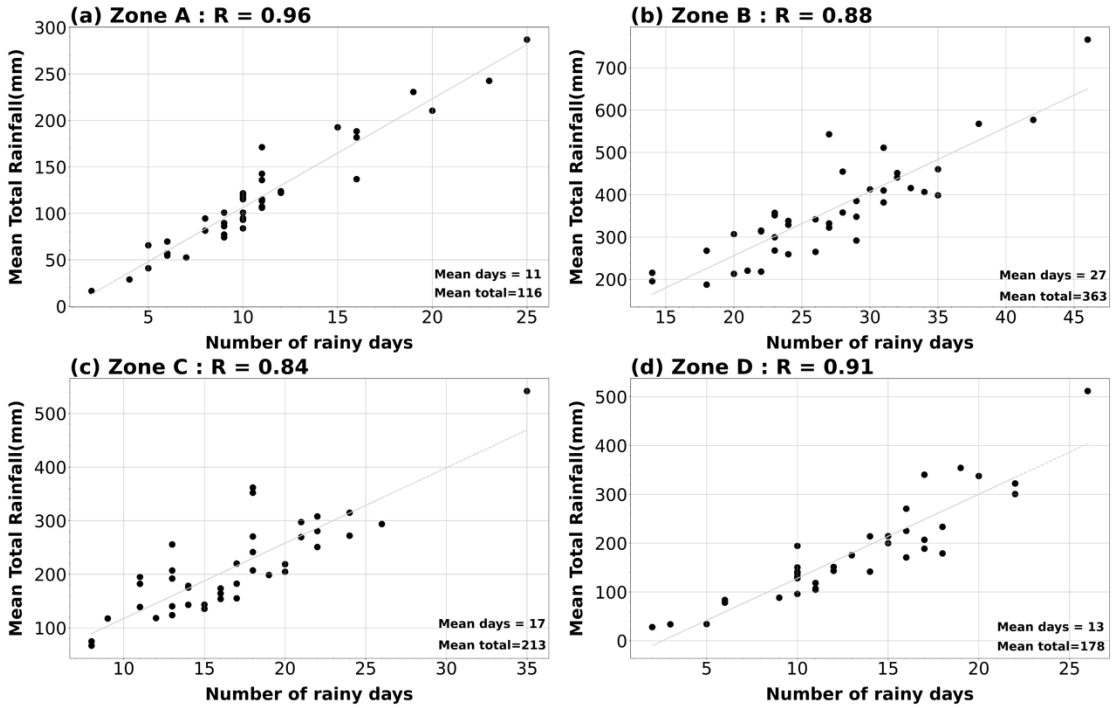

Figure 6.3*: The relationship between rainfall days and mean total rainfall (mm) during ONDJFM for (a) Zone A, (b) Zone B, (c) Zone C and (d) Zone D. The correlation between rainfall days and rainfall total is given at the top of each panel.*

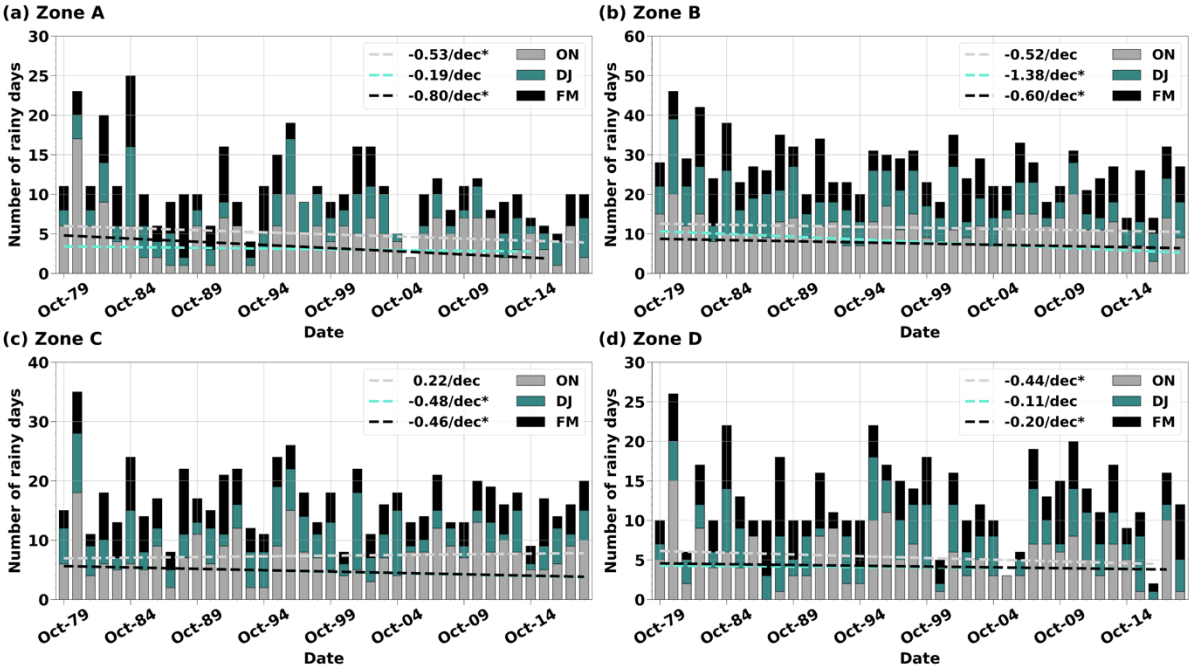

Figure 6.4*: The interannual variability in the number of rainfall days in bi-months October-November (ON), December-January (DJ) and February-March (FM) from 1979-2019 for (a) Zone A, (b) Zone B, (c) Zone C and (d) Zone D. The corresponding dashed lines represent the trends in each bi-month, with the trend value (given in days per decade) given in the legend (the * represents significance at the 95% level).*

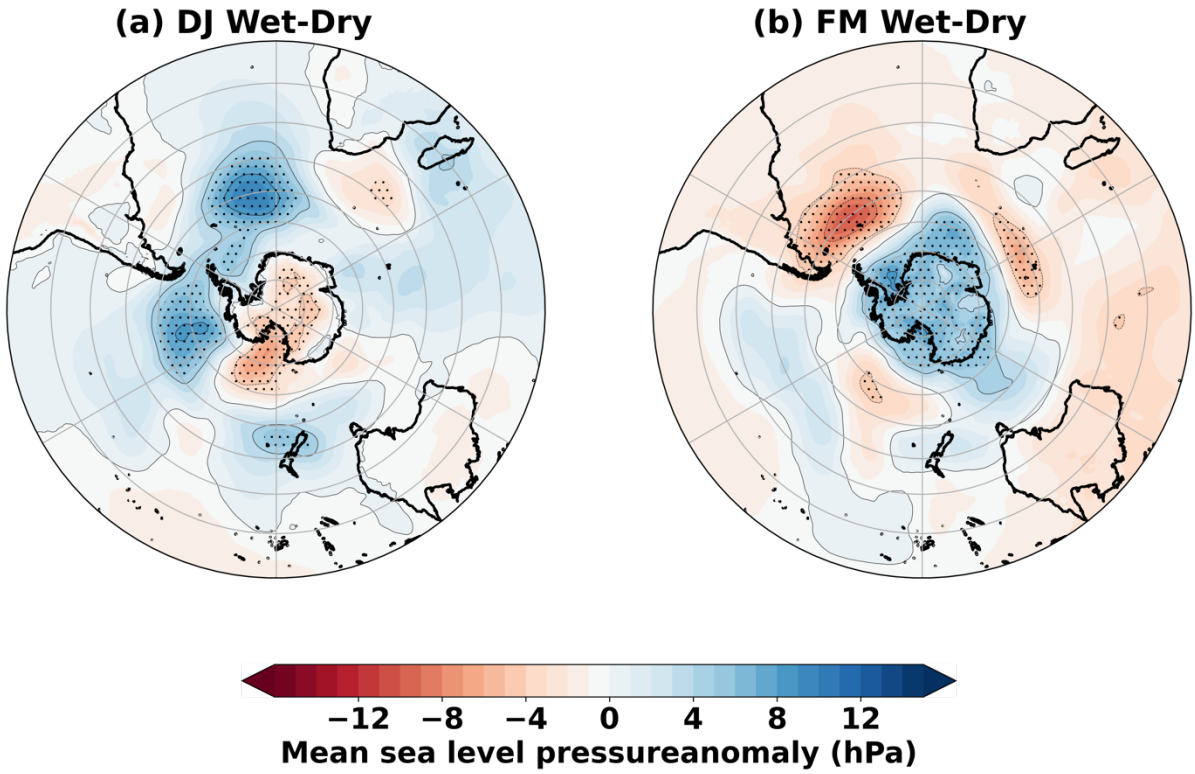

***Figure 6.5**: Mean Sea Level Pressure showing the difference between the five wettest and five driest seasons in (a) DJ and (b) FM for zones B and C. The black stippling represents areas that are statistically significant at the 95% level.*

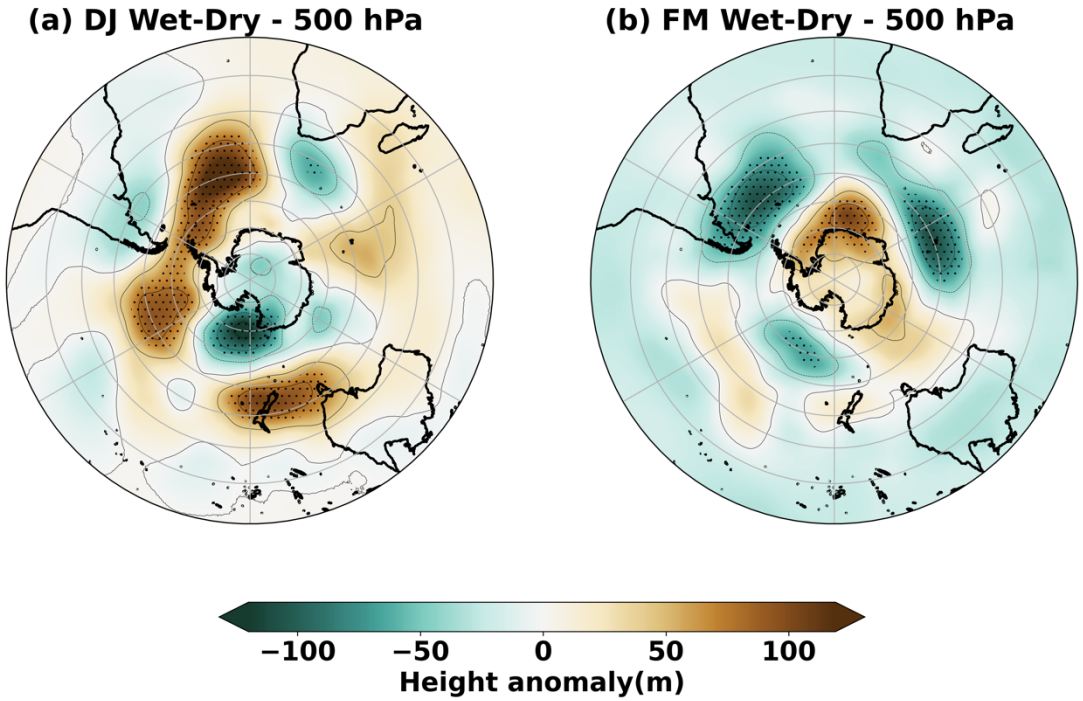

***Figure 6.6**: Geopotential height in the mid troposphere (500hPa) showing the difference between the five wettest and five driest seasons in (a) DJ and (b) FM for zones B and C. The black stippling represents areas that are statistically significant at the 95% level.*

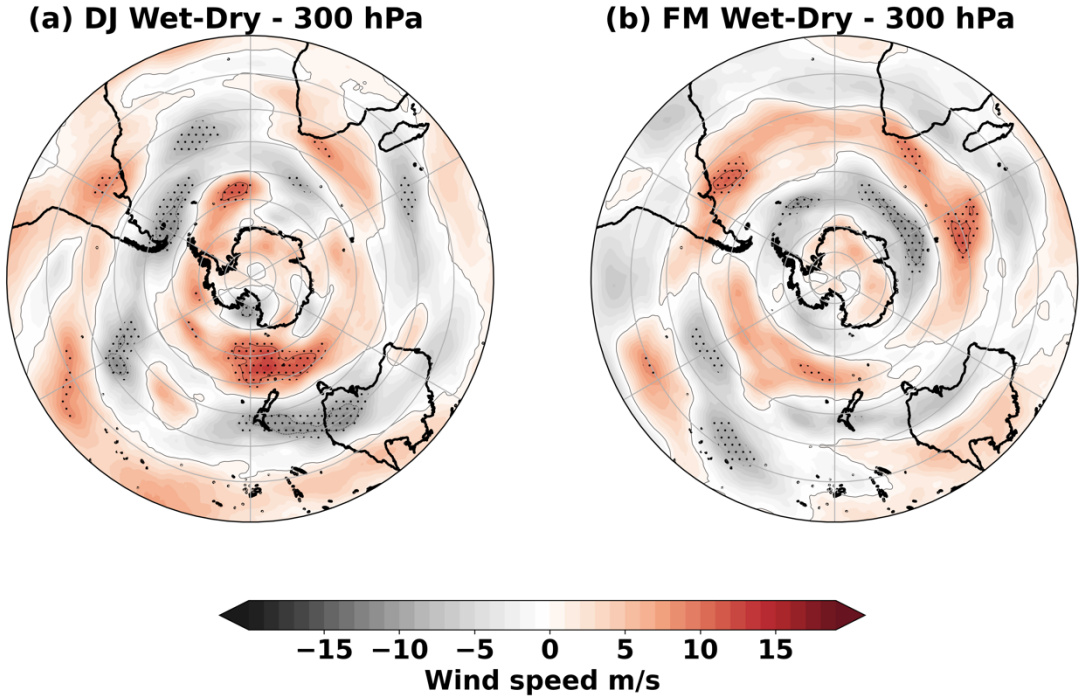

***Figure 6.7**: Upper troposphere zonal wind (300hPa) showing the difference between the five wettest and five driest seasons in (a) DJ and (b) FM for zones B and C. The black stippling represents areas that are statistically significant at the 95% level.*

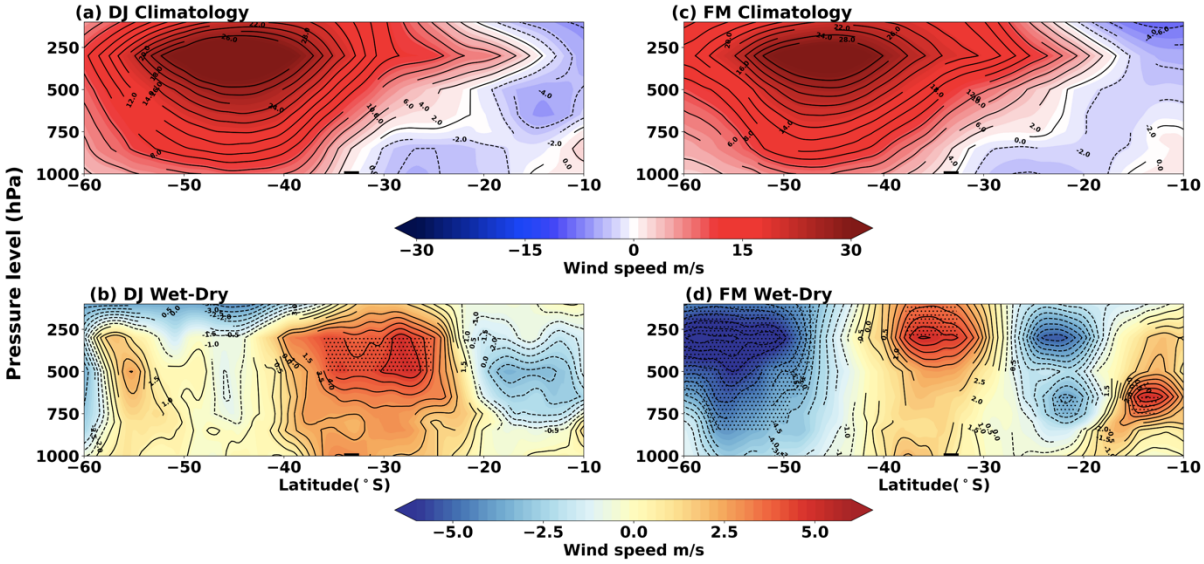

***Figure 6.8**: Cross sections of the mean zonal wind (m/s) at 10°E for (a) DJ and (b) FM. The difference in wet and dry composites for (b) DJ and (d) FM for zones B and C. Black stippling illustrates areas that are statistically significant, while the black bar along the x-axis represents the latitudinal position of the SWC.*

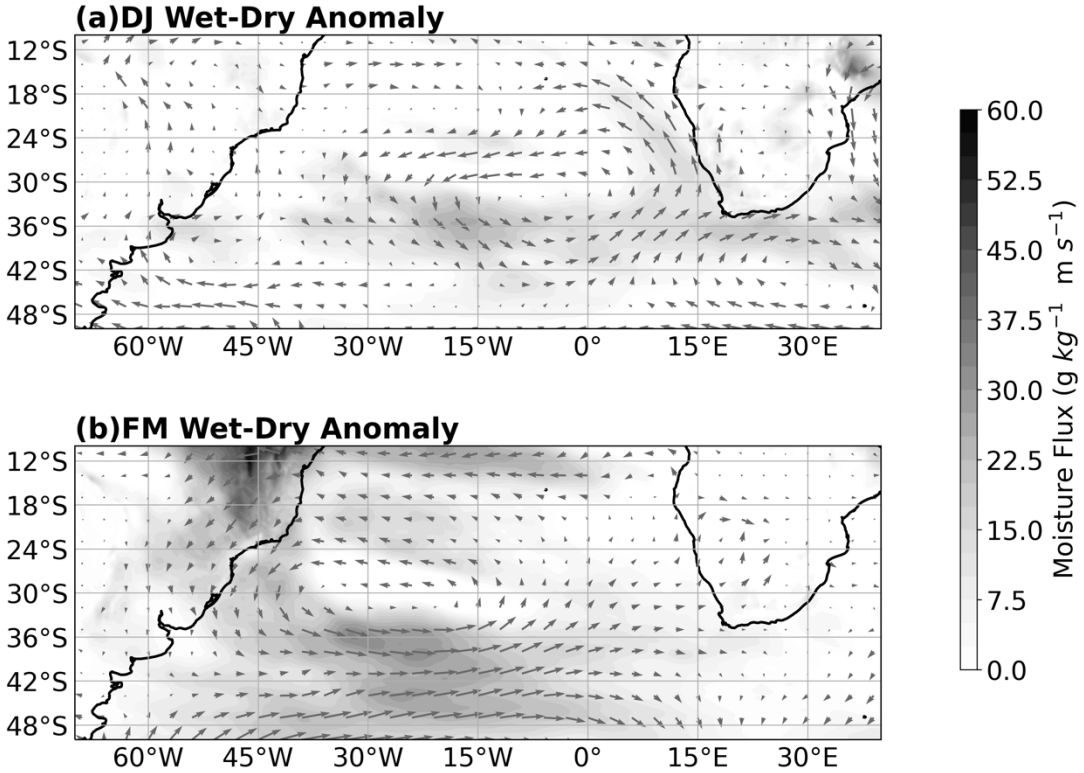

***Figure 6.9**: Moisture flux at 850hPa showing the difference between the five wettest and five driest seasons in (a) DJ and (b) FM for zones B and C. The vectors represent the relative strength and direction of the average resultant flux at 850hPa.*

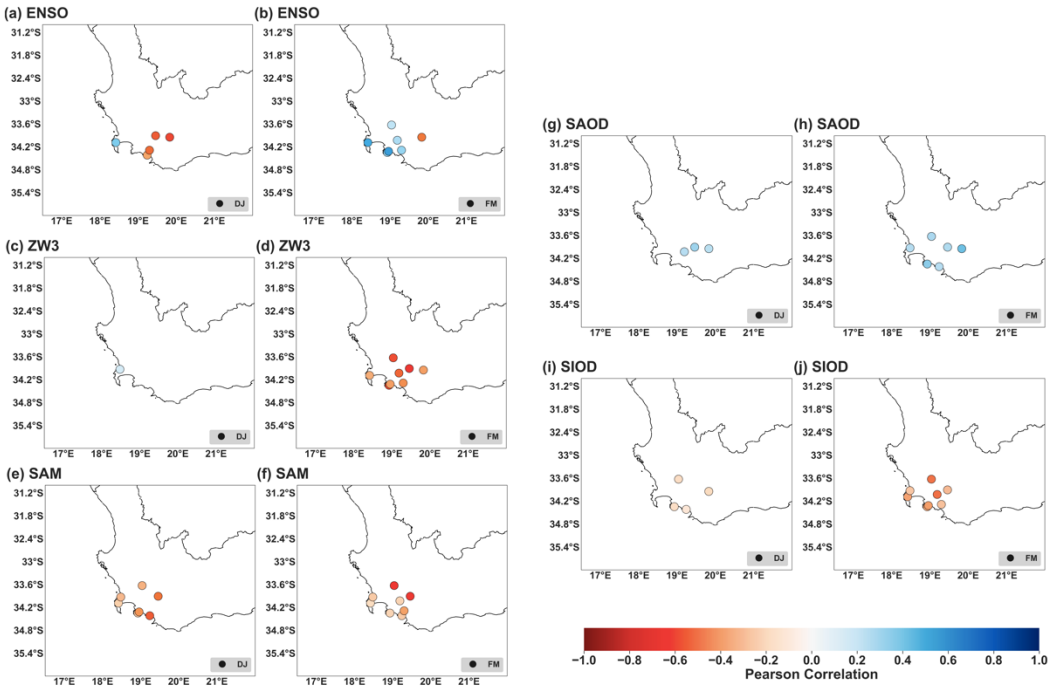

***Figure 6.10**: Pearson correlations between rainfall days at individual stations for zones B and C and various climate modes, namely the Niño 3.4 index (a-b), Zonal Wave Number 3 index (c-d), the Southern Annular Mode index (e-f), the South Atlantic Ocean Dipole index (g-h), and the South Indian Ocean Dipole index (i-j). Only stations with significant correlations at the 90% level are shown. Rainfall detrends were also considered.*

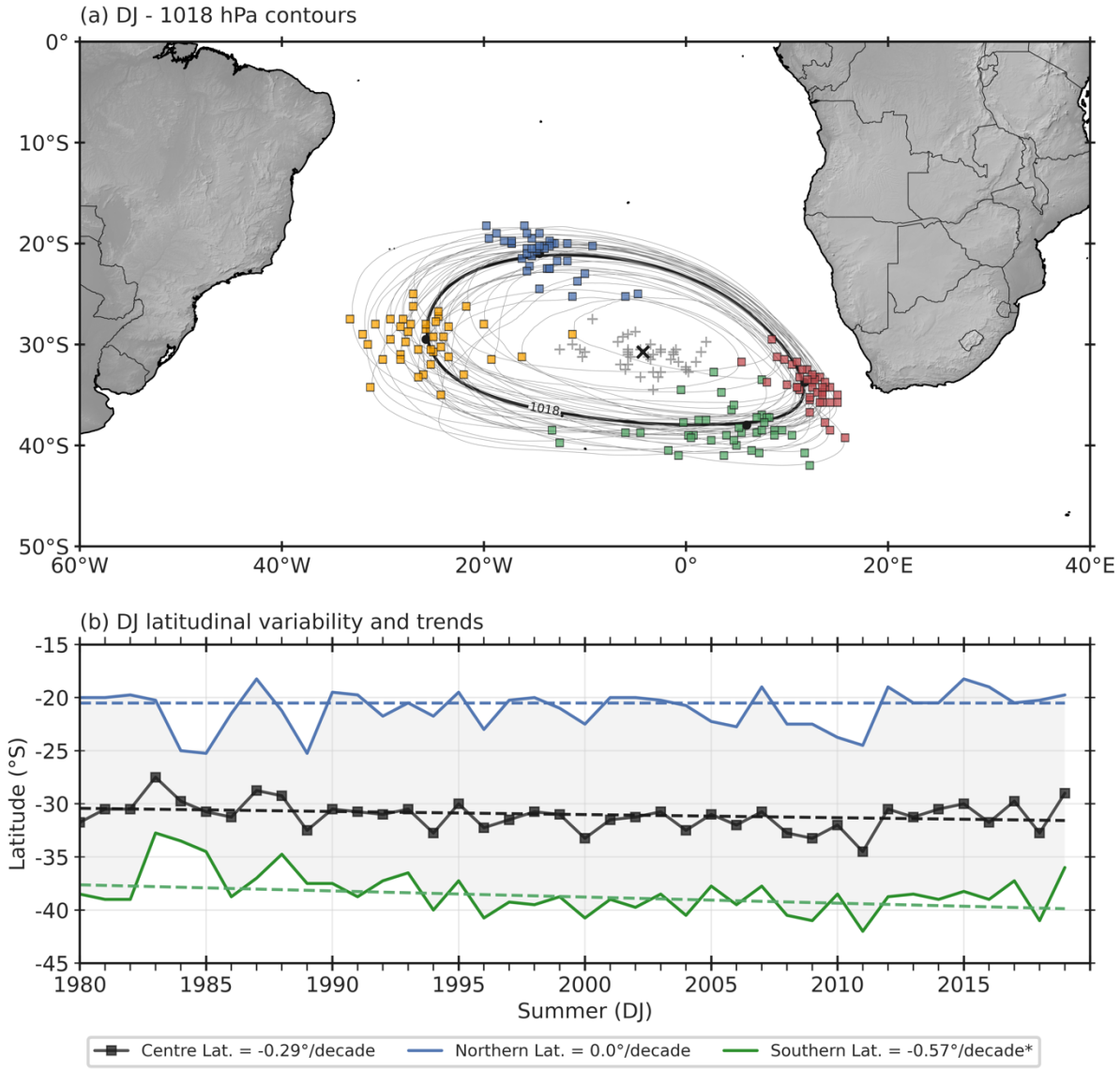

Figure 6.11: *(a) The 1018 hPa contour, representing the SAHP, for each DJ from 1979-2019. The coloured squares represent the outer boundary of the contour (see text), which is used to determine the shift and expansion of the SAHP, while the crosses represent the centre of the system. (b) The DJ interannual variability and trends in the latitudinal position of the northern boundary (blue), centre location (black) and southern boundary (green) of the SAHP. * denotes that the trend is significant at the 95% level, while ** is for the 90% level.*

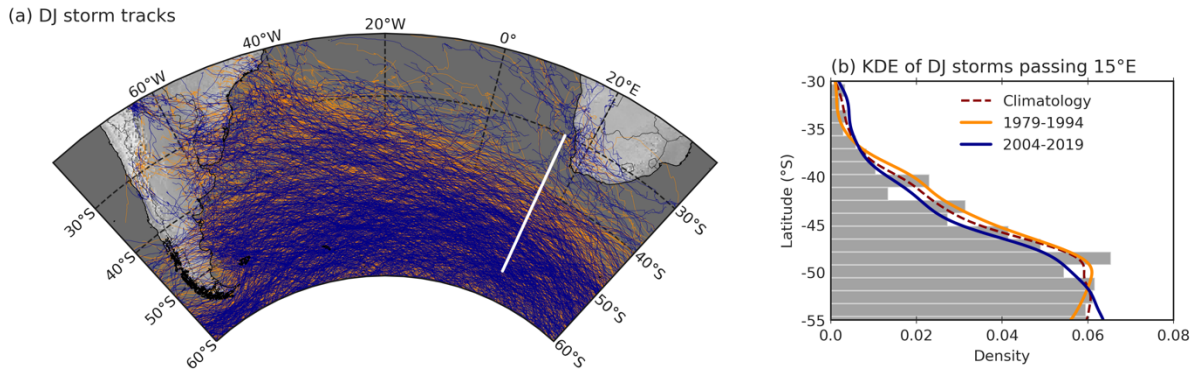

***Figure 6.12**: (a) All tracks of extratropical cyclones during DJ across the South Atlantic from 1979-1994 (orange) and 2004-2019 (blue) and (b) the density of storms that pass 15°E (see white line transect in panel a) in DJ during the first 15 years (1979-1994; orange line) and most recent 15 years (2004-2019; blue line). The dashed red line represents the density of all storms passing through 15°E during DJ from 1979-2019.*

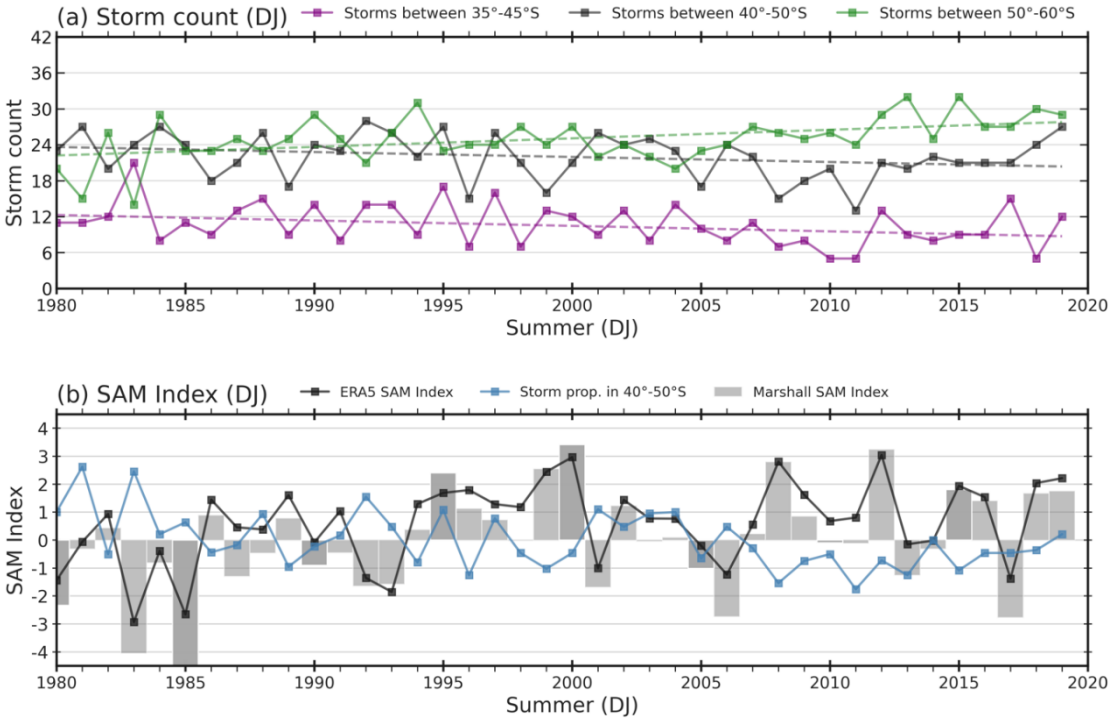

***Figure 6.13**: (a) Interannual variability and trends of storms that pass 15°E between 50-60°S (green), 40-50°S (black) and 35-45°S (purple) during DJ. The increasing (decreasing) trend for storms occurring between 50-60°S (35-45°S) is significant at the 95% (90%) level. (b) The ERA5 SAM index (black line), Marshall SAM index (grey bars) and the standardized anomaly of the proportion of storm tracks between 40-50°S versus 50-60°S (blue line) for DJ from 1979-2019.*

Chapter 7: Summary and Conclusions

The focus of this study has been to analyse rainfall in the SWC during the extended austral summer (October-March) and this is done by identifying the characteristics of large rainfall events (LREs) and their effects. The study also investigates the effects rainfall can have on surface temperatures and extreme hot days during this warmest and driest time of the year. Relationships between rainfall days and large-scale features are also investigated, highlighting differences between anomalously wet and dry seasons.

Although the SWC has relatively sufficient weather station rainfall data compared to the other regions of South Africa, identifying LREs remains a challenge as it is limited by satellite observations over longer periods. In this way *chapter four* only looked at identifying the top 75 events for October-March from 1979-2019. Over time, longer data periods can be developed due to the improvements in monitoring and the longer records of satellite as well as weather station data as they become available. These LREs were objectively identified based on rainfall amounts exceeding the 95th percentile and the extent of the area in the SWC meeting that criterion. Using satellite observations, reanalyses, and synoptic charts, it was shown that ARs and COLs are the most important synoptic system producing LREs in the summer. On average, LREs occur about twice in the summer half of the year but several summers have experienced more than five of these events and some none at all. Typically, COLs tend to contribute more at the beginning and end of the extended summer whereas AR events are more evenly distributed

The extended summer season is relatively understudied as the SWC receives the bulk of its rain from June-August and previous work has focussed largely on either these months, or in some cases May-September (Reason et al., 2002; Reason and Jagadheesha, 2005; Singleton and Reason, 2007a; Blamey et al., 2018; Wolski et al., 2020). Both municipal water managers, and the public at large, have historically been focussed on the amounts of winter rainfall and the associated dam levels before and at the end of the winter rains under the expectation that these need to last through the following summer until the beginning of the next winter rains. However, the recent multi-year 'Day Zero' drought' (2015-2017) has highlighted the vulnerability of greater Cape Town with its rapidly increasing population to winter droughts

(Wolski, 2018; Burls et al., 2019; Ramos et al., 2019) and the need to consider rainfall contributions in the typically much drier summer half of the year.

Based on *chapter four* findings (published as De Kock et al., 2021), LREs may contribute considerably to drought mitigation in the form of increasing dam reservoir levels across the SWC. It was found that COLs (46) and ARs (26) were responsible for ~ 95% of LREs during the extended summer. In *chapter four*, both COLs and ARs are shown to have unique characteristics which are supported by previous studies done on COLs (Singleton and Reason, 2007a; Weldon and Reason 2014) and ARs (Blamey et al., 2018; Ramos et al., 2019) for other times of the year in the region. COLs can be characterized as continuing relatively longer in supplying rainfall over the SWC compared to ARs. However, the generally shorter lived ARs may produce more intense rainfall and hence be more efficient at replenishing dam reservoir losses during the summer. What is concerning is that LREs appear to be happening less frequently during the more recent years in the study period. Should this tendency continue, then the potential for LREs to mitigate winter drought impacts may substantially decrease in future. Previous studies have highlighted the tendency for recent winters to be dry and for this to continue into the future (Reason and Rouault et al., 2005; Mahlalela et al., 2019; Omar and Abiodun, 2020; Roffe et al., 2021).

Chapter five also shows a similar tendency for warmer and drier conditions in the SWC in the last two decades compared to the first two. Only 1 out of the 5 wettest summers occur in the last two decades (2013/14), and this season had a well above average number of LREs (five). This shows the importance of such LREs bringing much needed rainfall into the region. Summer rainfall totals were shown to be inversely correlated ($r = -0.44$) with extreme hot days (90% decile) and this is significant at a 95% level. Rainfall can also bring much needed relief in temperature as well as evaporation rates due to cloud cover. Four out of the five wettest and coolest summers also show weaker winds and more cloud cover which aid in reducing evaporation rates. Such anomalously cool, wet and cloudy summers then lead to less water consumption by the public and agriculture than average and to a generally reduced fire risk over this fire-prone region. They can also mitigate existing late winter drought as well as provide some insurance should the following winter be significantly drier than average.

However, the tendency for less of these anomalously wet summers in the last two decades as well as the significantly increasing trend in extreme hot days (found in *Chapter five* to be 2.8

days/decade) is concerning. These tendencies suggest the likelihood of increasing water demands and fire risk in future. Coupled with the rapidly increasing population in the greater Cape Town region, such tendencies pose significant challenges for local and provincial government.

Chapter six (published in De Kock et al., 2022) examined variability and trends in rain day frequencies over the SWC during the summer and the associated circulation patterns and mechanisms. More rain days are associated with cyclonic anomalies over the SWC region and nearby South East Atlantic as well as increased moisture fluxes into the region. These anomalously wet summers can be most related to SAM and the positioning of the SAHP. Both SAM and SAHP position influence storm track trajectories in the region. Similar mechanisms have previously been suggested for increased winter rainfall (Reason et al., 2002; Reason and Rouault, 2005; Sousa et al., 2018; Burls et al., 2019; Mahlalela et al., 2019). Storm counts in the South Atlantic show that decreases around the SWC during unusually dry summers could be related to poleward positions and expansion of the SAHP. Recent poleward expansions of the SAHP have been well studied (Sousa et al., 2018; Burls et al., 2019) for the winter and have been suggested to influence rainfall in the region and promote drought-favourable conditions. Much like the decrease in LREs in recent years seen in *Chapter four*, a significant decrease in rainfall days is also seen in the core summer (December-January) and late summer (February-March).

Along with increased cyclonic activity off the coast of the SWC during anomalously wet summers, regional features such as shifts in the subtropical jet and moisture corridors with supporting wind fields, were also found. These anomalies, together with SAHP shifts, suggests that storm tracks veer towards the SWC during wet summers. However, recent years have tended to show a decrease in LREs (*Chapter four*) with COLs in particular showing lower occurrences in about the last 20 years while *Chapter six* found a decrease in storm tracks located further north in this period. These results are consistent with Reboita et al. (2018) who indicated future decreases in cyclone frequency in the South Atlantic Ocean. From *Chapter five* and **Appendix E**, more storms in the region generally mean fewer dry days and shorter dry spells during the summer. If these trends continue, then the SWC is likely to experience a drier climate with fewer cases of wet summers with substantial rainfall. *Chapter six (*published in De Kock et al., (2022) jointly demonstrate that in general, storms have cumulatively decreased in recent years with the midlatitude storms tending to be located further south, and the strong

linkage to the tendency for SAM to be more in positive phase in recent decades. Anomalies in rain day numbers at particular SWC locations were found to be related to SST modes (SAOD, SIOD) as well as to ENSO and the zonal wave number 3 pattern during the core and late summer (December to March), depending on the actual location of the station in the SWC .

It is important to note that, on average, the extended summer contributes about one third of the annual rainfall total. This is a not insignificant amount suggesting that the historical focus of research on variability in the winter rainfall only is inadequate for fully understanding the climate of the region. Furthermore, in some summers, relatively intense rainfall events occur. These results, those of Mahlalela et al. (2019) indicating early winter drying over the SWC in recent decades, and into the future, together with suggestions that rainfall seasonality over South Africa may change (Roffe et al., 2022) all argue for the need for increased research on SWC summer rainfall variability and trends. This thesis has provided evidence that some anomalously wet summers with their LREs can help mitigate winter drought. Whether or not these summers may continue to play this role in future remains to be fully investigated. However, more research on these anomalous summers would give a better understanding of the rainfall inputs into the water resources available for usage throughout the year and which need to be better managed by local authorities.

Another area needing more work concerns the characteristics, variability and trends of mid-latitude storms and associated surface heat fluxes over the poorly sampled Southern Ocean in general, and the South Atlantic sector in particular. These weather systems are crucial for SWC rainfall in both the winter (e.g., Tyson and Preston-Whyte, 2000; Reason et al., 2002; Reason and Jagadheesha, 2005) and, as shown in this thesis, the summer. Improved satellite observations and reanalyses with higher resolution such as ERA5 may help in better understanding these systems as well as those cases which are associated with ARs and COLs, and potentially LREs in the SWC. However, it must be noted that previous studies have shown significant differences between *in situ* data and various reanalyses such as for surface winds in the midlatitude South Atlantic (Schmidt et al., 2017).

In conclusion, this thesis has provided evidence of the importance of anomalously wet summers to annual rainfall totals in the SWC, and their potential for the mitigation of the effects of some severe winter droughts. However, these anomalously wet seasons appear to have occurred less frequently in the last two decades so their benefits may become less obvious in the future.

Nevertheless, any summer that is cooler and wetter than average reduces water consumption and reduces fire-risk in this highly fire-prone region. Since such summers also typically involve anomalous winds, there are also important implications for the coastal ocean either through changes in wind-driven upwelling or by changing the likelihood of harmful algal bloom events which occur in most late summers in parts of the west coast.

Given the importance of changes in the frequency and intensity of rain-bearing systems over the SWC to its economy, agriculture, and the reliance on a few large dams as the main water source, it is clear that better understanding of its rainfall variability and trends throughout the year is needed. Water resource managers face increasing challenges due to a rapidly increasing population in the greater Cape Town region and the expense and long lead time in improving water supply infrastructure, particularly large dams. The results of this thesis, together with previous work, suggests that the SWC has experienced drier conditions in the most recent decades, particularly in the later summer and the early winter. Should such tendencies continue, further efforts by the community to use available water more efficiently and reduce wastage that were emphasized during the recent "Day Zero" drought would then become increasingly important. Further research is therefore needed to establish more robustly whether these recent tendencies are likely to continue or worsen throughout the 21st Century.

References

Abram, N.J., Mulvaney, R., Vimeux, F., Phipps, S.J., Turner, J. and England, M.H., 2014. Evolution of the Southern Annular Mode during the past millennium. *Nat. Clim. Chang.,* **4**(7):564-569. https://doi.org/10.1038/nclimate2235

Al Fahad, A., Burls, N.J. and Strasberg, Z., 2020. How will southern hemisphere subtropical anticyclones respond to global warming? Mechanisms and seasonality in CMIP5 and CMIP6 model projections. *Climate Dyn.*, **55**(3): 703-718. https://doi.org/10.1007/s00382-020-05290-7

Allen, M.R. and Ingram, W.J., 2002. Constraints on future changes in climate and the hydrologic cycle. *Nature*, **419**(6903): 228-232. https://doi.org/10.1038/nature01092

Archer, E., Landman W.A., Malherbe, J., Tadross, M. and Pretorius, S. 2019. South Africa's winter rainfall region drought: a region in transition? *Clim. Risk Manag*., **25**: 100188. https://doi.org/10.1016/j.crm.2019.100188

Barnes, M.A., Ndarana, T. and Landman, W.A., 2021. Cut-off lows in the Southern Hemisphere and their extension to the surface. *Clim. Dyn.*, **56**(11): 3709-3732. https://doi.org/10.1007/s00382-021-05662-7

Behera, S.K. and Yamagata, T., 2001. Subtropical SST dipole events in the southern Indian Ocean. *Geophys. Res. Lett*., **28**(2): 327-330. https://doi.org/10.1029/2000GL011451

Bengtsson, L., Hodges, K.I. and Roeckner, E., 2006. Storm tracks and climate change. *J. Clim.*, **19**(15): 3518-3543. https://doi.org/10.1175/JCLI3815.1

Blamey, R.C., Ramos, A.M., Trigo, R.M., Tomé, R. and Reason, C.J.C., 2018: The influence of atmospheric rivers over the South Atlantic on winter rainfall in South Africa. *J. Hydrometeor.*, **19**(1):127-142, https://doi.org/10.1175/JHM-D-17-0111.1.

Botai, C.M., Botai, J.O., De Wit, J.P., Ncongwane, K.P. and Adeola, A.M., 2017. Drought characteristics over the western cape province, South Africa. *Water*, **9**(11): 876. https://doi.org/10.3390/w9110876

Burgess, A.J., Retkute, R., Preston, S.P., Jensen, O.E., Pound, M.P., Pridmore, T.P. and Murchie, E.H., 2016. The 4-dimensional plant: effects of wind-induced canopy movement on light fluctuations and photosynthesis. *Front. Plant Sci*., **7** :1392. https://doi.org/10.3389/fpls.2016.01392

Burls, N.J., Blamey, R.C., Cash, B.A., Swenson, E.T., al Fahad, A., Bopape, M.J.M., Straus, D.M. and Reason, C.J., 2019: The Cape Town "Day Zero" drought and Hadley cell expansion. *NPJ Clim. Atmos. Sci*., **2**(1):1-8. https://doi.org/10.1038/s41612-019-0084-6.

Burls, N. and Reason, C.J.C., 2008. Modelling the sensitivity of coastal winds over the Southern Benguela upwelling system to different SST forcing. *J. Mar. Syst*., **74**(1-2): 561-584. https://doi.org/10.1016/j.jmarsys.2008.04.009

Cai, W. and Cowan, T., 2006. SAM and regional rainfall in IPCC AR4 models: Can anthropogenic forcing account for southwest Western Australian winter rainfall reduction?. *Geophys. Res. Lett*., **33**(24). https://doi.org/10.1029/2006GL028037

Cai, W., Sullivan, A. and Cowan, T., 2011. Interactions of ENSO, the IOD, and the SAM in CMIP3 models. *J. Clim*., **24**(6): 1688-1704. https://doi.org/10.1175/2010JCLI3744.1

Clulow, A.D., Everson, C.S., Mengistu, M.G., Jarmain, C., Jewitt, G.P.W., Price, J.S. and Grundling, P.L., 2012. Measurement and modelling of evaporation from a coastal wetland in Maputaland, South Africa. *Hydrol. Earth Syst. Sci*., **16**(9): 3233-3247. https://doi.org/10.5194/hess-16-3233-2012

Codron, F., 2005. Relation between annular modes and the mean state: Southern Hemisphere summer. *J. Clim*., **18**(2): 320-330. https://doi.org/10.1175/JCLI-3255.1

Colberg, F., Reason, C.J.C. and Rodgers, K., 2004. South Atlantic response to El Niño–Southern Oscillation induced climate variability in an ocean general circulation model. *J. Geophys. Res.: Oceans*, **109**(C12). https://doi.org/10.1029/2004JC002301

Cordeira, J.M., Ralph, F.M., Martin, A., Gaggini, N., Spackman, J.R., Neiman, P.J., Rutz, J.J. and Pierce, R., 2017. Forecasting atmospheric rivers during CalWater 2015. *Bull. Am. Meteorol. Soc*., **98**(3): 449-459. https://doi.org/10.1175/BAMS-D-15-00245.1

De Coning, E., 2013. Optimizing satellite-based precipitation estimation for nowcasting of rainfall and flash flood events over the South African domain. *Remote Sens*., **5**(11): 5702-5724. https://doi.org/10.3390/rs5115702

De Kock, W.M., Blamey, R.C. and Reason, C.J.C., 2021. Large summer rainfall events and their importance in mitigating droughts over the South Western Cape, South Africa. *J. Hydrometeorol.*, **22**(3): 587-599. https://doi.org/10.1175/JHM-D-20-0123.1

De Kock, W.M., Blamey, R.C. and Reason, C.J.C., 2022. Large-scale mechanisms linked to anomalously wet summers over the southwestern Cape, South Africa. *Clim. Dyn*., **20**: 1-15. https://doi.org/10.1007/s00382-022-06280-7

de Waal, J. H., Chapman, A., and Kemp, J., 2017: Extreme 1-day rainfall distributions: Analysing change in the Western Cape, *S. Afr. J. Sci*., **113**(8):43–50, https://doi.org/10.17159/sajs.2017/20160301.

Dee, D.P., Uppala, S.M., Simmons, A.J., Berrisford, P., Poli, P., Kobayashi, S., Andrae, U., Balmaseda, M.A., Balsamo, G., Bauer, D.P. and Bechtold, P., 2011: The ERA-Interim reanalysis: Configuration and performance of the data assimilation system. *Q. J. R. Meteorol. Soc*., **137**(656):553-597, https://doi.org/10.1002/qj.828.

Dettinger, M.D., Ralph, F.M., Das, T., Neiman, P.J. and Cayan, D.R., 2011: Atmospheric rivers, floods and the water resources of California. *Water*, **3**(2):445-478, https://doi.org/10.3390/w3020445.

Donat, M.G., Lowry, A.L., Alexander, L.V., O'Gorman, P.A. and Maher, N., 2016. More extreme precipitation in the world's dry and wet regions. *Nat. Clim. Change*, **6**(5): 508-513. https://doi.org/10.1038/nclimate2941

Durgadoo, J.V., Loveday, B.R., Reason, C.J., Penven, P. and Biastoch, A., 2013. Agulhas leakage predominantly responds to the Southern Hemisphere westerlies. *J. Phys. Oceanogr.* , **43**(10): 2113-2131. https://doi.org/10.1175/JPO-D-13-047.1

Durre, I., Menne, M.J., Gleason, B.E., Houston, T.G. and Vose, R.S., 2010. Comprehensive automated quality assurance of daily surface observations. *J. Appl. Meteor. Climatol.*, **49**(8): 1615-1633. https://doi.org/10.1175/2010JAMC2375.1

Dyer, E., Hirons, L. and Taye, M.T., 2022. July–September rainfall in the Greater Horn of Africa: the combined influence of the Mascarene and South Atlantic highs. *Clim. Dyn.*, 1-21. https://doi.org/10.1007/s00382-022-06287-0

Eiras-Barca, J., Brands, S. and Miguez-Macho, G., 2016: Seasonal variations in North Atlantic atmospheric river activity and associations with anomalous precipitation over the Iberian Atlantic Margin. *J. Geophys. Res. Atmos.*, **121**(2):931-948, https://doi.org/10.1002/2015JD023379.

Engelbrecht, C.J., Landman, W.A., Engelbrecht, F.A. and Malherbe, J., 2015. A synoptic decomposition of rainfall over the Cape south coast of South Africa. *Clim. Dyn.*, **44**(9-10): 2589-2607. https://doi.org/10.1007/s00382-014-2230-5

Fauchereau, N., Trzaska, S., Richard, Y., Roucou, P. and Camberlin, P., 2003. Sea-surface temperature co-variability in the Southern Atlantic and Indian Oceans and its connections with the atmospheric circulation in the Southern Hemisphere. *Int. J. Climatol.*, **23**(6): 663-677. https://doi.org/10.1002/joc.905

Favre, A., Hewitson, B., Lennard, C., Cerezo-Mota, R. and Tadross, M., 2013. Cut-off lows in the South Africa region and their contribution to precipitation. *Clim. Dyn.*, **41**(9-10): 2331-2351. https://doi.org/10.1007/s00382-012-1579-6

Garreaud, R., 2013. Warm winter storms in Central Chile. *J. Hydrometeorol*., **14**(5): 1515-1534. https://doi.org/10.1175/JHM-D-12-0135.1

Geng, Q. and Sugi, M., 2003. Possible change of extratropical cyclone activity due to enhanced greenhouse gases and sulfate aerosols—Study with a high-resolution AGCM. *J. Clim.*, **16**(13): 2262-2274. https://doi.org/10.1175/1520-0442(2003)16<2262:PCOECA>2.0.CO;2

Gillett, N.P. and Stott, P.A., 2009. Attribution of anthropogenic influence on seasonal sea level pressure. *Geophys. Res. Lett*., **36**(23). https://doi.org/10.1029/2009GL041269

Gillett, N.P., Zwiers, F.W., Weaver, A.J. and Stott, P.A., 2003. Detection of human influence on sea-level pressure. *Nature*, **422**(6929): 292-294. https://doi.org/10.1038/nature01487

Gilliland, J.M. and Keim, B.D., 2018. Position of the South Atlantic Anticyclone and its impact on surface conditions across Brazil. *J. Appl. Meteor. Climatol*., **57**(3): 535-553. https://doi.org/10.1175/JAMC-D-17-0178.1

Gimeno, L., Dominguez, F., Nieto, R., Trigo, R., Drumond, A., Reason, C.J., Taschetto, A.S., Ramos, A.M., Kumar, R. and Marengo, J., 2016: Major mechanisms of atmospheric moisture transport and their role in extreme precipitation events. *Annu. Rev. Environ. Resour*., **41**:117-141. https://doi.org/10.1146/annurev-environ-110615-085558.

Gimeno, L., Nieto, R., Vázquez, M. and Lavers, D.A., 2014: Atmospheric rivers: A mini-review. *Front. Earth Sci*., **2**(2), https://doi.org/10.3389/feart.2014.00002

Grab, S. and Craparo, A., 2011. Advance of apple and pear tree full bloom dates in response to climate change in the southwestern Cape, South Africa: 1973–2009. *Agric. For. Meteorol.*, **151**(3): 406-413. https://doi.org/10.1016/j.agrformet.2010.11.001

Gramcianinov, C.B., Campos, R.M., de Camargo, R., Hodges, K.I., Guedes Soares, C., da Silva Dias, P.L., 2020. "Analysis of Atlantic extratropical storm tracks characteristics in 41 years of ERA5 and CFSR/CFSv2 databases", *Ocean Eng*.,216C, 108111. https://doi.org/10.1016/j.oceaneng.2020.108111

Gramcianinov, C.B., Hodges, K.I. and Camargo, R.D., 2019. The properties and genesis environments of South Atlantic cyclones. Climate Dynamics, 53(7), pp.4115-4140.

Grise, K.M., Davis, S.M., Staten, P.W. and Adam, O., 2018. Regional and seasonal characteristics of the recent expansion of the tropics. *J. Climate*, **31**(17): 6839-6856. https://doi.org/10.1175/JCLI-D-18-0060.1

Hall, A. and Visbeck, M., 2001. Ocean and Sea Ice response to the Southern Hemisphere Annular Mode: Results from a coupled climate model. *Clivar Exchanges*, **22**(6 (4)): 4-6.

Hart, R. and Grumm, R.H., 2001: Using normalized climatological anomalies to objectively rank extreme synoptic-scale events. *Mon. Wea. Rev.*, **129**:2426-2442, https://doi.org/10.1175/1520-0493(2001)129<2426:UNCATR>2.0.CO;2.

Hartmann, D.L. and Lo, F., 1998. Wave-driven zonal flow vacillation in the Southern Hemisphere. *J. Atmos. Sci.*, **55**(8): 1303-1315. https://doi.org/10.1175/1520-0469(1998)055<1303:WDZFVI>2.0.CO;2

Held, I.M. and Soden, B.J., 2006. Robust responses of the hydrological cycle to global warming. *J. Clim.*, **19**(21): 5686-5699. https://doi.org/10.1175/JCLI3990.1

Hermes, J.C. and Reason, C.J.C., 2005. Ocean model diagnosis of interannual coevolving SST variability in the South Indian and South Atlantic Oceans. *J. Clim.*, **18**(15): 2864-2882. https://doi.org/10.1175/JCLI3422.1

Hersbach, H., Bell, B., Berrisford, P., Hirahara, S., Horányi, A., Muñoz-Sabater, J., Nicolas, J., Peubey, C., Radu, R., Schepers, D. and Simmons, A., 2020. The ERA5 global reanalysis. *Q. J. R. Meteorol.*, **146**(730): 1999-2049. https://doi.org/10.1029/2012GL052910

Hoell, A. and Cheng, L., 2018. Austral summer Southern Africa precipitation extremes forced by the El Niño-Southern oscillation and the subtropical Indian Ocean dipole. Clim. Dyn., **50**(9): 3219-3236. https://doi.org/10.1007/s00382-017-3801-z

Hoffman, M.T., Cramer, M.D., Gillson, L. and Wallace, M., 2011. Pan evaporation and wind run decline in the Cape Floristic Region of South Africa (1974–2005): implications for vegetation responses to climate change. *Climatic Change*, **109**(3): 437-452. https://doi.org/10.1007/s10584-011-0030-z

Holmes, P.M., Esler, K.J., Geerts, S., Ngwenya, D.K., Rebelo, A.G., Dorse, C., van der Merwe, J., Retief, J., Hall, S.A., Grey, P. and Nsikani, M.N., 2022. Guidelines for restoring Lowland Sand Fynbos ecosystems. http://biodiversityadvisor.sanbi.org/planning-and-assessment/ecological-restoration/

Hoskins, B.J. and Hodges, K.I., 2005. A new perspective on Southern Hemisphere storm tracks. *J. Clim*., **18**(20): 4108-4129. https://doi.org/10.1175/JCLI3570.1

IPCC et al. 2013 Annex I: Atlas of global and regional climate projections ed G. J. van Oldenborgh et al Climate Change 2013: The Physical Science Basis. Contribution of Working Group I to the Fifth Assessment Report of the Intergovernmental Panel on Climate Change ed. T. F. Stocker (Cambridge, New York: Cambridge University Press)

Jakobson, E., Vihma, T., Palo, T., Jakobson, L., Keernik, H. and Jaagus, J., 2012: Validation of atmospheric reanalyses over the central Arctic Ocean. *Geophys. Res. Lett*., **39**(10), https://doi.org/10.1029/2012GL051591.

Jones, D.A. and Simmonds, I., 1993. A climatology of Southern Hemisphere extratropical cyclones. *Clim. Dyn*., **9**(3): 131-145. https://doi.org/10.1007/BF00209750

Jury, M.R., 1987. Aircraft observations of meteorological conditions along Africa's West Coast between 30–35 South. *J. Appl. Meteorol. Climatol*., **26**(11): 1540-1552. https://doi.org/10.1175/1520-0450(1987)026<1540:AOOMCA>2.0.CO;2

Jury, M.R., 1993. A preliminary note on rainfall and vegetation trends in the south-western Cape: 1985–1988. *S. Afr. J. Bot*., **59**(2):265-269.

Jury, M.R., 2020. Climate trends in the Cape Town area, South Africa. *Water SA*, **46**(3): 438-447. https://doi.org/10.17159/wsa/2020.v46.i3.8654

Kendall, M. G., 1975. Rank Correlation Methods. 4th Edition. London: Charles Griffin.

Kishore, P., Ratnam, M.V., Namboothiri, S.P., Velicogna, I., Basha, G., Jiang, J.H., Igarashi, K., Rao, S.V.B. and Sivakumar, V., 2011. Global (50 S–50 N) distribution of water vapor observed by COSMIC GPS RO: Comparison with GPS radiosonde, NCEP, ERA-Interim, and JRA-25 reanalysis data sets. *J. Atmos. Sol.-Terr. Phys*., **73**(13): 1849-1860. https://doi.org/10.1016/j.jastp.2011.04.017

Kishore, P., Ratnam, M.V., Namboothiri, S.P., Velicogna, I., Basha, G., Jiang, J.H., Igarashi, K., Rao, S.V.B. and Sivakumar, V., 2011: Global (50 S–50 N) distribution of water vapor observed by COSMIC GPS RO: Comparison with GPS radiosonde, NCEP, ERA-Interim, and JRA-25 reanalysis data sets. *J. Atmos.. Sol.-Terr. Phys*., **73**(13):1849-1860, https://doi.org/10.1016/j.jastp.2011.04.017.

Kruger, A.C. and Nxumalo, M.P., 2017. Historical rainfall trends in South Africa: 1921–2015. *Water SA*, **43**(2): 285-297. https://doi.org/10.4314/wsa.v43i2.12

Kruger, A.C., Goliger, A.M., Retief, J.V. and Sekele, S., 2010. Strong wind climatic zones in South Africa. http://hdl.handle.net/10204/4187

Lavers, D.A., Beljaars, A., Richardson, D.S., Rodwell, M.J. and Pappenberger, F., 2019. A forecast evaluation of planetary boundary layer height over the ocean. *J. Geophys. Res: Atmospheres*, **124**(9): 4975-4984. https://doi.org/10.1029/2019JD030454

Lindesay JA. 1988. South African rainfall, the Southern Oscillation and a Southern Hemisphere semi-annual cycle. J.
Climatol. 8: 17–30.

Loveday, B.R., Durgadoo, J.V., Reason, C.J., Biastoch, A. and Penven, P., 2014. Decoupling of the Agulhas leakage from the Agulhas Current. *J. Phys. Oceanogr.*, **44**(7): 1776-1797. https://doi.org/10.1175/JPO-D-13-093.1

Lu, J., Deser, C. and Reichler, T., 2009: Cause of the widening of the tropical belt since 1958. *Geophys. Res. Lett*., **36**(3), https://doi.org/10.1029/2008GL036076.

Lübbecke, J.F., Burls, N.J., Reason, C.J. and McPhaden, M.J., 2014. Variability in the South Atlantic anticyclone and the Atlantic Niño mode. Journal of Climate, 27(21), pp.8135-8150.

Lucas, C., Timbal, B. and Nguyen, H., 2014: The expanding tropics: a critical assessment of the observational and modeling studies. Wiley Interdiscip. *Rev. Clim. Change*, **5**(1):89-112, https://doi.org/10.1002/wcc.251.

Lutjeharms, J.R.E., 1981. Satellite studies of the South Atlantic upwelling system. In Oceanography from space (195-199). Springer, Boston, MA.

Mächel, H., Kapala, A. and Flohn, H. (1998a) Behaviour of the centres of action above the Atlantic since 1881. Part I: characteristics of seasonal and interannual variability. *Int. J. Climatol*., **18**: 1–22. https://doi.org/10.1002/(SICI)1097-0088(199801)18:1<1::AID-JOC225>3.0.CO;2-A

Mahlalela, P.T., Blamey, R.C. and Reason, C.J.C., 2019. Mechanisms behind early winter rainfall variability in the southwestern Cape, South Africa. *Clim. Dyn*., **53**(1): 21-39. https://doi.org/10.1007/s00382-018-4571-y

Mann, H. B., 1945. Nonparametric tests against trend. Econometrica: *J. Econom. Soc*., 245–259. https://doi.org/10.2307/1907187

Marchant, R., Mumbi, C., Behera, S. and Yamagata, T., 2007. The Indian Ocean dipole–the unsung driver of climatic variability in East Africa. *Afr. J. Ecol*., **45**(1): 4-16. https://doi.org/10.1111/j.1365-2028.2006.00707.x

Marshall, G.J., 2003. Trends in the Southern Annular Mode from observations and reanalyses. *J. Clim*., **16**(24): 4134-4143.Error! Hyperlink reference not valid.

Molekwa, S., Engelbrecht, C.J. and Rautenbach, C.D., 2014: Attributes of cut-off low induced rainfall over the Eastern Cape Province of South Africa. *Theor. Appl. Climatol*, **118**(1-2):307-318. https://doi.org/10.1007/s00704-013-1061-3

Muller, M., 2018. Cape Town's drought: don't blame climate change. *Nature*, **559**: 174-176. https://doi.org/10.1038/d41586-018-05649-1

Murray, R.J. and Simmonds, I., 1991. A numerical scheme for tracking cyclone centres from digital data. *Aust. Meteorol. Mag.*, **39**(3): 155-166.

Naik, M. and Abiodun, B.J., 2020. Projected changes in drought characteristics over the Western Cape, South Africa. *Meteorol. Appl.*, **27**(1): 1802. https://doi.org/10.1002/met.1802

Ndebele, N.E., Grab, S. and Turasie, A., 2020. Characterizing rainfall in the south-western Cape, South Africa: 1841–2016. *Int. J. Climatol.*, **40**(4): 1992-2014. https://doi.org/10.1002/joc.6314

Neiman, P.J., Ralph, F.M., White, A.B., Kingsmill, D.E. and Persson, P.O.G., 2002: The statistical relationship between upslope flow and rainfall in California's coastal mountains: Observations during CALJET. *Mon. Wea. Rev.*, **130**(6):1468-1492, https://doi.org/10.1175/1520-0493(2002)130<1468:TSRBUF>2.0.CO;2.

Nguyen, H., Evans, A., Lucas, C., Smith, I. and Timbal, B., 2013. The Hadley circulation in reanalyses: Climatology, variability, and change. *J. Clim.*, **26**(10): 3357-3376. https://doi.org/10.1175/JCLI-D-12-00224.1

Nicholson SE, Kim J. 1997. The relationship of the El Nin˜o–Southern Oscillation to African rainfall. *Int. J. Climatol.*17: 117–135. https://doi.org/10.1002/(SICI)1097-0088(199702)17:2<117::AID-JOC84>3.0.CO;2-O

Nieto, R., Castillo, R. and Drumond, A., 2014. The modulation of oceanic moisture transport by the hemispheric annular modes. *Front. Earth Sci.*, **2**: 11. https://doi.org/10.3389/feart.2014.00011

Nieto, R., Gimeno, L., de La Torre, L., Ribera, P., Gallego, D., García-Herrera, R., García, J.A., Nuñez, M., Redaño, A. and Lorente, J., 2005: Climatological features of cutoff low systems in the Northern Hemisphere. *J. Clim.*, **18**(16):3085-3103, https://doi.org/10.1175/JCLI3386.1.

Nieto, R., Sprenger, M., Wernli, H., Trigo, R.M. and Gimeno, L., 2008: Identification and Climatology of Cut-off Lows near the Tropopause. *Ann. NY. Acad. Sci.*, **1146**(1):256-290, https://doi.org/10.1196/annals.1446.016.

Nnamchi, H.C., Li, J. and Anyadike, R.N., 2011. Does a dipole mode really exist in the South Atlantic Ocean?. *J. Geophys. Res.*: Atmospheres, **116**(D15). https://doi.org/10.1029/2010JD015579

Nnamchi, H.C., Li, J., Kang, I.S. and Kucharski, F., 2013. Simulated impacts of the South Atlantic Ocean Dipole on summer precipitation at the Guinea Coast. *Clim. Dyn*., **41**(3): 677-694. https://doi.org/10.1007/s00382-012-1629-0

Omar, S.A. and Abiodun, B.J., 2020. Characteristics of cut-off lows during the 2015–2017 drought in the Western Cape, South Africa. *Atmos. Res.*, **235**: 104772. https://doi.org/10.1016/j.atmosres.2019.104772

Onoda, Y. and Anten, N.P., 2011. Challenges to understand plant responses to wind. *Plant Signaling & Behavior*, **6**(7): 1057-1059. https://doi.org/10.4161/psb.6.7.15635

Pascale, S., Kapnick, S.B., Delworth, T.L. and Cooke, W.F., 2020. Increasing risk of another Cape Town "Day Zero" drought in the 21st century. *Proc. Natl. Acad. Sci. U.S.A*., **117**(47): 29495-29503. https://doi.org/10.1073/pnas.2009144117

Payne, A.E., Demory, M.E., Leung, L.R., Ramos, A.M., Shields, C.A., Rutz, J.J., Siler, N., Villarini, G., Hall, A. and Ralph, F.M., 2020. Responses and impacts of atmospheric rivers to climate change. *Nat. Rev. Earth Environ*., **1**(3): 143-157. https://doi.org/10.1038/s43017-020-0030-5

Pezza, A.B., Durrant, T., Simmonds, I. and Smith, I., 2008. Southern Hemisphere synoptic behavior in extreme phases of SAM, ENSO, sea ice extent, and southern Australia rainfall. *J. Clim*., **21**(21): 5566-5584. https://doi.org/10.1175/2008JCLI2128.1

Pezza, A.B., Simmonds, I. and Renwick, J.A., 2007. Southern Hemisphere cyclones and anticyclones: Recent trends and links with decadal variability in the Pacific Ocean. *Int. J. Climatol.: J. Roy. Meteorol. Soc*., **27**(11): 1403-1419. https://doi.org/10.1002/joc.1477

Philippon, N., Rouault, M., Richard, Y. and Favre, A., 2012. The influence of ENSO on winter rainfall in South Africa. *Int. J. Climatol*., **32**(15): 2333-2347. https://doi.org/10.1002/joc.3403

Pienaar, A., Brent, A.C., Musango, J.K. and De Kock, I.H., 2017: Water resource infrastructure implications of a green economy transition in the Western Cape Province of South Africa: A system dynamics approach. *S. Afr. J. Ind. Eng*., **28**(2):78-94. http://dx.doi.org/10.7166/28-2-1639.

Pohl, B. and Matthews, A.J., 2007. Observed changes in the lifetime and amplitude of the Madden–Julian oscillation associated with interannual ENSO sea surface temperature anomalies. *J. Clim*., **20**(11): 2659-2674. https://doi.org/10.1175/JCLI4230.1

Poli, P., Healy, S.B. and Dee, D.P., 2010: Assimilation of Global Positioning System radio occultation data in the ECMWF ERA–Interim reanalysis. *Q. J. R. Meteorol. Soc*., **136**(653):1972-1990, https://doi.org/10.1002/qj.722.

Preston-Whyte, R.A., Diab, R.D. and Tyson, P.D., 1977. Towards an inversion climatology of Southern Africa: Part II, non-surface inversions in the lower atmosphere. S. Afr. Geogr. J. .**59**(1): 45-59. https://doi.org/10.1080/03736245.1977.9713494

Ralph, F.M., Coleman, T., Neiman, P.J., Zamora, R.J. and Dettinger, M.D., 2013: Observed impacts of duration and seasonality of atmospheric-river landfalls on soil moisture and runoff in coastal northern California. *J. Hydrometeor*., **14**(2):443-459, https://doi.org/10.1175/JHM-D-12-076.1.

Ralph, F.M., Neiman, P.J. and Wick, G.A., 2004: Satellite and CALJET aircraft observations of atmospheric rivers over the eastern North Pacific Ocean during the winter of 1997/98. *Mon. Wea. Rev.*, **132**(7):1721-1745, https://doi.org/10.1175/1520-0493(2004)132<1721:SACAOO>2.0.CO;2.

Ramos, A.M., Blamey, R.C., Algarra, I., Nieto, R., Gimeno, L., Tomé, R., Reason, C.J. and Trigo, R.M., 2018: From Amazonia to southern Africa: atmospheric moisture transport through low-level jets and atmospheric rivers. *Ann. NY. Acad. Sci*., **1436**(1):217-230, doi: https://10.1111/nyas.13960.

Ramos, A.M., Trigo, R.M., Liberato, M.L. and Tomé, R., 2015: Daily precipitation extreme events in the Iberian Peninsula and its association with atmospheric rivers. *J. Hydrometeor*., **16**(2):579-597, https://doi.org/10.1175/JHM-D-14-0103.1.

Raphael, M.N., 2004. A zonal wave 3 index for the Southern Hemisphere. *Geophys. Res. Lett.*, **31**(23). https://doi.org/10.1029/2004GL020365

Reason, C.J.C., Allan, R.J., Lindesay, J.A. and Ansell, T.J., 2000. ENSO and climatic signals across the Indian Ocean basin in the global context: Part I, Interannual composite patterns. *Int. J. Climatol. : J R Meteorol Soc.*, **20**(11): 1285-1327. https://doi.org/10.1002/1097-0088(200009)20:11<1285::AID-JOC536>3.0.CO;2-R

Reason, C.J.C. and Jagadheesha, D., 2005. Relationships between South Atlantic SST variability and atmospheric circulation over the South African region during austral winter. *J. Clim.*, **18**(16): 3339-3355. https://doi.org/10.1175/JCLI3474.1

Reason, C.J.C. and Jury, M.R., 1990: On the generation and propagation of the southern African coastal low. *Q. J. R. Meteorol. Soc*., **116**(495): 1133-1151, https://doi.org/10.1002/qj.49711649507.

Reason, C.J.C. and Rouault, M., 2002: ENSO-like decadal variability and South African rainfall. *Geophys. Res. Lett*., **29**(13):16-1, https://doi.org/10.1029/2002GL014663.

Reason, C.J.C. and Rouault, M., 2005. Links between the Antarctic Oscillation and winter rainfall over western South Africa. *Geophys. Res. Lett*., **32**(7). https://doi.org/10.1029/2005GL022419

Reason, C.J.C., 2001. Subtropical Indian Ocean SST dipole events and southern African rainfall. *Geophys. Res. Lett*., **28**(11): 2225-2227. https://doi.org/10.1029/2000GL012735

Reason, C.J.C., 2002. Sensitivity of the southern African circulation to dipole sea-surface temperature patterns in the south Indian Ocean. *Int. J. Climatol.*, **22**(4): 377-393. https://doi.org/10.1002/joc.744

Reason, C.J.C., Allan, R.J., Lindesay, J.A. and Ansell, T.J., 2000. ENSO and climatic signals across the Indian Ocean basin in the global context: Part I, interannual composite patterns. *Int. J. Climatol.*, **20**: 1285-1327. https://doi.org/10.1002/1097-0088(200009)20:11<1285::AID-JOC536>3.0.CO;2-R

Reason, C.J.C., Landman, W. and Tennant, W., 2006. Seasonal to decadal prediction of southern African climate and its links with variability of the Atlantic Ocean. *Bull. Am. Meteorol. Soc.*, **87**(7): 941-956. https://doi.org/10.1175/BAMS-87-7-941

Reason, C.J.C., Rouault, M., Melice, J.L. and Jagadheesha, D., 2002: Interannual winter rainfall variability in SW South Africa and large scale ocean–atmosphere interactions. *Meteorol. Atmos. Phys.*, **80**(1-4):19-29, https://doi.org/10.1007/s007030200011.

Reboita, M.S., Ambrizzi, T., Silva, B.A., Pinheiro, R.F. and Da Rocha, R.P., 2019. The South Atlantic subtropical anticyclone: present and future climate. *Front. Earth Sci.*, **7**: 1-15. https://doi.org/10.3389/feart.2019.00008

Reboita, M.S., Da Rocha, R.P. and Oliveira, D.M.D., 2018. Key features and adverse weather of the named subtropical cyclones over the Southwestern South Atlantic Ocean. *Atmosphere*, **10**(1): 6. https://doi.org/10.3390/atmos10010006

Reboita, M.S., Da Rocha, R.P., Ambrizzi, T. and Gouveia, C.D., 2015. Trend and teleconnection patterns in the climatology of extratropical cyclones over the Southern Hemisphere. *Clim. Dyn.*, **45**(7): 1929-1944. https://doi.org/10.1007/s00382-014-2447-3

Reboita, M.S., Reale, M., da Rocha, R.P., Giorgi, F., Giuliani, G., Coppola, E., Nino, R.B.L., Llopart, M., Torres, J.A. and Cavazos, T., 2021. Future changes in the wintertime cyclonic activity over the CORDEX-CORE southern hemisphere domains in a multi-model approach. *Clim. Dyn.*, **57**(5): 1533-1549. https://doi.org/10.1007/s00382-020-05317-z

Roffe, S.J., Steinkopf, J. and Fitchett, J.M., 2022. South African winter rainfall zone shifts: A comparison of seasonality metrics for Cape Town from 1841–1899 and 1933–2020. *Theor. Appl. Climatol*., **147**(3): 1229-1247. https://doi.org/10.1007/s00704-021-03911-7

Rutz, J.J., Steenburgh, W.J. and Ralph, F.M., 2014: Climatological characteristics of atmospheric rivers and their inland penetration over the western United States. *Mon. Wea. Rev.*, **142**(2):905-921,https://doi.org/10.1175/MWR-D-13-00168.1.

Saji, N.H., Goswami, B.N., Vinayachandran, P.N. and Yamagata, T., 1999. A dipole mode in the tropical Indian Ocean. *Nature*, **401**(6751): 360-363. https://doi.org/10.1038/43854

Scheff, J. and Frierson, D.M., 2012. Robust future precipitation declines in CMIP5 largely reflect the poleward expansion of model subtropical dry zones. *Geophys. Res. Lett*., **39**(18). https://doi.org/10.1029/2012GL052910

Schmidt, K.M., Swart, S., Reason, C. and Nicholson, S.A., 2017. Evaluation of satellite and reanalysis wind products with in situ wave glider wind observations in the Southern Ocean. *J. Atmos. Ocean. Technol.,* **34**(12): 2551-2568. https://doi.org/10.1175/JTECH-D-17-0079.1

Seager, R., Naik, N. and Vecchi, G.A., 2010. Thermodynamic and dynamic mechanisms for large-scale changes in the hydrological cycle in response to global warming. *J. Clim.*, **23**(17): 4651-4668. https://doi.org/10.1175/2010JCLI3655.1

Sen, P. K., 1968. Estimates of the regression coefficient based on Kendall's tau. *J. Am. Stat. Assoc*. **63**(324):1379–1389. https://doi.org/10.1080/01621459.1968.10480934

Shepherd, N., 2019. Making sense of "Day Zero": Slow catastrophes, anthropocene futures, and the story of Cape Town's water crisis. *Water*, **11**(9): 1744. https://doi.org/10.3390/w11091744

Silvestri, G.E. and Vera, C.S., 2003. Antarctic Oscillation signal on precipitation anomalies over southeastern South America. *Geophys. Res. Lett*., **30**(21).

https://doi.org/10.1029/2003GL018277

Simmonds, I. and Keay, K., 2000. Mean Southern Hemisphere extratropical cyclone behavior in the 40-year NCEP–NCAR reanalysis. *J. Clim.*, **13**(5): 873-885. https://doi.org/10.1175/1520-0442(2000)013<0873:MSHECB>2.0.CO;2

Sinclair, M.R., 1997. Objective identification of cyclones and their circulation intensity, and climatology. *Weather Forecast.*, **12**(3): 595-612. https://doi.org/10.1175/1520-0434(1997)012%3C0595:OIOCAT%3E2.0.CO;2

Singleton, A.T. and Reason, C.J.C., 2006: Numerical simulations of a severe rainfall event over the Eastern Cape coast of South Africa: sensitivity to sea surface temperature and topography. Tellus A: Dyn. *Meteorol. Oceanogr.*, **58**(3):335-367, https://doi.org/10.1111/j.1600-0870.2006.00180.x.

Singleton, A.T. and Reason, C.J.C., 2007a. Variability in the characteristics of cut-off low pressure systems over subtropical southern Africa. *Int. J. Climatol.*, **27**(3): 295-310. https://doi.org/10.1002/joc.1399

Singleton, A.T. and Reason, C.J.C., 2007b: A numerical model study of an intense cutoff low pressure system over South Africa. *Mon. Wea. Rev.*, **135**(3):1128-1150, https://doi.org/10.1175/MWR3311.1.

Sousa, P.M., Barriopedro, D., Ramos, A.M., García-Herrera, R., Espírito-Santo, F. and Trigo, R.M., 2019: Saharan air intrusions as a relevant mechanism for Iberian heatwaves: The record breaking events of August 2018 and June 2019. *Weather. Clim. Extremes*, **26**:100224, https://doi.org/10.1016/j.wace.2019.100224.

Sousa, P.M., Blamey, R.C., Reason, C.J., Ramos, A.M. and Trigo, R.M., 2018: The 'Day Zero'Cape Town drought and the poleward migration of moisture corridors. *Environ. Res. Lett.*, **13**(12):124025, https://doi.org/10.1088/1748-9326/aaebc7.

Staten, P.W., Lu, J., Grise, K.M., Davis, S.M. and Birner, T., 2018. Re-examining tropical expansion. *Nat. Clim.*, **8**(9): 768-775. https://doi.org/10.1038/s41558-018-0246-2

Sun, X., Cook, K.H. and Vizy, E.K., 2017. The South Atlantic subtropical high: climatology and interannual variability. *J. Clim*., **30**(9): 3279-3296. https://doi.org/10.1175/JCLI-D-16-0705.1

Taljaard, J.J., 1953. The mean circulation in the lower troposphere over southern Africa. *S. Afr. Geo. J*., **35**(1): 33-45. https://doi.org/10.1080/03736245.1953.10559299

Taljaard, J.J., 1985. Cut-off lows in the South African region (No. 14). Weather Bureau, Department of Transport.

Taszarek, M., Allen, J.T., Marchio, M. and Brooks, H.E., 2021. Global climatology and trends in convective environments from ERA5 and rawinsonde data. *NPJ climate and atmospheric science*, **4**(1): 1-11. https://doi.org/10.1038/s41612-021-00190-x

Telesca, L., Pierini, J.O. and Scian, B., 2012. Investigating the temporal variation of the scaling behavior in rainfall data measured in central Argentina by means of detrended fluctuation analysis. *Phys. A: Stat. Mech. Appl.*, **391**(4): 1553-1562. https://doi.org/10.1016/j.physa.2011.08.042

Theil, H., 1950. A rank-invariant method of linear and polynimical regression analysis. In Proceedings of the Royal Netherlands Academy of Sciences, 53: Part I, 386-392, Part II, 521-525, Part III, 1397-1412

Theron, S.N., Archer, E., Midgley, S.J.E. and Walker, S., 2021. Agricultural perspectives on the 2015-2018 western cape drought, South Africa: Characteristics and spatial variability in the core wheat growing regions. *Agric. For. Meteorol*., **304**: 108405.

Tyson, P.D. and Preston-Whyte, R.A., 2000: The Weather and Climate of Southern Africa. Oxford University Press.

Usman, M.T. and Reason, C.J.C., 2004: Dry spell frequencies and their variability over southern Africa. *Clim. Res*., **26**(3):199-211, https://doi.org/10.3354/cr026199.

van Loon, H. and Jenne, R.L., 1972. The zonal harmonic standing waves in the Southern Hemisphere. *J. Geophys. Res*., **77**(6): 992-1003. https://doi.org/10.1029/JC077i006p00992

Van Wilgen, B.W., 1984. Fire climates in the southern and western Cape Province and their potential use in fire control and management. *S. Afr. J. Sci*., **80**(8): 358.

Van Wilgen, B.W., 2009. The evolution of fire and invasive alien plant management practices in fynbos. *S. Afr. J. Sci.*, **105**(9): 335-342. https://hdl.handle.net/10520/EJC96966

Veitch, J.A., Florenchie, P. and Shillington, F.A., 2006. Seasonal and interannual fluctuations of the Angola–Benguela Frontal Zone (ABFZ) using 4.5 km resolution satellite imagery from 1982 to 1999. *Int. J. Remote Sens*., **27**(05): 987-998. https://doi.org/10.1080/01431160500127914

Vigaud, N., Richard, Y., Rouault, M. and Fauchereau, N., 2009. Moisture transport between the South Atlantic Ocean and southern Africa: relationships with summer rainfall and associated dynamics. *Clim. Dyn*., **32**(1): 113-123. https://doi.org/10.1007/s00382-008-0377-7

Vowinckel, E., 1955. Beitrag zur Witterungsklimatologie Südafrikas. *Archiv für Meteorologie, Geophysik und Bioklimatologie, Serie B*, **7**(1): 11-31.

Walker, N.D., 1990. Links between South African summer rainfall and temperature variability of the Agulhas and Benguela Current systems. *J. Geophys. Res.: Oceans*, **95**(C3): 3297-3319. https://doi.org/10.1029/JC095iC03p03297

Walker, ND and Lindesay, J.A., 1989. Preliminary observations of oceanic influences on the February March 1988 floods in central South Africa. *S. Afr. J. Sci*., **85**(3): 164.

Weldon, D. and Reason, C.J.C., 2014. Variability of rainfall characteristics over the South Coast region of South Africa. *Theor. Appl. Climatol.*, **115**(1): 177-185. https://doi.org/10.1007/s00704-013-0882-4

Wolski, P., 2018. How severe is Cape Town's "Day Zero" drought? *Significance* **15**(2): 24-27. https://doi.org/10.1111/j.1740-9713.2018.01127.x

Wolski, P., Conradie, S., Jack, C. and Tadross, M., 2021. Spatio-temporal patterns of rainfall trends and the 2015–2017 drought over the winter rainfall region of South Africa. *Int. J. Climatol.*, **41**: 1303-1319. https://doi.org/10.1002/joc.6768

Zarrin, A., Ghaemi, H., Azadi, M. and Farajzadeh, M., 2010. The spatial pattern of summertime subtropical anticyclones over Asia and Africa: A climatological review. *Int. J. Climatol*., **30**(2): 159-1. https://doi.org/10.1002/joc.1879

Zhu, Y. and Newell, R.E., 1998: A proposed algorithm for moisture fluxes from atmospheric rivers. *Mon. Wea. Rev*., **126**(3):725-735,https://doi.org/10.1175/1520-0493(1998)126<0725:APAFMF>2.0.CO;2.

Zilli, M.T., Carvalho, L.M. and Lintner, B.R., 2019: The poleward shift of South Atlantic Convergence Zone in recent decades. *Clim. Dyn*., **52**(5-6): 2545-2563. https://doi.org/10.1007/s00382-018-4277-1

Appendix A

Appendix A: The average monthly percentage contributions toward annual rainfall from 1979-2019 together with total average percentage for the extended summer

	Average Rainfall Day Contribution(%)			
	Zone A	Zone B	Zone C	Zone D
Jan	3.2	5.3	4.9	3.7
Feb	3.2	4.9	4.4	4.2
Mar	4.8	6.0	5.9	6.2
Apr	8.5	7.4	8.0	8.8
May	11.5	10.3	10.4	10.4
Jun	14.8	12.1	12.1	13.0
Jul	13.0	11.5	12.6	13.0
Aug	13.7	11.8	12.5	12.4
Sep	10.6	10.3	9.7	9.4
Oct	6.7	7.7	8.1	6.9
Nov	5.5	6.7	6.4	6.3
Dec	4.5	5.9	5.2	5.5
ONDJFM % contribution to annual rainy days	27.9	36.5	34.8	32.9

Appendix B

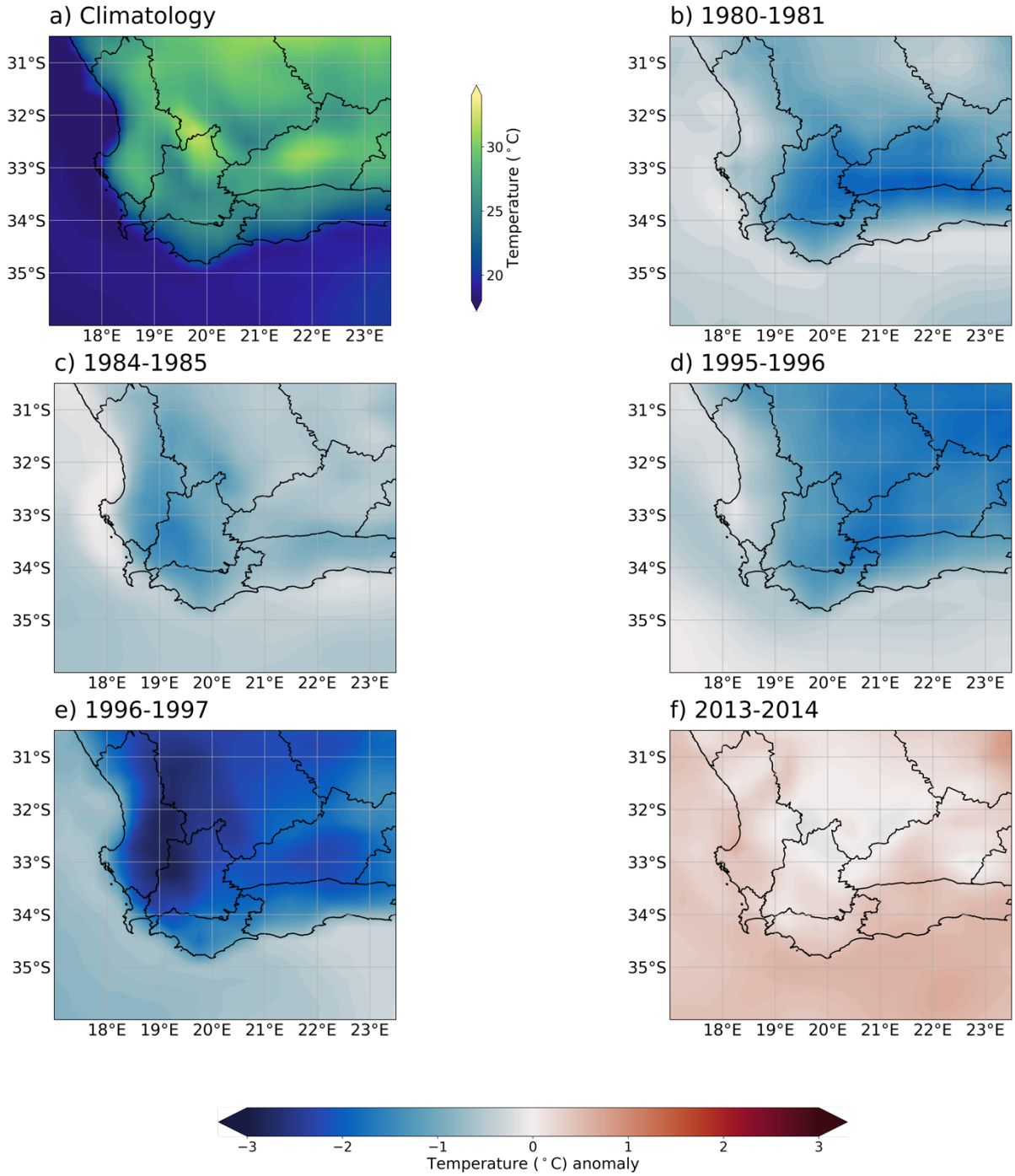

Same as **Fig 5.4-5.5** but for the entire ONDJFM season

Appendix C

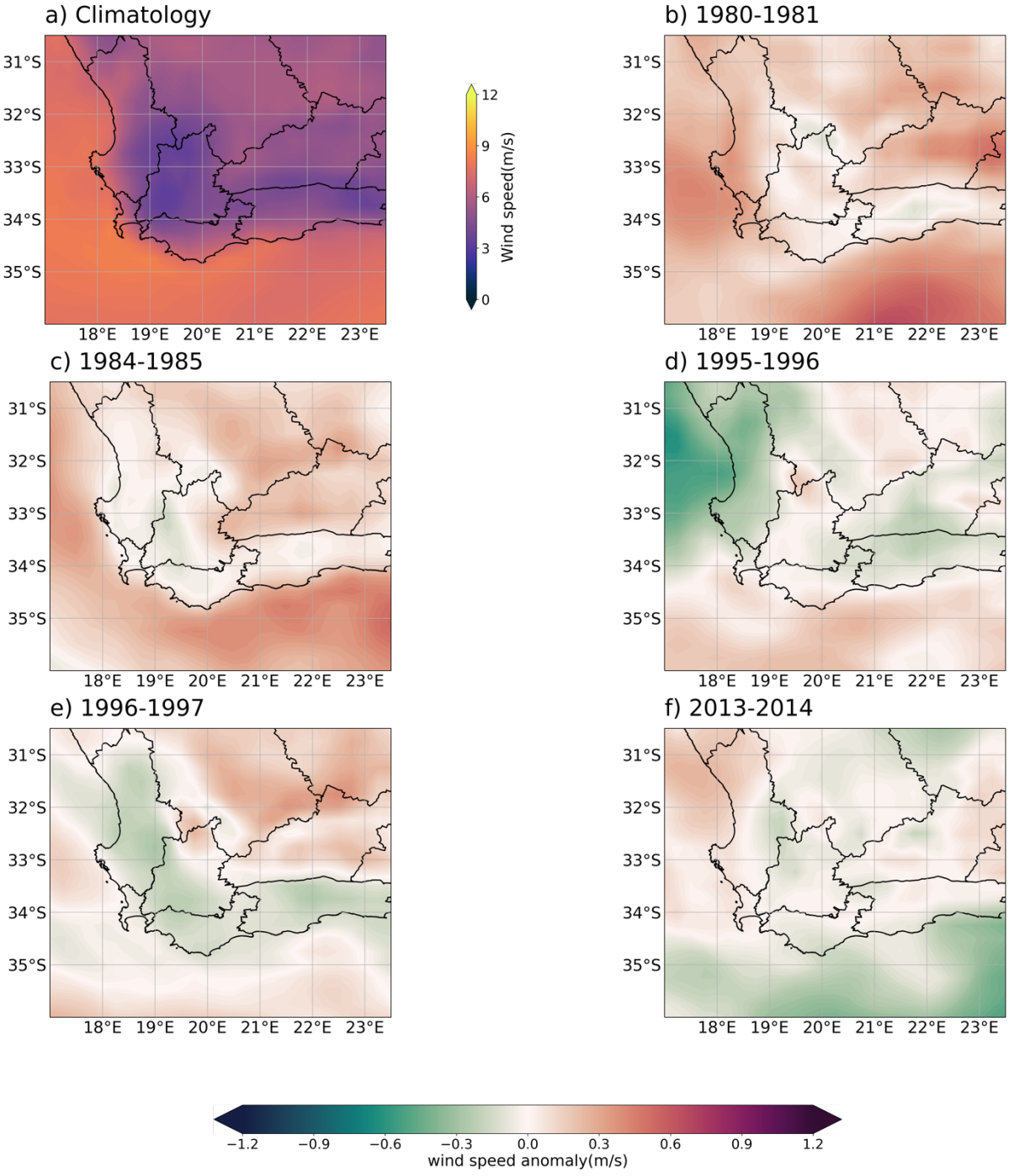

Same as **Fig 5.6-5.7** but for the entire ONDJFM season

Appendix D

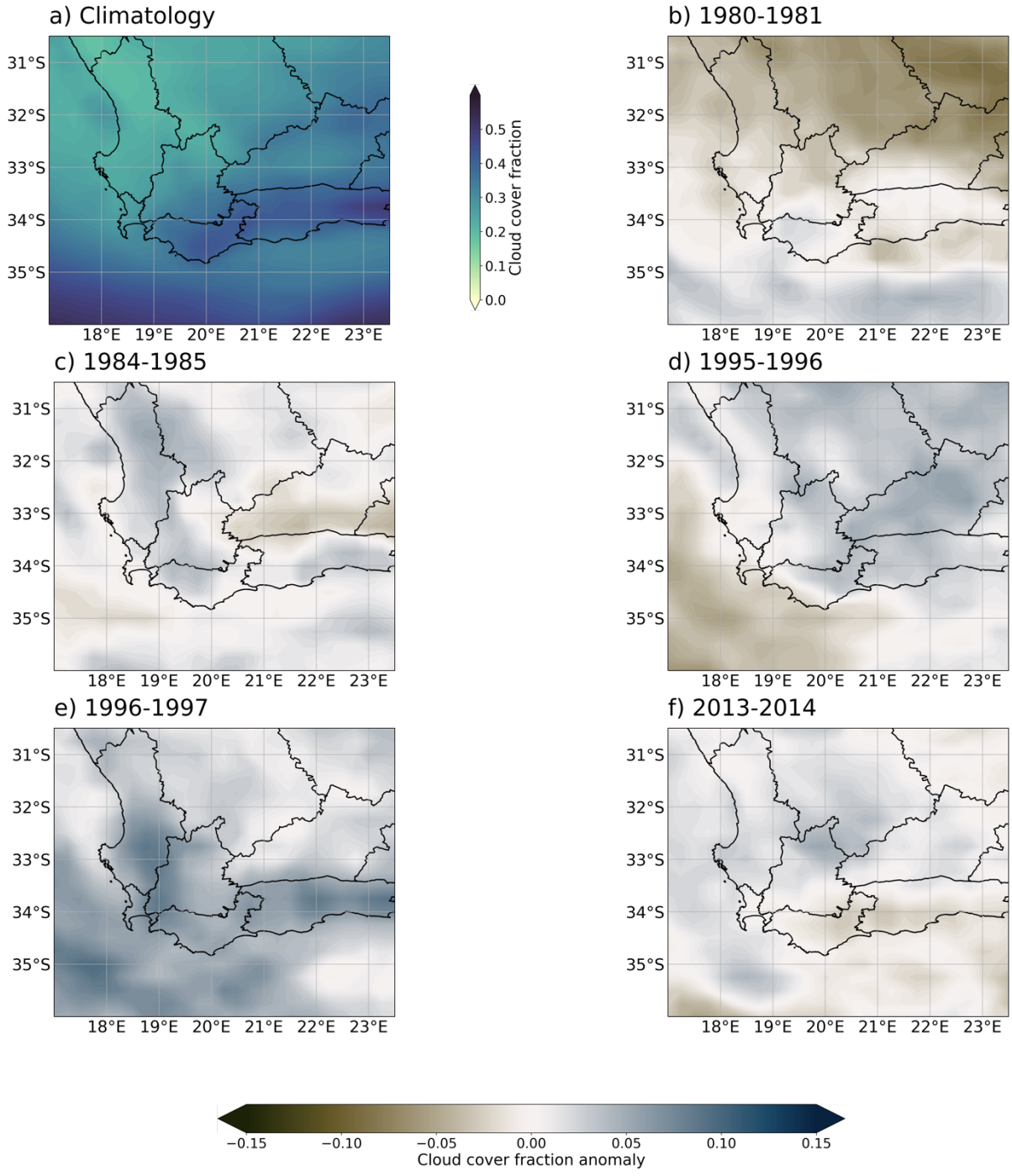

Same as **Fig 5.8-5.9** but for the entire ONDJFM season

Appendix E

Appendix E: The five wettest seasons over the catchment area between 1979-2019 and the number of storm between 30-50° S at the 10° E line. The table also indicates the longest dry spell (consecutive 0mm days) and the number of dry days per season.

Wet Season	Storm counts between 30-50° S	Longest Dry Spell	Days of 0mm rain
1980/81	41	20	139
1984/85	47	21	141
1995/96	37	41	155
1996/97	52	34	147
2013/14	40	30	151